Studies on 6-sector-site deployment in downlink LTE

Studies on 6-Sector-Site Deployment in Downlink LTE

Dipl. Eng. Damiano Scanferla

Eindhoven University of Technology (TU/e)

Department of Electrical Engineering

Electromagnetics Group

Stan Ackermans Institute (SAI)

Information and Communication Technology (ICT)

KPN Supervisor: ir. Arie Verschoor

TU/e Supervisor: prof. dr. ir. Erik Fledderus

April 30, 2012

Summary

Mobile data traffic is expected to increase massively in the following years. Consequently, service operators are induced to increase the capacity of their networks continually to attract more subscribers and maximize their revenues. At the same time, they want to minimize operational costs and capital expenditures. Among the alternatives that aim to increase the network capacity, higher order sectorization, and in particular a six sectorized configuration, is nowadays attracting a lot of attention for LTE macro-cell deployments since a higher number of sectors per site results in improved site capacity and coverage. A six sectorized configuration is attractive for both roll-out phase and growth phase of the network. In the roll-out phase, the radio access network is planned with 6-sector sites instead of 3-sector sites with the advantage that less sites are needed for the same capacity and coverage requirements. In the growth phase, the six sectorized configuration can be used to upgrade existing 3-sector sites where the traffic grows beyond the current sites' capabilities. Therefore, no additional expensive and time consuming contracts need to be signed for the locations of the new sites, while the existing sites are used more efficiently. However, although potentially a 6-sector site can offer a double capacity than a 3-sector site, several factors prevent the capacity from growing proportionately to the number of sectors. Consequently, there is an uncertainty on whether the capacity gain is high enough to justify the extra costs of the additional equipment and, more specifically, whether the 6-sector-site deployment is more economically attractive than a 3-sector-site deployment. The aim of this report is to solve this uncertainty. First, we present the main factors that affect the capacity gain. Next, we quantify the impact of these factors on the capacity gain in downlink LTE with the use of a system level simulator. Finally, we use the results of the simulation study as inputs for an economic study to access the reasons for a possible deployment of 6-sector sites instead of 3-sector sites for LTE.

Contents

Chapter 1

Introduction

1.1 Overview of LTE

The Long Term Evolution (LTE) standard, specified by the 3rd Generation Partnership Project (3GPP) in Release 8, defines the next evolutionary step in 3G technology. The work towards LTE started in 2004 with the definition of the targets, but it took more than 5 years for the first commercial deployment using an interoperability standard to enter the market. A few factors led to LTE deployment: wireline capability evolution, the need for additional wireless capacity, the need for lower cost wireless data delivery, and the competition with other wireless technologies [1]. The continuous improving of wireline technology requires a similar evolution for the wireless domain, to guarantee fluent usage of applications in both domains. There are also other wireless technologies, such as WiMAX, that promise high data capabilities, so LTE had to match and exceed the competition. Further, flat rate pricing keeps pushing wireless technologies to a higher efficiency for what concerns both the spectrum and the network architecture.
LTE aims to provide superior performance compared to High Speed Packet Access (HSPA) technology as defined in Release 6. The main performance targets are listed below [1]:

- Spectral efficiency two to four times higher than with HSPA release 6.
- Peak rates to exceed 100 Mbps in downlink and 50 Mbps in uplink.
- Enables a round trip time of < 10 ms.
- Packet switching optimized.
- High level of mobility and security.
- Optimized terminal power efficiency.
- Frequency flexibility from below 1.5 MHz up to 20 MHz.

The fulfillment of the performance targets outlined above is only possible with radical advances on both radio technology and network architecture. Three technologies characterize the LTE radio interface design: multicarrier technology, multiple-antenna technology, and the application of packet-switching to the radio interface. As an overview, we briefly introduce here the advantages of each radio technology and the changes in the network architecture.

Multicarrier Technology

The Orthogonal Frequency Division Multiple Access (OFDMA) and the Single-Carrier Frequency Division Multiple Access (SC-FDMA) were chosen as the multiple-access schemes for the LTE downlink and uplink, respectively. OFDM has a relative high Peak-to-Average Power

Ratio (PAPR), resulting in a need for a highly linear RF power amplifier. While this is not a problem for downlink transmissions, since high-cost implementations are tolerated at the base station, it represents a limitation for the uplink transmission, since low-cost implementations are more desirable at the mobile terminal. SC-FDMA benefits from the advantages of multicarrier technology and has a significantly lower PAPR, so it was chosen as multiple-access technology for the LTE uplink. The use of the frequency domain in addition to the time-division multiplexing enabled a high flexibility in the system: the transmission bandwidth can be selected between 1.4 MHz and 20 MHz, depending on the spectrum availability without changing the fundamental system parameters or equipment design; transmission resources of variable bandwidth can be allocated to different users and scheduled freely in the frequency domain; both fractional frequency re-use and interference coordination between cells are facilitated.

Multiple-antenna technology

Multi Input Multi Output (MIMO) technology is a key component of LTE, allowing for the targeted throughput and spectral efficiency. MIMO refers to the use of multiple antennas at the transmitter and receiver side. The capacity of MIMO can be up to $min(N_t, N_r)$ times larger than the single-antenna capacity, where N_t and N_r are the number of transmit and receive antennas respectively. For the LTE downlink, a 2x2 MIMO configuration is assumed as the baseline configuration, i.e. two transmit antennas at the base station and two receive antennas at the terminal side. Configuration with four transmit or receive antennas are also expected and reflected in specifications. Different downlink MIMO schemes are envisaged in LTE and can be adjusted according to channel conditions, traffic requirements, and UE capability. The following transmission schemes are possible in LTE [2]:

- Single antenna transmission (SISO)
- Transmit diversity
- Open-loop spatial multiplexing (OLSM)
- Closed-loop spatial multiplexing (CLSM)
- Multi-user MIMO (MU-MIMO)
- Closed-loop precoding for rank 1
- Beamforming

Packet-switching Technology

LTE was designed to support only packet-switched services, in contrast to the circuit-switched model of the previous cellular systems. It aims to provide seamless Internet Protocol (IP) connectivity between User Equipment (UE) and the Packet Data Network (PDN), without any disruption to the end users' applications during mobility. In order to improve the system latency, the packet duration was further reduced to 1 ms from the 2 ms used in HSDPA.
LTE uses the concept of bearer to route IP traffic from a gateway in the PDN to the UE. A bearer is an IP packet flow with a defined Quality of Service (QoS) between the gateway and the UE. Multiple bearers can be established for a user to provide different QoS streams or connectivity to different PDNs.

Network Architecture

While the term LTE covers the evolution of the radio access through the Evolved-UMTS Terrestrial Radio Access Network (E-UTRAN), it is accompanied by an evolution of the

non-radio aspects under the term System Architecture Evolution (SAE), which includes the Evolved Packet Core (EPC) network. Together LTE and SAE comprise the Evolved Packet System (EPS).
3GPP believed in the reduction of the number of network elements as the means to improve the network scalability and to minimize the end-to-end latency. All radio protocols, mobility management, header compression and packet retransmissions are located in one single node called eNodeB, rather than being located in two nodes, named Radio Network Controller (RNC) and NodeB, as it was in 3GPP Release 6. Moreover, the core network functionalities are split into a control plane and a user plane. The Mobility Management Entity (MME) is involved in the control plane only, while the user plane bypasses the MME directly to the System Architecture Evolution Gateway (SAE-GW).

1.2 Mobile Data Traffic Forecast

Despite the continued economic downturn, global mobile data traffic increased immensely in the last few years and the same tendency is expected for the next few years. According to The Cisco Visual Networking Index, Global Mobile Data Traffic Forecast, the overall mobile data traffic is expected to grow at a CAGR (Compound Annual Growth Rate) of 78 percent from 2011 to 2016 and it is expected to reach 10.8 Exabytes per month by 2016, a 18-fold increase over 2011. Figure 1.1 shows the mobile data traffic forecast between 2011 and 2016.

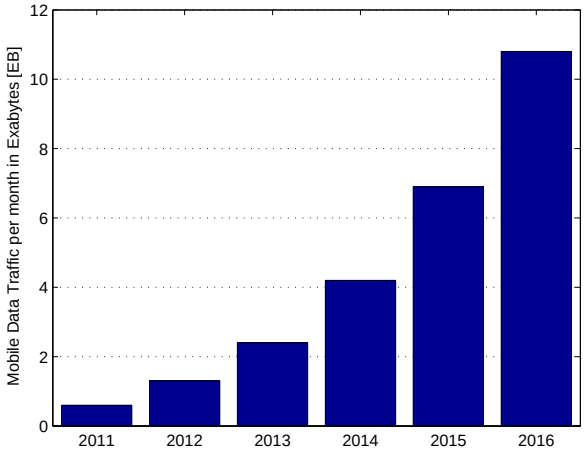

Figure 1.1: Cisco VNI Global Mobile Data Traffic per month [3]

One reason for the strong growth is the accelerated adoption of smartphones by mobile phone subscribers, in combination with the much higher usage profile of smartphones relative to basic handsets (operators such as Vodafone have indicated that smartphone users generate 10 to 20 times the traffic of their non-smartphone counterparts). The increase in smartphone adoption is expected to be even sharper for those smartphones that have the highest usage profile, such as iPhones and Android phones, that generate 5 to 10 times the traffic of the average smartphone. In addition, other high-usage devices, such us mobile-connected tablets, laptops, and netbooks will increase their presence on the mobile network. The introduction of these devices is a major generator of traffic. Firstly, these devices offer the consumer contents and applications not supported by the previous generation of mobile devices. Secondly, a

Device Type	Growth in Users, 2011-2016 CAGR	Growth in Mobile Data Traffic, 2011-2016 CAGR
Smartphone	24%	119%
Portable gaming console	56%	76%
Tablet	50%	129%
Laptop and netbook	17%	48%
M2M module	42%	86%

Table 1.1: Comparison of Global Device Unit Growth and Global Data Traffic Growth [3]

large percentage of mobile-connected laptop users consider mobile broadband their primary means of accessing the Internet, and in many regions there is a pronounced mobile broadband substitution effect over the fixed broadband.
Another reason for the strong growth of the mobile traffic is the rapid increase of the traffic per device. The increasing high-definition video and TV services demands, along with a higher usage of VoIP applications, mobile gaming, mobile P2P, and mobile M2M (machine-to-machine) are the main promoters of the growth in average usage per device. A comparison of the global device unit growth and the global data traffic growth is shown in Table 1.1.
In order to support the rapid growth in mobile subscribers and bandwidth demand per subscriber, mobile service providers must increase the capacity of their networks. Addressing this need is complicated by the fact that the highest site traffic demand (and, therefore, capacity requirements) is found within only a small percentage of the overall network. For example, a recent HSDPA traffic analysis in RNC shows that during the early morning hours, 10% of the cells contribute to 70-85% of the total RNC level data volume, whereas during the busiest hours the same 70-85% data volume is contributed by 19-25% of the cells [1].

1.3 Techniques to Increase Network Capacity

The network capacity can be increased by either adding new sites or enhancing the capacity of the existing sites. The addition of a new macrocell site can be a long process that lasts for a couple of years, since it involves network planning, agreements with landlords, permissions acquisition from the city hall, etc. The capacity increase of the existing sites can be addressed in several ways: adding additional spectrum capacity, updating the transmission mode, and using a higher order of sectorization.

Spectrum Capacity

The spectrum capacity of an LTE service operator can be increased either purchasing additional spectrum or refarming to the GSM spectrum. The former solution requires long auctions and large upfront investments. The latter solution does not require investments because it reuses the GSM spectrum of the operator and it is facilitated by the flexibility of the LTE bandwidth. In fact, LTE can start with 1.4 MHz or 3 MHz bandwidth and then gradually grow as soon as the GSM traffic has decreased. However, it is worth noting that the spectrum efficiency is expected to be lower for narrower bandwidths, since the frequency selectivity of the channel offers a lower potential.

Transmission mode

First LTE deployments are expected to support 2x2 Single-User MIMO (SU-MIMO) with OLSM scheme for downlink transmissions. At later stages, when capacity requirements will exceed the offered capacity, the number of transmitter antennas at the base station may be doubled, resulting in a 4x2 SU-MIMO, and Multi-User MIMO (MU-MIMO) may also be adopted. In addition, as mobile devices with 4 receiver antennas will enter the market, 4x4 MIMO will be realizable. Beamforming technologies such as fixed beam switching and adaptive beamforming are also considered as options to increase the site capacity [4].

Higher Order Sectorization

In the baseline configuration, LTE employes three sectors per site. A higher order sectorization with 6 or more sectors is considered a favorable economic option to increase the capacity of the site by exploiting the spatial dimension. Rather than adding new sites to the network, the addition of sector antennas to existing sites requires a lower investment and less deployment time. However, the capacity gains with higher order sectorizations depend on a number of factors that are difficult to predict and to estimate. Studies presented in [5] concluded that higher order sectorizations give higher capacity but the increase is not proportional to the number of sectors.

1.4 Motivations and Objectives

As the number of subscribers and the amount of mobile data traffic will substantially increase in the next years, LTE service providers will need to improve the capacity offered by their networks. Moreover, the highest site traffic demand is found within only a small percentage of the overall network. Among the solutions that service providers are investigating, higher order sectorization is gaining more and more attention, as it can improve the capacity and service quality within network hotspots as required, without altering and re-engineering the overall network (which is needed when adding new sites). However, despite several studies being available in the literature on the performance gain of a 6-sector site compared to a 3-sector site for WCDMA, only a few studies have been conducted for LTE. This report describes the work that has been done at KPN in the framework of my final project in the second year of the PDEng program in SAI/ICT. The first goal of this report is to determine the capacity gain that can be achieved with a 6-sector site compared to the 3-sector site in the Physical Downlink Shared Channel (PDSCH) of UTRAN LTE. The second goal is to access the reasons for a possible deployment of 6-sector sites instead of 3-sector sites for LTE.

1.5 Strategy

The initial plan to address the capacity gain was to follow two parallel methodologies. The first methodology involves the use of a system level simulator to evaluate and compare the performance of a three and a six sectorized configuration. The second methodology involves throughput measurements in a 3- and a 6-sector site of the KPN Friendly User Pilot (FUP) network in Utrecht. The choice of this particular strategy has two main goals: to increase the reliability of the results, and to determine whether the simulator uses the right models and parameter settings to predict the channel propagation or if it requires further adjustments.

Unfortunately, the construction of the FUP network had been delayed beyond the duration of the project and the measurements couldn't take place. Therefore, only the first methodology is followed to determine the capacity gain. Nevertheless, the report includes the test cases that were developed in the second methodology to allow the execution of the measurements in a follow-up project in KPN.
The results of the capacity gain investigation are the inputs for an economic study that aims to determine whether the capacity gain is high enough to justify the extra costs derived by the additional equipment of a 6-sector site, and more specifically, to determine whether the 6-sector-site deployment is economically more attractive than the 3-sector-site deployment. Since the analysis that is conducted in the economic study contains confidential information, it is not included in this report and it is only available at KPN. Nevertheless, the main conclusions of the economic study are presented in this report.

1.6 Report Outline

The report is organized as follows. Chapter 2 introduces the concept of sectorization. It describes the factors that affect the capacity gain of a 6-sector site, and presents the latest innovations that may benefit a 6-sector upgrade. Chapter 3 describes the simulation study. It includes a description of the simulated scenarios, a selection of the metrics, and the results. Chapter 4 describes the test cases to perform the measurements. Finally, Chapter 5 provides the overall conclusions of the report and discusses future research issues.
Appendix A describes the LTE standardization background and process. Appendix B describes the LTE physical layer solutions along with the system architecture. Appendix C reviews the LTE system level simulator that has been used in this project. Appendix D presents a feasibility study on a particular antenna array deployment for a 6-sector site. Finally, Appendix E presents the baseline document of the project.

Chapter 2

Sectorization in LTE

2.1 Introduction

The term 'sectorization' refers to the process of partitioning each site radially into multiple sectors and reusing the spectral resources across sectors and sites. Sectorization is primarily used as a technique to increase system capacity, although service coverage is generally improved at the same time as a result of the increased antenna gain associated with more directional antennas. The configuration associated with various degrees of sectorization are presented in Table 2.1.

Level	Application
1 sector	Micro-cell or low capacity macro-cell
2 sectors	Micro-cell or macro-cell providing roadside coverage
3 sectors	Standard macro-cell configuration providing medium capacity
4 or 5 sectors	Not commonly used but may be chosen to support a specific traffic scenario
6 sectors	High capacity macro-cell configuration

Table 2.1: The application of various levels of sectorization [5]

In the remaining part of the section, an overview of sectorization in GSM, WCDMA, and LTE will be presented along with some considerations on the 6-sector site deployment feasibility in these systems. Section 2 describes the factors that affect the capacity gain of a 6-sector site in LTE. Finally, section 3 presents the latest innovation that may favour a 6-sector upgrade.

2.1.1 Overview of Sectorization in GSM

Initial GSM deployments were based on omnidirectional base stations, due to the low capacity requirement and the simplicity of the network planning. As the number of subscribers increased considerably, sectorization was considered an economically attractive solution for network operators to increase the site capacity. Sectorization in GSM requires a larger frequency reuse pattern[1] than the omnidirectional configuration to guarantee a comparable level of co-channel carrier-to-interference ratio (C/I). While a reuse pattern of 7/7 is nominal for an omnidirectional base station configuration, a reuse pattern of 4/12 has to be used for a

[1]The frequency reuse factor indicates the cluster size of cells within which each frequency is used only once. It is typically denoted as N/M and indicates that each frequency is reused every N sites and every M sectors.

Reuse Factor	Co-channel C/I [dB]	Channels per site	Channel capacity gain over 7/7	Channel capacity gain over 4/12
7/7	18.66	S/7	1	0.57
4/12	18.57	S/4	1.75	1
3/18	19.08	S/3	2.33	1.33
2/12	15.56	S/2	3.5	2

Table 2.2: C/I and channel capacity for various reuse factors. S is the total number of GSM channels.

three sectorized configuration to provide the co-channel interference protection required by GSM specifications. Values of C/I are reported in Table 2.2 and are calculated as follows:

$$\frac{C}{I} = 10log\left[\frac{(3N)^{r/2}}{L}\right] \tag{2.1}$$

where N is the cluster size, L is the number of co-channel interferers, and r is the pathloss exponent that is set equal to 4. Table 2.2 also reports the number of available channels per site for each reuse factor along with the channel capacity gain over the omnidirectional site. Although a channel capacity gain of 3 can be expected in a three sectorized configuration over an omnidirectional configuration, only a channel capacity gain of 1.75 is achievable due to the larger reuse factor. Nevertheless, this capacity gain was considered high enough to justify the migration to three sectorized sites.
The capacity of a GSM site can be further improved upgrading a three-sector site to a six-sector site. In order to guarantee the same level of co-channel C/I, a reuse factor of 3/18 needs to be adopted. However, in this configuration the achievable channel capacity gain is only 1.33 (see Table 2.2). A reuse factor of 2/12 was also investigated, as it offers a double channel capacity than the 4/12 reuse factor. Even so, since the closest separation between co-channel sites is shorter than that of the 4/12 reuse plan, the expected co-channel C/I is 3 dB lower. Therefore, techniques to mitigate the co-channel interference need to be considered. For these reasons, along with difficulties in increasing the amount of required equipment, cabling, and number of antennas in the traditional site models and base stations, the migration to a six sectorized configuration was not economically attractive enough and it was set aside. Instead, the site capacity was improved increasing the number of three sectorized sites.

2.1.2 Overview of Sectorization in WCDMA

After the success and the experience gained with sectorization in GSM, the three sectorized configuration was adopted as a standard configuration in WCDMA macro-cell deployments. The gains that can be achieved from sectorization in WCDMA are much higher that in the GSM systems, because of the frequency reuse factor 1/1, which results in the entire reuse of the allocated bandwidth in each sector. However, the radiation patterns of the sector antennas are not ideal and result in sector overlaps. Sector overlapping causes interference leakage between adjacent sectors, which results in reduced capacity. Furthermore, although a certain degree of cell coverage overlap is required for the smooth functioning of soft and softer handovers to provide ubiquitous service coverage, excess adjacent sector overlaps result in increased soft and softer handover probabilities and overhead, which in turn reduces system capacity. Therefore, the degree of overlap between sectors must be controlled, for example by a careful choice of antenna beamwidth, so that overlap reduces to an acceptable level. As

the level of sectorization increases then so also do the sector overlaps and thus the level of inter-cell interference, probability of handovers, and handover overhead. Antenna sidelobes are also likely to be greater for more directional antennas.
Several simulation studies have been conducted to investigate the performance of a WCDMA six sectorized site. An investigation of WCDMA system capacity for omnidirectional, 3-sector, and 6-sector site is presented in [5]. This study showed a capacity gain of 2.6-2.8 for a 3-sector site compared to an omnidirectional site, and a capacity gain of 1.7-1.8 for a 6-sector site compared to a 3-sector site. A study presented in [6] confirmed these results. It showed a capacity gain of 2.97 and 1.7, respectively. It also reported a 23% soft handover overhead for the omnidirectional site, and an increase of 4% and 9% for the 3-sector site and the 6-sector site respectively.
An investigation of the performances of a 3-sector and a 6-sector deployments is presented in [7] for two case studies. In the first case study, the performance are evaluated in a homogeneous and regular hexagonal deployment, with a resulting capacity gain of 1.86 when doubling the sectors from 3 to 6. The second case study, instead, addresses a real Vodafone network in the Stuttgart area. The dynamic simulator has been extended and adapted in order to mimic the real environment conditions including: sites positions and configurations, RNC parameter settings, deployed antennas, orientation and tilting, pathloss raster maps, and traffic distribution raster map. The results showed an increased covered area (+23%), an increased capacity (+77%), and a non-significant change of soft handover ratio (less then 10% relative change) when doubling the number of sectors per site from 3 to 6.
It comes without doubt that a 3-sector-site deployment was long preferable compared to the omnidirectional configuration, since the site capacity is almost three times higher. As the mobile data traffic increased substantially in the last few years, solutions to increase the capacity of WCDMA, including higher order sectorization, were considered. However, a migration to a six sectorized configuration was hindered by the fact that deploying highly sectorized sites requires a corresponding high quantity of hardware in terms of both the antenna sub-system and the modules to be fitted within the BS cabinet. In some cases the additional transceivers and power amplifiers may require a second BS cabinet. For this reasons, it was preferable to improve the capacity by adding new frequency carriers or new sites rather than adding new sectors to existing sites. Even so, in 2009, Nokia Siemens Network (NSN) launched the High-Performance Site Solution [8] which enables a lean and cost-efficient 6-sector-site. This technology was adopted in 2010 by Telefonica O2 UK Limited to upgrade a congested site in London, resulting in the ability to carry significantly more voice data calls in O2's network [9]. The upgrade also helped conserve smartphone battery life while decreasing the signaling load on the network. Interest in 6-sector deployments for WCDMA has also been shown by SK Telecom, which is planning to expand to 500 6-sector base stations the 20 base stations that were beta-tested at the end of 2010 [10].

2.1.3 Overview of Sectorization in LTE

Three sectorized macro-cell sites is the standard configuration for LTE. OFDMA minimizes the intra-sector interference by orthogonal allocation of the sub-carriers to the scheduled users. However, due to a 1/1 reuse factor and non-ideal radiation pattern of the sector antennas, intra-site and inter-site interference[1] are still present. Furthermore, the higher number of interferers and the wider overlapping regions of a 6-sector site lead to a higher interference

[1]Intra-site interference is defined as the interference that is received from the sectors of the serving site. Inter-site interference is defined as the interference that is received from the sectors of the surrounding sites.

compared to a 3-sector-site deployment. So far, a performance evaluation of 6-sector site for downlink UTRAN LTE has been presented only in [11]. No other studies are available in open literature. A site capacity gain of 88% and a cell-edge throughput[2] gain of 63% are achieved in an homogeneous network when doubling the number of sectors from 3 to 6. The effect of different antenna beamwidths was also investigated showing a reduction of the average site throughput of 1% and 4% with a 5 degrees and 10 degrees larger beamwidths, respectively. Finally, a mixed network topology with two different combinations of 3- and 6-sector-site deployment has also been considered to determine if the 6-sector-site deployment is a viable option to meet high traffic demands in a localized area such as hot spots. In the first configuration the network consists of a single 6-sector site surrounded by 3-sector sites, while in the second configuration, the network consists of a cluster of 6-sector-sites surrounded by 3-sector-sites. The results showed an average capacity gain in the upgraded sites of 110% and 96%, respectively.
Presently, no studies are available in the open literature that evaluate the effects of different radiation patterns, antenna gains, users' speed, CQI compression techniques, and uplink delays for both 3- and 6-sector-site deployments and that provides a capacity gain study based on the service provider requirements. Not even measurements studies have been conducted to access the site capacity. The main goal of this report is to cover these two gaps in the literature and to provide the network operators with useful insights into the six sectorized deployment.

2.1.4 Considerations

In GSM, the 6-sector-site deployment was not considered technologically and economically feasible. On the one hand, the reuse factor 3/18 provides a theoretical capacity gain of 1.33 which is not economically attractive. On the other hand, the reuse factor of 2/12 requires additional techniques to mitigate the co-channel interference to have a comparable level of co-channel carrier-to-interference ratio with a 3-sector-site deployment. In addition, with the technology that was available 5-10 years ago, the equipment upgrade would have required much more space at the base station and the installation of additional feeder cables. Nowadays, the equipment upgrade is far more compact, easy to install, and less expensive; however, the GSM network is quite mature and the capacity requirements are well satisfied. Furthermore, a migration of GSM users to WCDMA is expected while new subscribers are likely to be WCDMA users. Therefore, a 6-sector solution is not attractive for GSM nowadays either.
In WCDMA, simulation studies showed a 6-sector-site capacity gain of 1.7-1.8. However, due to the lack of measurements with 6-sector sites, operators were doubtful concerning the real capacity gain that can be achieved. In addition, the technology limitations in terms of space and installation were still an issue to be solved. Therefore, the network capacity was increased either with the addition of new carriers, which provide a guaranteed capacity gain, or with the addition of new sites. Recently, innovations in site equipment solved the site implementation issues raised above and resulted in a lean and cost-effective 6-sector site. Therefore, nowadays the six sectorized configuration can be thought as a feasible solution to increase the capacity of a WCDMA network. The examples provided in 2.1.2 confirm what stated.
In LTE, simulations showed that a 6-sector site is expected to offer a capacity gain of 1.88. In addition, a compact and cost-effective 6-sector-site solution is already available in the market, thus making the 6-sector-site deployment a realistic solution to increase the network capacity. The only issue to be solved is to determine whether this solution is economical attractive. Therefore, operators should conduct appropriate measurements to validate the simulation

[2]The cell-edge throughput is defined as the 5% user throughput percentile

results and determine whether the capacity gain is high enough to justify the additional equipment that is needed in a 6-sector site.

2.2 Factors Affecting Capacity Gain

Since LTE reuses all available resources in each sector, a 6-sector site can allocate twice the resources that can be allocated with a 3-sector site. In other words, for a fixed number of users per site and for an equal distribution of resources per user, the number of resources that are allocated to each user is doubled. Thus, the capacity gain of a 6-sector site potentially is 2. However, factors such as interference, handovers, etc. have a stronger impact in the 6-sector site. Therefore, although users have twice the resources, the channel conditions are worse and the capacity gain that can be achieved is lower than 2. This section presents the most relevant factors that have an impact on the capacity gain of a 6-sector-site deployment compared to a 3-sector-site deployment.

Inter-cell Interference

The most important factor influencing the system performance of a sectorized site is the choice of the antennas. Since the antenna radiation patterns are not ideal, the radiation of the sector antenna is not confined to the target sector but it covers a wider area resulting in overlapping regions[2] between adjacent sectors. The extent of the overlapping region determines the level of inter-cell interference. Figure 2.1 shows the overlapping regions for a 3- and a 6-sector-site deployment. The antenna radiation patterns considered in Figure 2.1 follow the idealized

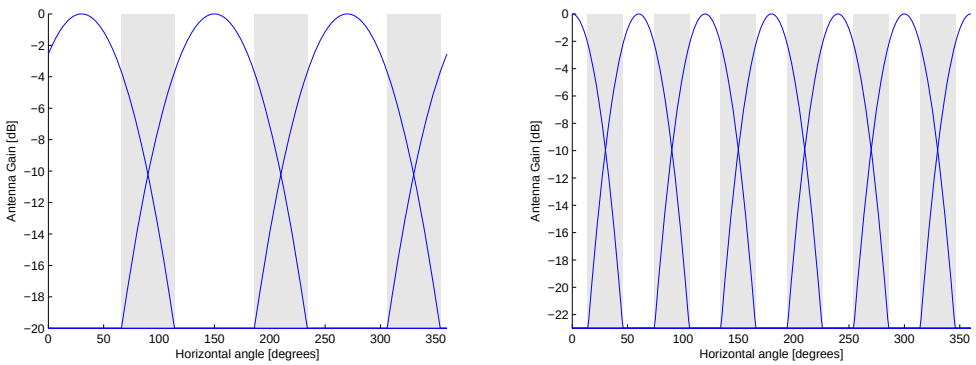

(a) 3-sector-site deployment (b) 6-sector-site deployment

Figure 2.1: Overlapping regions

parabolic response defined in [18]. The beamwidth and sidelobe attenuation are 65 degrees and -20 dB for the 3-sector antenna pattern, and 33 degrees and -23dB for the 6-sector antenna pattern. For the 3-sector-site deployment the total overlapping region is 144 degrees, while for the 6-sector-site deployment it increases to 192 degrees.
In addition, 6-sector antennas have stronger sidelobes than 3-sector antennas, so the power radiated in the adjacent sectors is higher. The reason is that the narrower the antenna beamwidth, the worse the sidelobe suppression.

[2]The overlapping region is defined as the region in which at least two signals are above the sidelobe attenuation.

Consequently, due to the wider overlapping regions, higher number of interfering sectors, and stronger sidelobes, the inter-cell interference is expected to be higher in the 6-sector site.

Intra-site and Inter-site Handovers

Because of the narrower coverage areas of the sectors and the wider overlapping regions, the number of intra-site handovers is expected to be higher or even double in the 6-sector-site deployment. On the other hand, the number of inter-site handovers is expected to remain unchanged or to slightly increase because the site coverage is approximately unchanged. Therefore, the total amount of intra-site and inter-site handovers will be higher in the 6-sector-site deployment but not as much as twice the number of handovers than the 3-sector-site deployment. From an user perspective, a higher number of handovers results in worse performance both in terms of throughput and service interruptibility. Instead, from a sector perspective, since the number of sectors is doubled in the 6-sector-site deployment whereas the total number of handovers is less then doubled, the number of handovers per sector will be smaller. Consequently, a smaller percentage of resources will be used to handle the handovers. As a result, the capacity gain of a 6-sector-site deployment is expected to be higher in the presence of handovers compared with a static situation with no handovers.

Azimuth Spread

Signals that transverse a radio channel become subject to spatial and temporal dispersions. The spatial distribution of the signal power is known as the Power Azimuth Spread (PAS). The standard deviation of the PAS is commonly referred to as the azimuth spread. The degree of azimuth spread directly impacts the signal strength at the mobile and correlates the signal power from adjacent sector antennas. As the azimuth spread increases, the effective sector beamwidth increases, resulting in additional inter-cell interference. The effective radiation pattern of a sector antenna can be obtained by convolving the baseline radiation pattern of the sector (that has zero azimuth spread), in the angular domain, with the PAS of a typical urban macrocellular channel. Experimental investigations reported in [12] showed that the PAS of both urban and rural macrocellular environments is accurately modeled by a Laplacian function. The median azimuth spread was found to equal 5° for an antenna mounted 32 m above ground level, and 10° when mounted 20 m above ground level. Because the PAS is relatively narrow compared to the 3-sector response, the resulting 3-sector effective response is similar to the baseline response. Instead, the 6-sector effective response is wider than the baseline response resulting in additional inter-cell interference and thus lower capacity gain.

Spatial Distribution of Users

The capacity of a site depends, to some extent, on the number of users that are allocated. In fact, the higher the number of users, the higher the probability that users experience different channel conditions for the same frequency. Therefore, as the number of users per sector increases, the resource utilization improves resulting in a higher throughput per sector.
For a fixed number of users per site, the number of users per sector is lower in a 6-sector site than in a 3-sector site. From what said above, this results in a worse resource utilization and therefore a lower sector throughput. The effect is more definite when the total number of users per site is small.

Site Planning

Ideally, when doubling the number of sector from 3 to 6, two 6-sector antennas are intended to cover the same area of one 3-sector antenna. However, this is not the case because of the non-ideal radiation patterns and the higher antenna gain. Therefore, upgrading a single 3-sector site or a cluster of 3-sector site requires an accurate radio tilt adjustment in the interested sites and in the surrounding sites. A non-accurate radio settings may affect both the capacity gain of the 6-sector sites and the capacity of the surrounding 3-sector sites.

Deployment of Inter-cell Interference Coordination Techniques

Inter-cell Interference Coordination involves the intelligent coordination of Physical Resource Blocks (PRBs) between various neighboring cells to reduce the inter-cell interference and improve the performance especially for cell-edge users. Although several techniques are available in literature, the common strategy is to give up some resources in a coordinated fashion. As the resources are not fully reused in each sector, the throughput is lower. These techniques can be adopted in the 6-sector-site deployments to cope with the higher inter-cell interference resulting in lower capacity gains.

2.3 Technology for 6-sector-site deployment

As stated in the previous paragraphs, the migration from a three sectorized configuration to a six sectorized configuration has been hindered mainly by two factors: uncertainty on the capacity gain; and site implementation issues. This section presents the most encouraging solutions to address these problems.

Enhancing the capacity gain

Simulation studies on WCDMA and LTE showed that the capacity gain of a 6-sector site is affected to a large extent by the higher interference and the higher number of handovers compared to a 3-sector site. The three reasons behind these phenomenons are the double number of interfering antennas, wider overlapping regions, and stronger effect of the AS. This results in capacity improvements in the order of 70-80% compared to a 3-sector site. However, although simulations use accurate models to emulate real environment conditions, performance of real applications may be much lower. Therefore service providers are reluctant to invest in a solution that may fail to deliver the anticipated performance gains.
Normally, when upgrading a 3-sector site to a 6-sector site, the 65°-beamwidth antenna in one sector is replaced by two conventional narrower 33°-beamwidth antennas. However, the symmetrical patterns of the two antennas result in wide coverage gaps and handover area that lead to the consequences explained above.
Advances in adaptive array technology have been used to develop single dual-sector panel antennas that allow a one-to-one update of the sector antennas. Among the alternatives that are available in the market, the TenXc Multi Band Bi-Sector Array Antenna [13] provides asymmetrical dual beams optimized to match existing 65°-pattern, thus avoiding the need of radio adjustments, and to reduce the overlap bewtween adjacent sectors. This solution is capable of limiting the inter-sector interference and the number of handovers, potentially improving the capacity gain of a 6-sector site.

Addressing site implementation issues

A site upgrade from a 3-sector configuration to a 6-sector configuration requires a new set of antennas, and a considerable amount of additional equipment and cables. In particular, six extra heavy feeder cables are required to connect the antennas with the equipment at the basement. Obviously, while this upgrade can be easily achieved in a solid mast, many issues may arise if the base station is located in a less convenient location.
Recent research topics focus from one side on optimizing the size and the power consumption of the base station, and from the other side on extending the support to multi-technology and multi-band systems. For example, Nokia Siemens Network (NSN) developed the Flexi Multi-radio 10 Base Station [14] that supports GSM/EDGE, WCDMA/HSPA+, LTE(FDD/TDD), and LTE-Advanced. It is a rather compact solution that combines one Flexi System Module and one Flexi 3-sector RF Module. When adopting this technology, a 3-sector LTE eNodeB with 2-Tx MIMO and 10 MHz bandwidth consists of three cross-polar 65°-beamwidth antennas, one Flexi System Module, and two Flexi 3-sector RF Modules[3]. The volume of the platform is 75 liter for around 70 Kg weight, excluding the antennas. A site upgrade to a 6-sector configuration requires the replacement of the existing sector antennas with either six cross-polar 33°-beamwidth antennas or three cross-polar bi-sector antennas, two extra Flexi 3-sector RF Modules, and extra cables[4], as shown in Figure 2.2. The volume of this platform is 125 liter for around 120 Kg weight, excluding the antennas.
The NSN's solutions for a 3-sector LTE eNodeB and for a 6-sector LTE eNodeB can be easily mounted next to the antennas, instead of being placed on the basement, with the advantage that the long, rigid, and heavy feeder cables can be replaced by short, flexible, and light feeder cables. The compactness of the solution proposed by NSN for the 6-sector eNodeB along with the light feeder cables clearly extends the chance to install a 6-sector site in almost any location.

[3]One Flexi 3-sector RF Module controls 3 sectors with 1-Tx per sector. Therefore, two Flexi 3-sector RF Modules are required for 3 sectors and 2-Tx MIMO.

[4]Note that one extra Flexi System Module is required for 2-Tx MIMO and 20 MHz bandwidth.

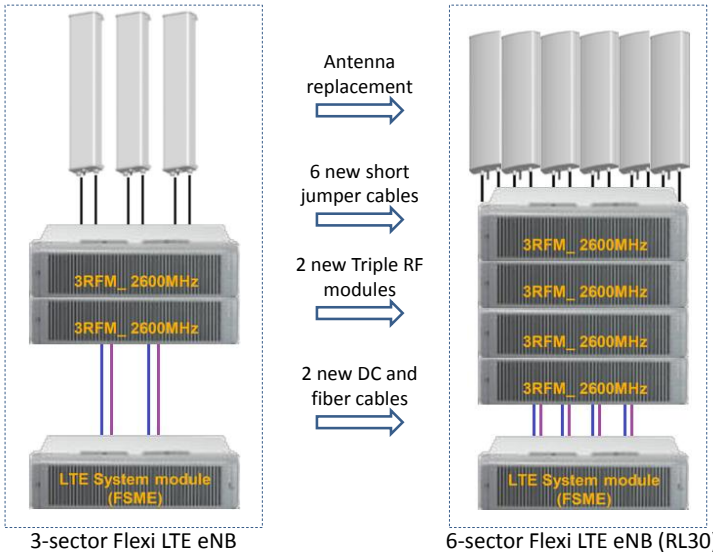

Figure 2.2: NSN's 3-sector and 6-sector LTE eNodeB RL30 (available from Q1/2012).

Chapter 3

Simulation Study

3.1 Introduction

The performance evaluation of the Physical Downlink Shared Channel (PDSCH) of LTE networks with 3-sector or 6-sector sites requires a system level simulator. Indeed, while link-level simulators allow for the investigation of physical layer related issues such as MIMO gains, Adaptive Modulation and Coding (AMC) feedback, or modeling of channel encoding and decoding, system-level simulators focus more on network-related issues such as scheduling, mobility handling, interference management, or site configuration and network layout.
Among the system-level simulators that were available in the market at the time this project was started, none of them allows the simulation of LTE networks with 6-sectors sites. This feature was found only in the simulator used in [11] that was unfortunately developed within a company for private use only. In order to identify the most suitable simulator for this project, we defined the following requirements:

- the simulator is implemented according to the 3GPP standards
- the simulator is well documented and on-line support is available
- OLSM transmission scheme is implemented
- the source code is available
- the 6-sector capability and other additional features can be implemented

The definition of the above requirements narrowed the set of choices to the LTE system-level simulator developed by the Vienna University of Technology [15]. The simulator is offered for free under an academic, non-commercial use license, and its source code is available. Further, being implemented in MATLAB making extensive use of the object-oriented programming capabilities, new functionalities and algorithms can be easily added and tested. The version of the simulator that is used in this project is the v1.3r427. Please refer to Appendix C for an overview of the simulator.

3.1.1 Developed Functionalities

The following features and functionalities have been added to the original version of the simulator:

- Extension of the macroscopic pathloss to the 2.6 GHz frequency.
- Possibility to choose the number of sectors (either 3 or 6) of each site independently.
- Possibility to choose the number of users in each sector independently.

- Addition of horizontal and vertical radiation patterns of two Kathrein sector antennas that are used for 3- and 6-sector site, respectively.
- New metrics such as Intra- and Inter-site interference, and cell-edge throughput;
- Technique to avoid network edge effects.
- Support of a frequency reuse factor of 1/3, in addition of the standard 1/1.
- Wideband CQI reporting technique.
- New action to take when a UE exits the ROI: the last position inside the ROI is set as current position and the UE's direction is inverted.

3.2 Simulation Setup

3.2.1 Simulation Parameters

A hexagonal cellular layout composed of 19 sites is assumed in the simulation study. Each site is composed of either 3 or 6 sectors based on the simulation requirements. Site refers to the area covered by one eNodeB, and sector refers to the area covered by one of the 3 or 6 sector antennas in that eNodeB. Only the center site and the sites within the first ring have been simulated with active user terminals, whereas the sites within the second ring are taken as interfering sites assumed with full downlink load (Figure 3.1). The location of users is randomly generated from a uniform distribution within the center area (center site and first ring). The serving sector is selected among all sectors of the center area with the highest received signal power, that is calculated including pathloss and shadow fading but excluding fast fading. A total of 60 users per site is considered and scaled per sector according to the number of sectors, resulting in 20 users/sector for 3-sector site and 10 users/sector for 6-sector site.
The infinite full buffer traffic model has been chosen for the simulations, therefore all eNodeBs have always data to transmit to every attached UEs. In addition, the Proportional Fair (PF) scheduler[1] has been selected as frequency domain packet scheduler [17]. Since no scheduling are done in the time domain, all active users will be allocated every TTI. If the number of users per sector is high, this solution results in high overhead in the PDCCH channel because the scheduler needs to send the resource allocation of all active users every TTI. A Time Domain PF scheduler needs to be added in order to limit the number of users that can be allocated

[1]The allocation strategy of the frequency domain PF scheduler is based on the calculation of a metric, $M_{u,i}$, that is defined for the UE u and the PRB i as the ratio between the achievable throughput of the UE u with PRB i and the average throughput of UE u. The PRB i is assigned to the users that maximizes the metric $M_{u,i}$.

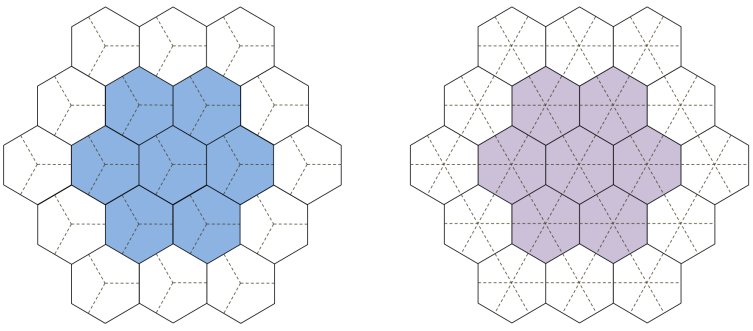

Figure 3.1: Modeled homogeneous network topologies

in one TTI. The addition of this stage is left as future work since the number of active users considered in study is not high.
An important parameter to be defined is the Minimum Coupling Loss (MCL). MCL describes the minimum loss in signals between eNodeB and UE and it is defined as the minimum distance loss including antenna gains measured between antenna connectors [18]. In a macro cell deployment, MCL is set equal to 70 dB for urban area and 80 dB for rural area. With the above definition, the received power in downlink and uplink can be expressed as:

$$P_{RX} = P_{TX} - max\left(pathloss - G_{TX} - G_{RX}, MCL\right) \tag{3.1}$$

Therefore, even the users that are close to the base station will have a signal attenuation at least equal to MCL.
The propagation model that has been adopted is the macro cell propagation model for urban area specified in [18]. The pathloss is expressed as:

$$L(R) = 40\left(1 - 4 \cdot 10^{-3} \cdot Dhb\right) log_{10}R - 18log_{10}Dhb + 21log_{10}f + 80dB \tag{3.2}$$

where Dhb is the base station antenna height measured from the average rooftop level in [m], R is the UE-eNodeB distance in [Km], and f is the carrier frequency in [MHz]. Dhb is set equal to 15 m and f to 2600 MHz.
The shadow fading is modeled by the Claussen model presented in [19]. It generates for every site a lognormal-distributed 2D space-correlated shadow fading map. The parameters of the model are reported in Table 3.1. The number of neighbors indicates the number of pixels

Parameter	Value
Map resolution	5 m/pixel
Number of neighbors	8
Mean	0
Standard deviation	8 dB
Inter-site correlation	0.5
Intra-site correlation	1

Table 3.1: Parameters of the Claussen model for the shadow fading

the algorithm takes into account when the space-correlated maps are generated. Inter-site correlation is the shadow fading correlation between maps of different sites. Similarly, intra-site correlation is the shadow fading correlation between maps of different sectors of the same site. In this case, it is set to 1 indicating that sectors of the same site will have the same shadow fading map.
The fast fading is generated using the Rosa Zheng model [20]. The considered channel models includes the Extended Pedestrian B, for users' speed of 3 km/h, and the Extended Vehicular A, for users' speed of 30 km/h. These models are presented in [21] as extensions of the ITU Pedestrian B and ITU Vehicular A for channels with bandwidth larger than 5 MHz. Table 3.2 summarizes the simulation parameters used.

3.2.2 Antenna Patterns

Three categories of radiation patterns of the sector antennas have been considered in the simulations. The first category follows the antenna pattern equation presented in [18]:

$$A(\theta) = -min\left[12\left(\frac{\theta}{\theta_{3dB}}\right)^2, A_m\right], -180 \leq \theta \leq 180 \tag{3.3}$$

Parameter	Setting
Carrier Frequency	2.6 GHz
System Bandwidth	10 MHz
No. of Subcarriers	600
No. of PRBs	50 (12 Subcarriers/PRB)
Subframe Duration	1 ms (14 OFDM Symbols)
Total eNodeB Transmit Power	46 dBm (1-Tx Antenna)
Transmission Scheme	2x2 OLSM
HARQ Model	Not implemented
Uplink delay	2 TTIs
No. of Sectors per Site	3 or 6
No. of UEs	20 UEs/sector (for 3-sector site) or 10 UEs/sector (for 6-sector site)
Power Delay Profile	Extended Ped-B, Extended Veh-A
Users' speed	3 km/h, 30 km/h
BLER Target	10%
Cellular Layout	Hexagonal grid with 19 sites
Inter-site Distance	500 m
Minimum Coupling Loss	70 dB
Interfering cells	First interfering ring
Simulation Time	100 TTIs

Table 3.2: Main parameters and simulation assumptions

where θ_{3dB} is the half power beamwidth (HPBW) and A_m is the maximum attenuation. Thus, the antenna gain can be expressed as $G(\theta) = A(\theta) + G_m$, where G_m is the maximum antenna gain. Values for these parameters for a 3-sector-site deployment and for a 6-sector-site deployment are reported in Table 3.3.

	θ_{3dB}	A_m	G_m
3-sector	65°	20 dB	15 dBi
6-sector	33°	23 dB	18 dBi

Table 3.3: Parameters of the TR 36.942 antenna radiation pattern

The second category consists of measured horizontal radiation patterns. For the 3-sector-site deployment, the horizontal radiation pattern of the antenna Kathrein 80010622 has been considered for a frequency of 2620 MHz, −45° polarization, and 5° downtilt. For the 6-sector-site deployment, no radiation pattern with HPBW of 33° were available for a frequency of 2600 MHz. Therefore, we adopted the horizontal radiation pattern of the antenna Kathrein 80010251 that has been measured at 2140 MHz, −45° polarization, and 5° downtilt. Data has been provided by [22]. A comparison of the radiation patterns of the first two categories is presented in Figure 3.2.
Finally, the third category consists of 3D radiation patterns. In particular, the horizontal radiation pattern is combined with the vertical radiation pattern in order to obtain a 3D radiation pattern. The same Kathrein antennas of the second category have been considered.

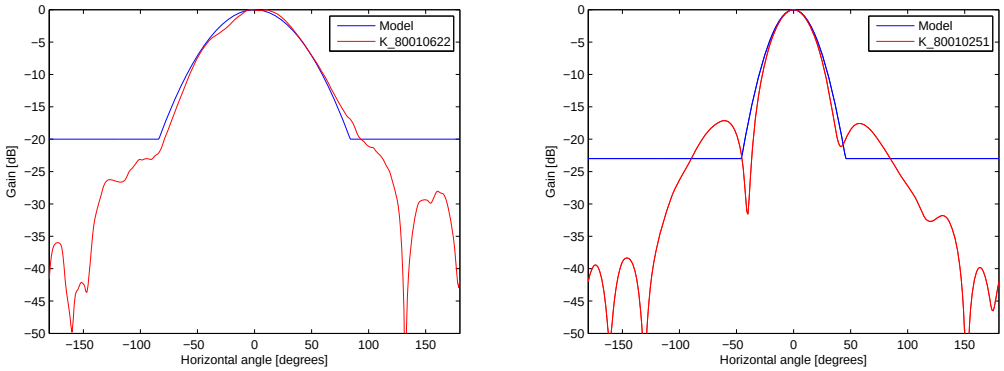

(a) 3-sector site (b) 6-sector site

Figure 3.2: Comparison of adopted radiation patterns

3.2.3 Scenarios

Homogeneous network topologies of 3 and 6 sectors per site have been considered in the first part of the simulation study. All sites are composed of identically sectorized antennas over the assumed cellular network consisting of 19 sites as shown in Figure 3.1. Firstly, we evaluate the performances of a 3-sector-site deployment and a 6-sector-site deployment with different radiation patterns for the sector antennas, i.e. (3.3), 2D, and 3D radiation patterns. Secondly, we evaluate the effect of the parameters of Table 3.3 on the performance of both deployments. Different values of maximum antenna gain, maximum attenuation, and half power beamwidth are considered. The latter parameter helps understanding the effect of the channel dispersion. In fact, channel dispersion can be taken into account in the simulations by considering a wider beamwidth for the sector antenna. Next, we compare the performance of the two deployments with a reuse factor of 1/3. Finally, we evaluate the capacity gain of a 6-sector-site deployment compared with a 3-sector-site deployment under different users' speed, CQI reporting delay, and CQI compression techniques.
In the second part of the simulation study, a mixed network topology with a combination of 3- and 6-sector sites has been considered, as shown in Figure 3.3. The goal of this study is to evaluate if a partial migration to a six sectorized configuration is a viable option to meet high traffic demands in localized areas such as hot spots. The results are presented in paragraph 3.5.

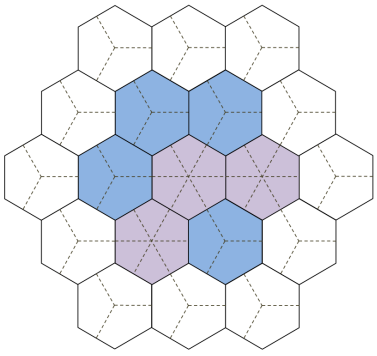

Figure 3.3: Modeled mixed network topology

3.3 Metrics

This section defines the metrics that are used to evaluate the performance of all the scenarios that are considered in this study. Among these metrics, site capacity and capacity gain are defined in a separated paragraph within this section because they are used exclusively for the analysis that is performed in 3.5.6.

- The **Intra-site interference** is defined as the interference that a UE receives from the sectors of the serving site averaged over simulation time and PRBs.

- The **Inter-site interference** is defined as the interference that a UE receives from the sectors of the neighboring sites averaged over simulation time and PRBs.

- **Geometry Factor** is defined as the ratio between the desired received signal power that a UE receives and the total amount of interference plus noise averaged over simulation time. It is expressed as:

$$GF = \frac{1}{TTI_{length}} \sum_{i=1}^{TTI_{length}} \frac{P_{rx}(i)}{P_{int}(i) + P_{noise}(i)} \tag{3.4}$$

  where P_{rx}, P_{int}, and P_{noise} represent the signal power, total amount of interference, and noise that are received at time i, respectively. P_{rx} includes the effect of shadow fading but excludes the fast fading, therefore the GF is constant among the PRBs.

- The **User Throughput** for the uth user is defined as:

$$Th_u = \frac{\text{Total bits correctly received by user } u}{\text{Simulation time}} \tag{3.5}$$

- **Cell-edge throughput** is denoted by Th_{edge} and is defined as the 5%-ile of the User Throughput, i.e. only 5% of the UEs experience a lower average data. It can be expressed as:

$$prob(Th_{user} < Th_{edge}) = 0.05 \tag{3.6}$$

  The cell-edge throughput is used as an indicator to represent the throughput achieved by the users located at the cell-edge, where the experienced inter-site interference is high.

- The **Sector Throughput** is defined as:

$$Th_{sector} = \frac{\text{Total bits correctly delivered}}{\text{Simulation time}} \tag{3.7}$$

  where the numerator is an aggregate of the correctly delivered bits over the simulation time by the sector.

- The **Site Throughput** is defined as the product of the Sector Throughput and the number of sectors within the site.

Site Capacity and Capacity Gain

This paragraph introduces the definitions of site capacity and capacity gain that are used in subsection 3.5.6. We assume that user applications require a throughput of at least 300 Kbps. Below this value, the user's expectations for the application are not satisfied. In order to guarantee a certain level of QoS for the users, service providers are required to offer a throughput higher than 300 Kbps for at least 90% of the users. In other words, the percentage of users with throughput lower than 300 Kbps should be kept below 10%. According to this requirement, *site capacity* is defined as the average site throughput and the average number of UEs in the site, when the percentage of UEs with throughput lower than 300 Kbps is 10%. *Capacity gain* is defined as the ratio of the 6-sector-site capacity and the 3-sector-site capacity. These definitions allow for a fair comparison of the performance of the two deployments because both are evaluated at the same load conditions.

3.4 Results

3.4.1 Performance using different antenna patterns

Figure 3.4, 3.5, and 3.6 show the simulation results achieved in the 3-sector-site and 6-sector-site deployment with the radiation patterns presented in chapter 3.3.2: equation (3.3), Kathrein 2D, and Kathrein 3D, respectively. The comparison of the antenna patterns, as

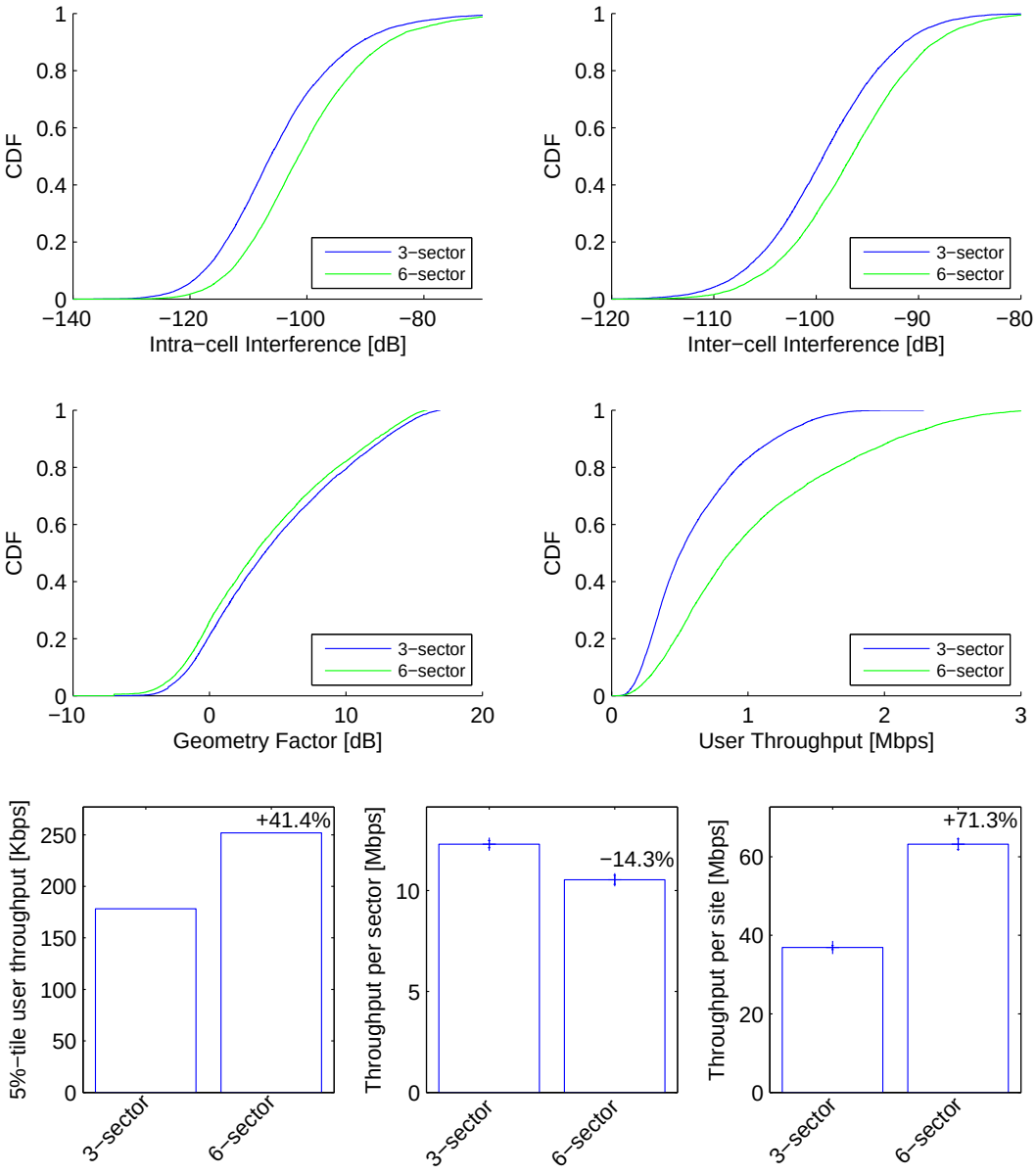

Figure 3.4: Performance with the antenna pattern specified by (3.3)

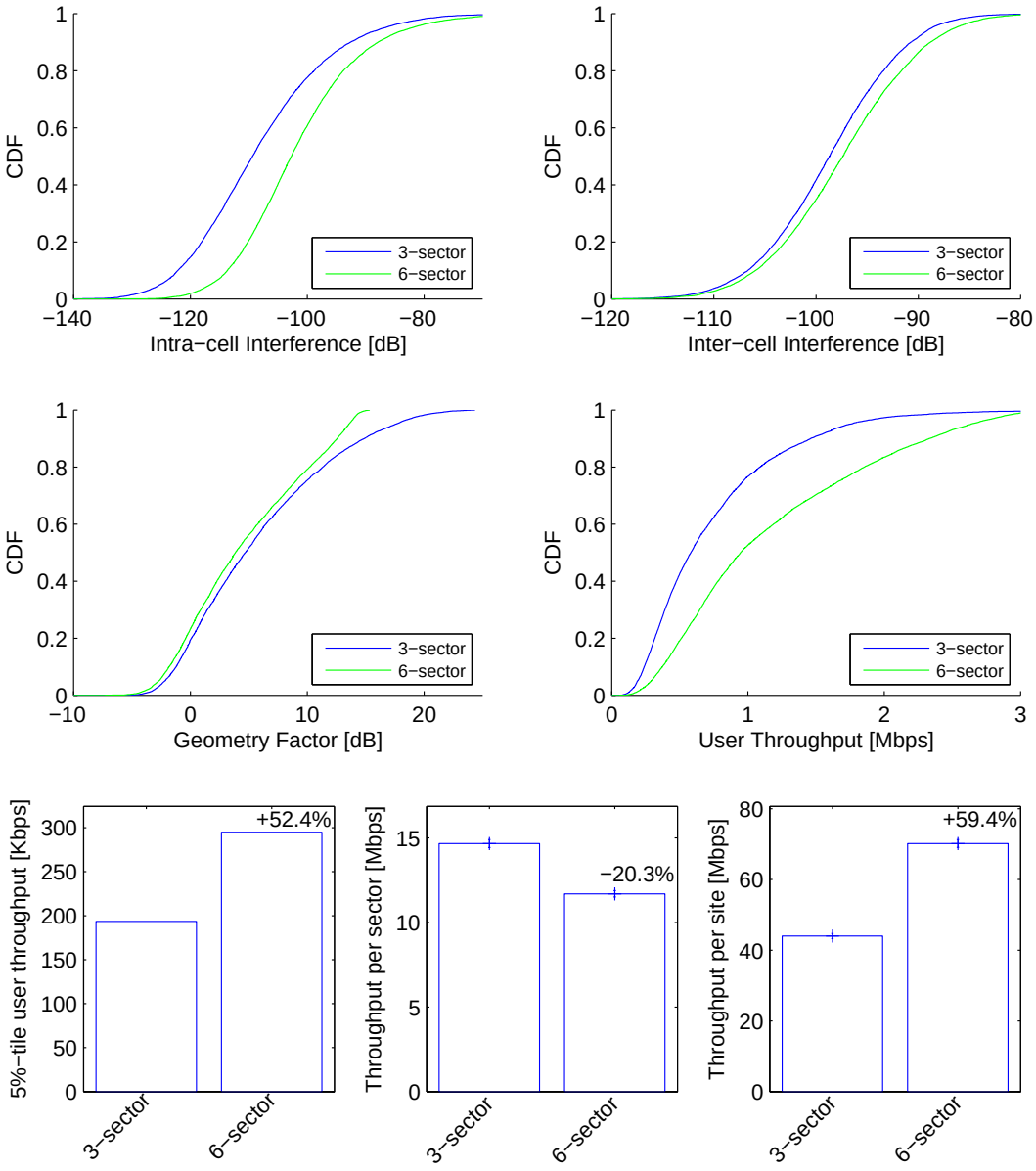

Figure 3.5: Performance with Kathrein 2D antenna pattern

depicted in Figure 3.2, showed that the gap between the 3-sector radiation pattern defined by (3.3) and the realistic pattern of a 3-sector Kathrein antenna is quite different than the gap between a 6-sector radiation pattern defined by (3.3) and the realistic pattern of a 6-sector Kathrein antenna. Consequently, the performance of the two deployments are affected to a different extent by the choice of the antenna radiation pattern among the options of this study. This results in different coverage and throughput gains. However, the comparison of the 3-sector-site with the 6-sector-site deployment reveals a similar trend among the scenarios.

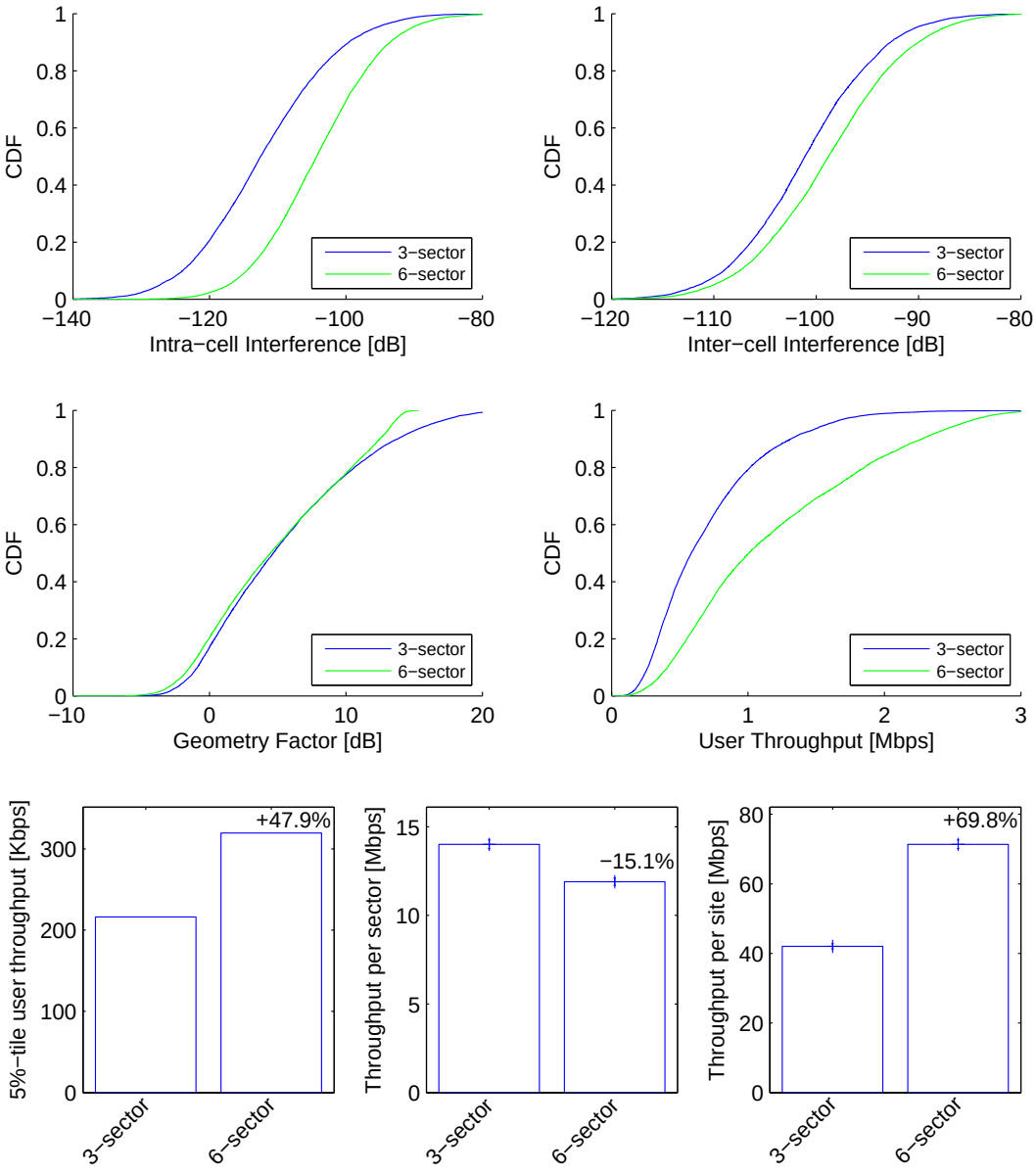

Figure 3.6: Performance with Kathrein 3D antenna pattern

In a 6-sector-site deployment, users experience an higher intra-site and inter-site interference that result in a worse SINR. Therefore, the sector throughput is lower than that of a 3-sector site, and a twice higher site throughput cannot be achieved. From the user point of view, although the resources of a sector are shared among half users than in the 3-sector site, the worse channel conditions prevent to achieve a double user throughput.

3.4.2 Effect of antenna sidelobe attenuation

Figure 3.7 and 3.8 show the simulation results achieved in the 3-sector-site and 6-sector-site deployment, respectively, for different values of antenna sidelobe attenuation. In both cases we considered a sidelobe attenuation of 10 dB and 20 dB lower than the value of Table 3.3. The antenna pattern expressed in (3.3) has been used in these simulations. The magnitude of the antenna sidelobe attenuation affects to a large extent the intra-site interference while only

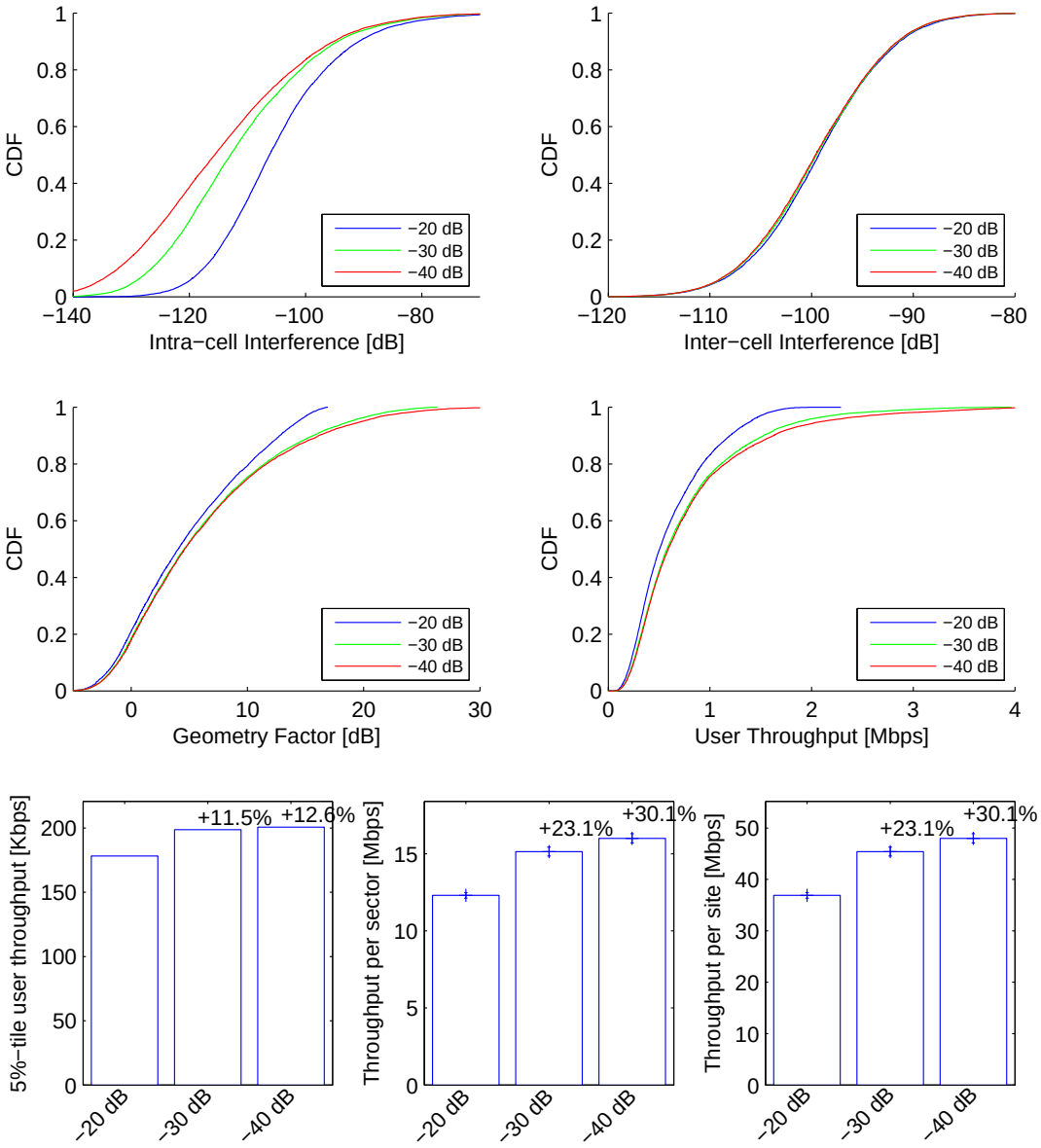

Figure 3.7: Performance of 3-sector site with different values of antenna sidelobe attenuation

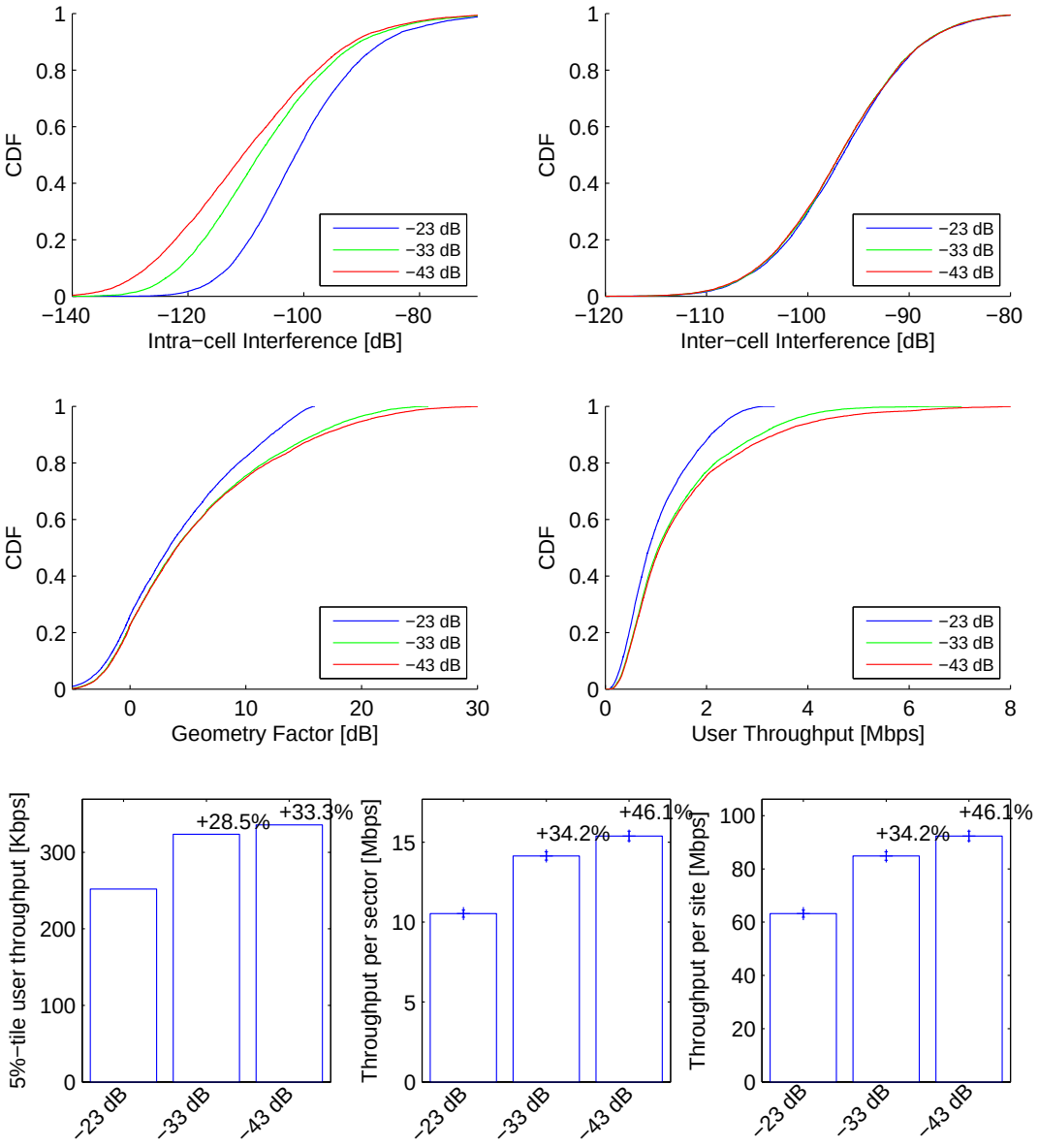

Figure 3.8: Performance of 6-sector site with different values of antenna sidelobe attenuation

slightly affects the inter-site interference. As depicted in Figure 2.1, users are in the sidelobe region of either 1 or 2 sectors in a 3-sector site, and either 4 or 5 sectors in a 6-sector site, therefore the sidelobe attenuation is a dominant factor in the intra-site interference. The lower numbers in both deployments (1 and 4) are experienced by users in the overlapping regions, where the signal of one interfering sector is above the sidelobe level. Since this signal is not affected by the value of the sidelobe attenuation, it becomes the dominant part of the intra-site interference when the sidelobe attenuation is reduced beyond a certain limit. The result is that

beyond that limit the intra-site interference is less influenced by the sidelobe attenuation. The effect is shown in Figure 3.7, where the reduction of the intra-site interference is higher when going from -20 dB to -30 dB than when going from -30 dB to -40 dB. The same effect is shown in Figure 3.8, although with minor intensity. In fact, since the number of interfering sectors in the sidelobe region is higher in a 6-sector site, the interfering sector above the sidelobe level becomes dominant at an higher sidelobe attenuation then in a 3-sector site deployment.
Regarding the inter-site interference, its magnitude is dominated by the signal received from the sectors of other sites that radiate in the direction of the user. Those signals are not affected by the level of sidelobe attenuation and therefore the inter-site interference stays almost constant in the simulations.
The reduction in the intra-site interference results in higher throughputs in both 3-sector-site and 6-sector-site deployment. The effect is stronger in a 6-sector-site deployment due to the higher number of interfering sectors in the sidelobe region.

3.4.3 Effect of maximum antenna gain

Figure 3.9 and 3.10 show the simulation results achieved in the 3-sector-site and 6-sector-site deployment, respectively, for different values of maximum antenna gain. In both cases we consider a maximum gain 3 dB lower and 3 dB higher than the standard value presented in Table 3.3. The antenna pattern expressed in (3.3) has been used in these simulations. In principle, the maximum antenna gain should not affect the simulation results because to an

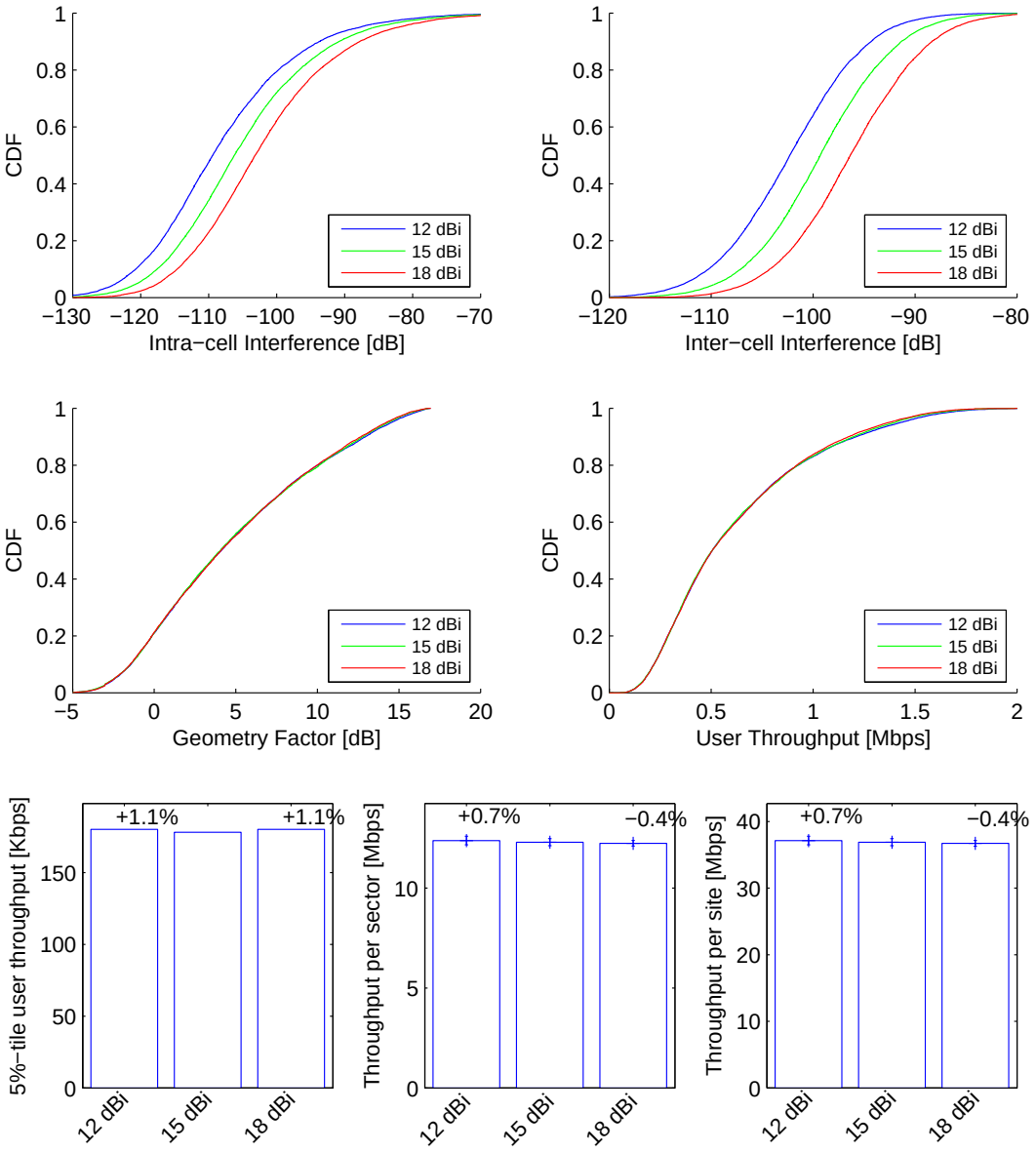

Figure 3.9: Performance of 3-sector site with different values of maximum antenna gain

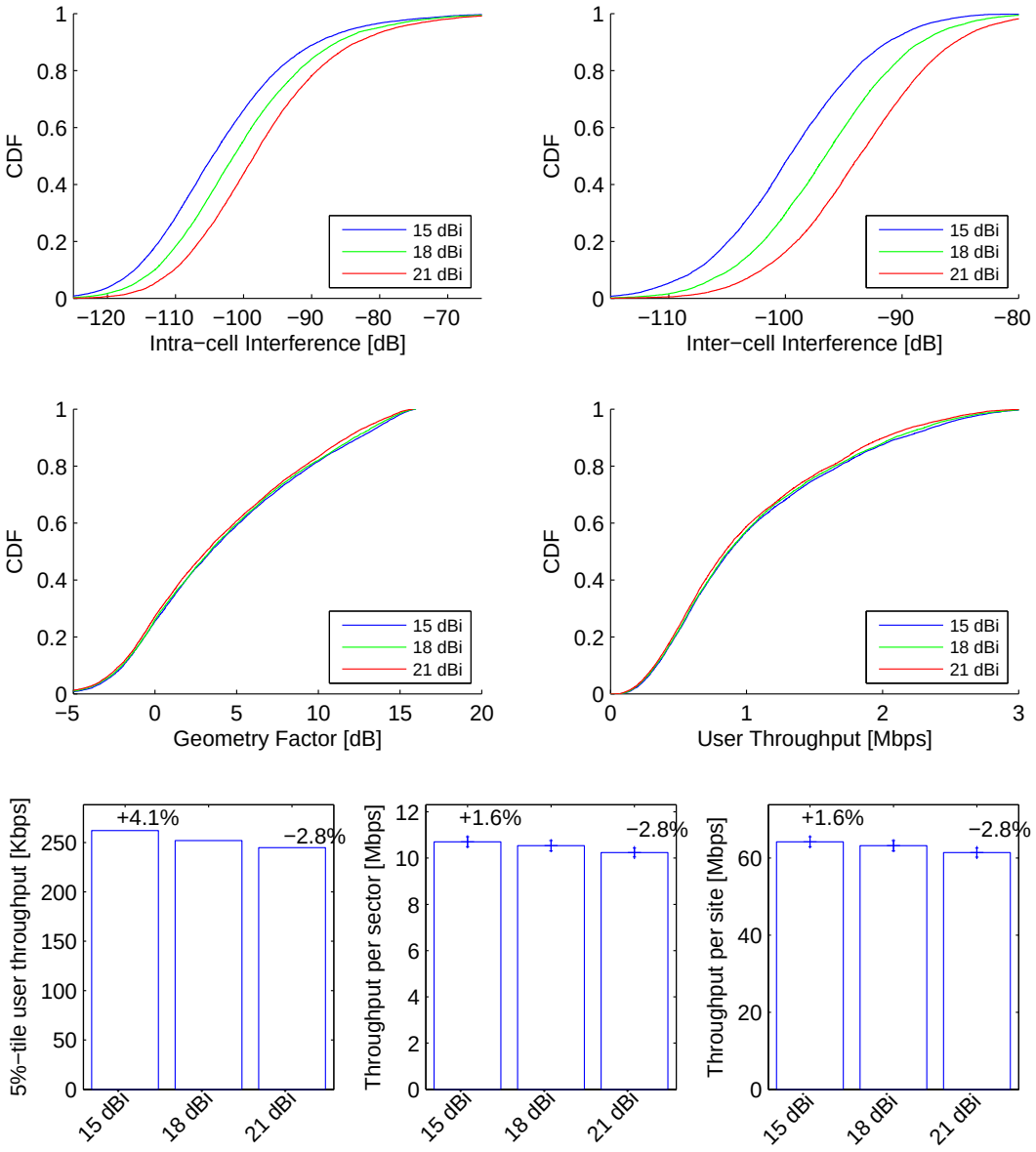

Figure 3.10: Performance of 6-sector site with different values of maximum antenna gain

increase (decrease) of 3 dB in the desired received signal corresponds an increase (decrease) of 3 dB in the received interference, thus the SIR remains constant. However, in both Figure 3.9 and 3.10 we can see that the geometry factor is somehow affected, resulting in a lower throughput for higher maximum antenna gain. The reason is in the parameter Minimum Coupling Loss that describes the minimum loss in signal [dB] between eNodeB and UE and it is defined as the minimum distance loss including antenna gains measured between antenna connectors. If the coupling loss is lower than the Minimum Coupling Loss, it is set to the

Minimum Coupling Loss. Let us consider a situation in which the signal received by a user has a coupling loss equal to the Minimum Coupling Loss. If we increase the maximum antenna gain by 3 dB, both the desired signal and the interference are increased by 3 dB. However, the coupling loss of the desired signal is now 3 dB lower than the Minimum Coupling Loss and it is increased to the Minimum Coupling Loss. As result, the received power of the desired signal is the same as in the case with lower gain while the received interference power is 3 dB higher, resulting in a worse SIR and worse performance.

3.4.4 Effect of channel dispersion

Figure 3.11 and Figure 3.12 show the simulation results achieved in the 3-sector-site and 6-sector-site deployment, respectively, for different values of half power beamwidth (HPBW). In both scenarios, 5 and 10 degrees higher HPBWs than the standard value have been considered in order to take into account different levels of channel dispersion. The antenna pattern expressed in (3.3) has been used in these simulations. The wider the HPBW of the sector

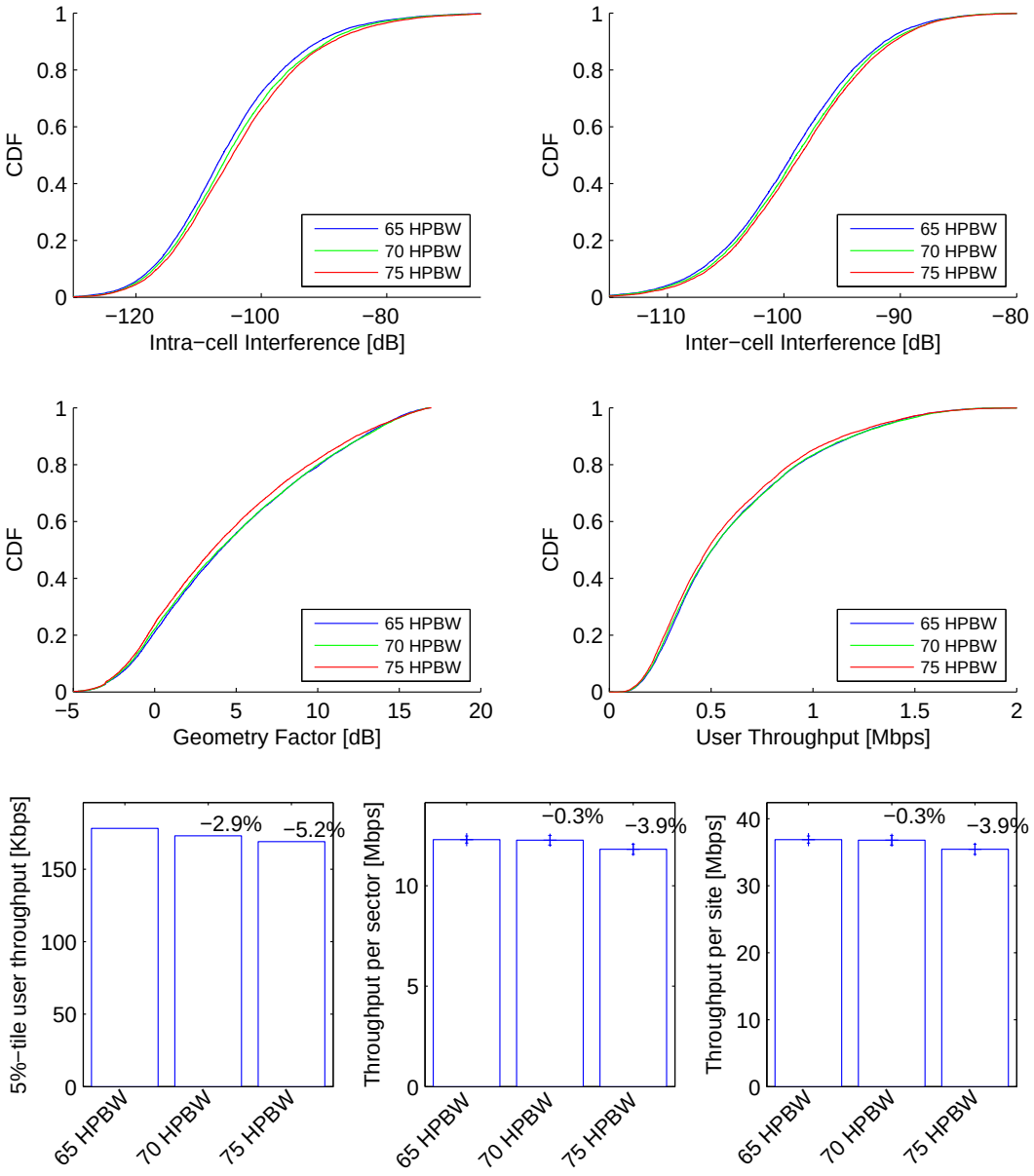

Figure 3.11: Performance of 3-sector site with different values of HPBW

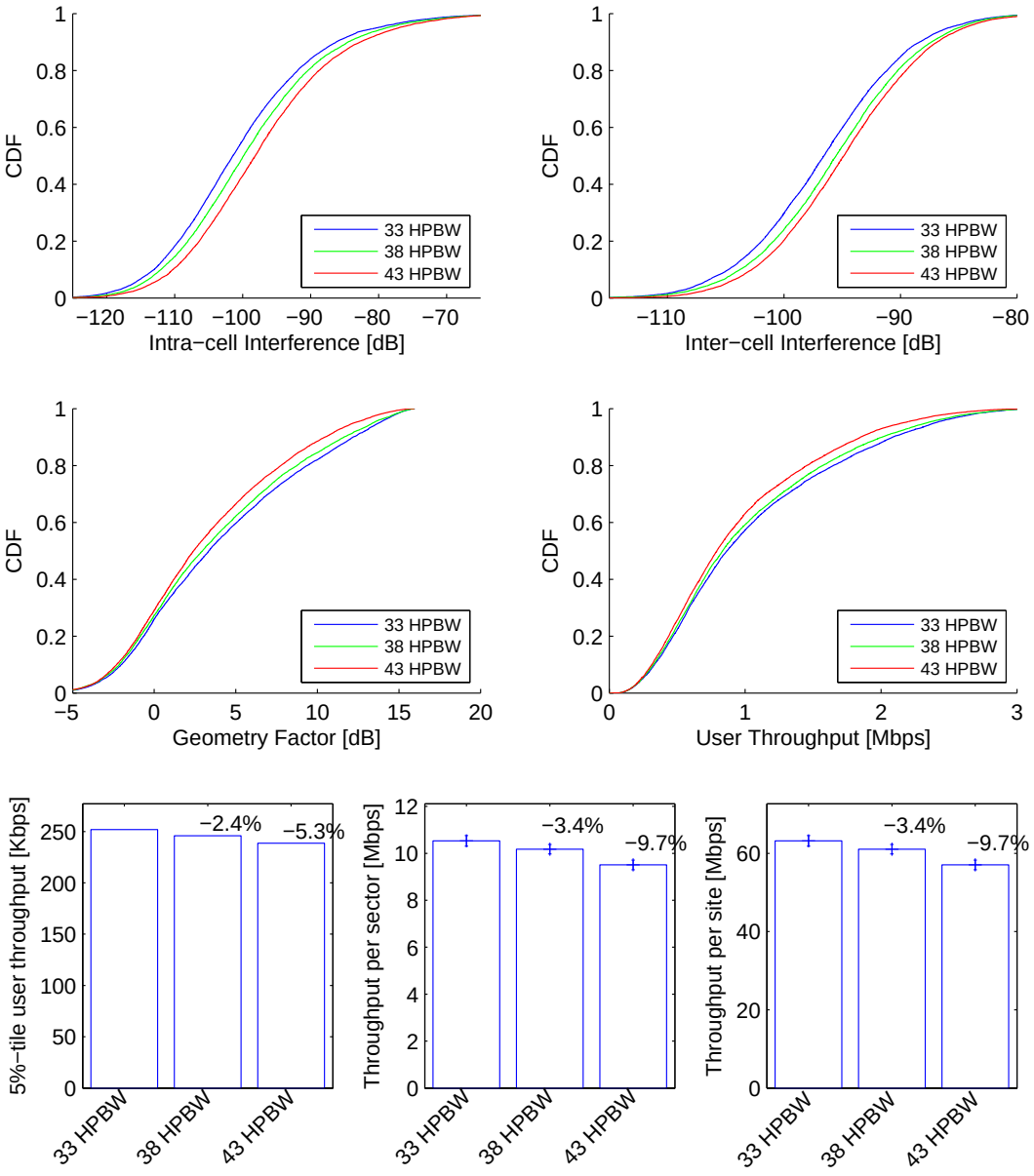

Figure 3.12: Performance of 6-sector site with different values of HPBW

antennas, the wider the overlapping regions between adjacent sectors and therefore the higher the intra-site interference. Further, given a certain direction between a user and an interfering sector of an other site, increasing the HPBW of the sector antenna results in a stronger signal from that sector. Therefore, the inter-site interference is increased too. Higher intra- and inter-site interference cause worse performances in terms of coverage and throughout. The effect is more definite in the 6-sector site deployment because of the double number of interferers.

3.4.5 Performance with a Reuse Factor of 1/3

Figure 3.13 and 3.14 show the simulation results achieved in the 3-sector-site and 6-sector-site deployment, respectively, for a frequency reuse factor of 1/1 and 1/3. The frequency reuse factor 1/1 indicates that each sector can use all the 50 available PRBs, while the frequency reuse factor 1/3 indicates that each sector can use only one third of the available PRBs. More specifically, the first 16 PRBs are assigned to sectors 1 and 4, the second 16 PRBs to sectors 2 and 5, and the last 18 PRBs to sectors 3 and 6. Although the resources per sector are reduced

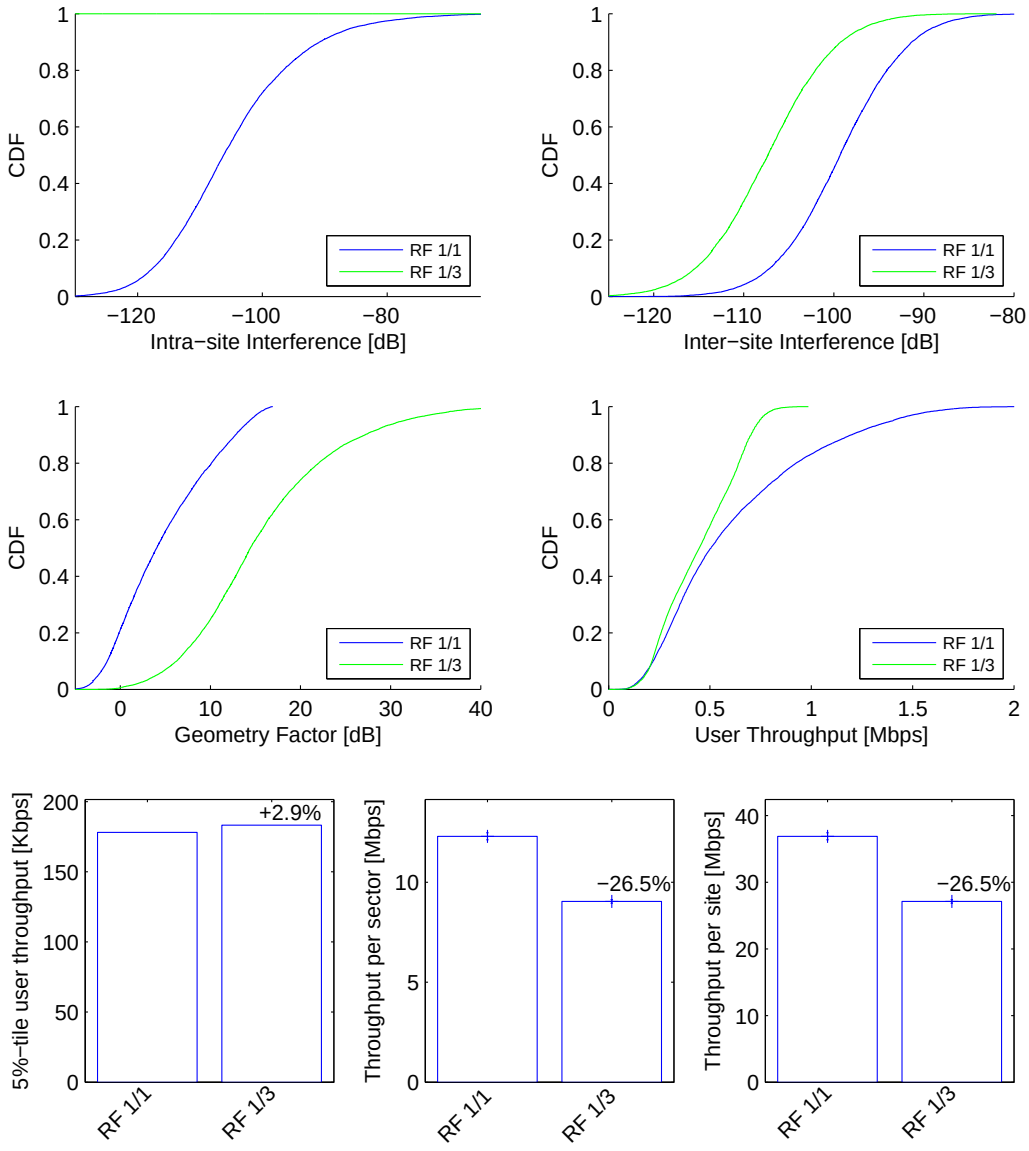

Figure 3.13: Performance of 3-sector site with frequency reuse factors of 1/1 and 1/3

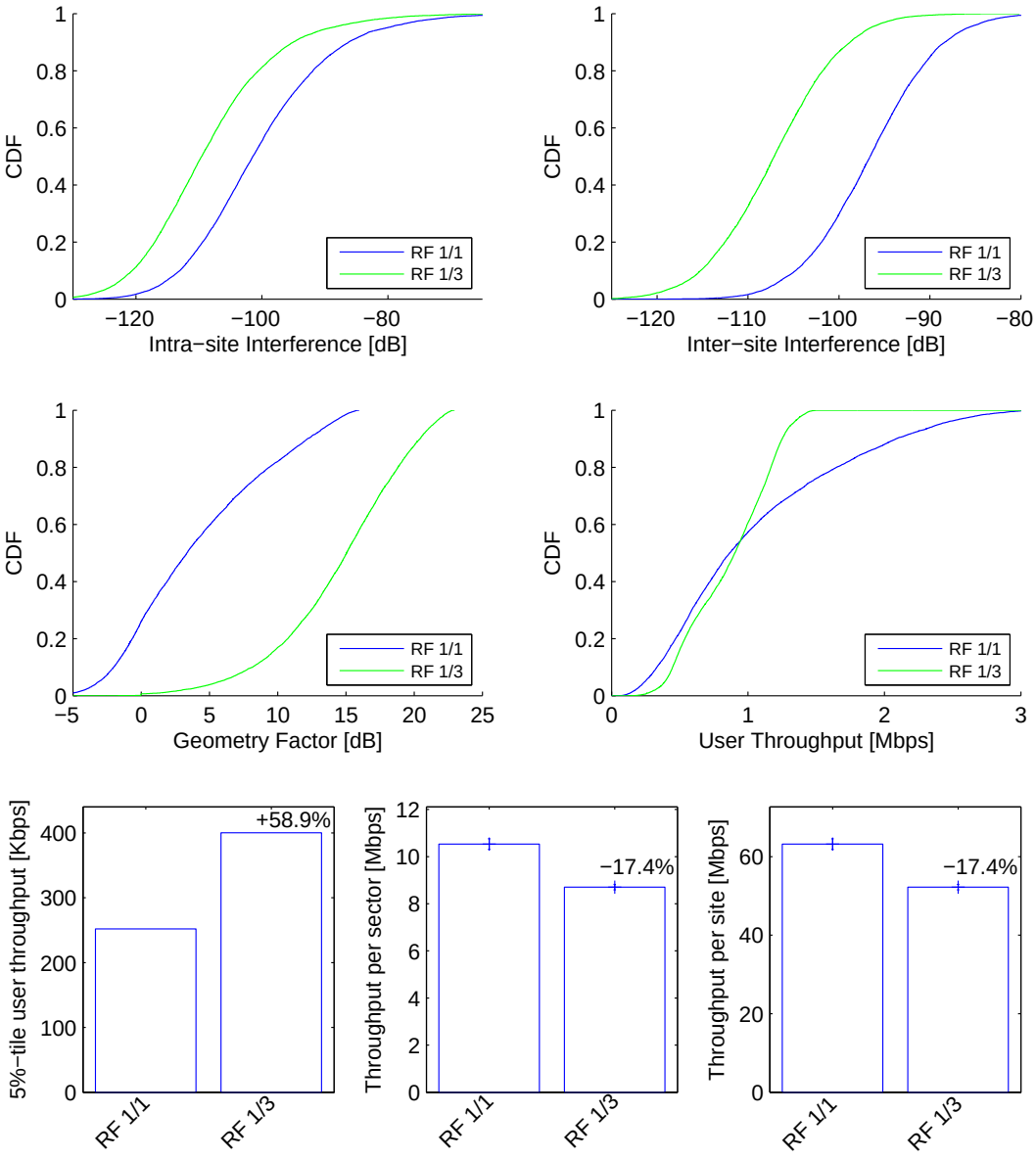

Figure 3.14: Performance of 6-sector site with frequency reuse factors of 1/1 and 1/3

by a factor of three, we observe a reduction in the site throughput of only 26.5% and 17.4% in the two deployments, respectively. Further, the 5%-tile user throughput is improved by 2.9% in the 3-sector-site deployment and by 58.9% in the 6-sector-site deployment. The reason is the intelligent allocation of frequencies among the sectors that consistently reduces the amount of intra-site and inter-site interference. The effect is stronger in the six sectorized configuration where the frequency reuse factor 1/3 can even be thought as a technique to increase the cell-edge coverage at the cost of a reasonable reduction of site throughput. Finally, it is worth

noting that, due to the lower availability of resources, the peak user throughput is reduced with a frequency reuse factor of 1/3.

3.4.6 Capacity gain evaluation

This section evaluates the capacity gain of the 6-sector-site deployment compared to the 3-sector-site deployment. The capacity gain is calculated as the ratio between the capacities of the 6-sector site and the 3-sector site. Site capacity, in turn, is defined as the site throughput and the number of active UEs in the site when the user throughput is lower than 300 Kbps for 10% of the active UEs. The constraint on the user throughput has been added to the definition of site capacity in order to compare the two deployments under the same load conditions. Four scenarios are considered with different users' speeds, CQI compression techniques, and feedback delays. The parameters are summarized in Table 3.4.

Scenario	**Users' speed**	**CQI compression scheme**	**Uplink delay**
1	3 km/h	uncompressed	2 TTI
2	30 km/h	uncompressed	2 TTI
3	3 km/h	wideband	2 TTI
4	3 km/h	uncompressed	4 TTI

Table 3.4: Scenarios for the capacity gain

In the uncompressed scheme, the CQI feedback consists of one CQI value for each PRB, while in the wideband scheme, the CQI feedback consists of one single value calculated as the average CQI among the PRBs. The feedback delay corresponds to the delay between the time the user measures and generates the feedback information and the time the base station uses these information for scheduling and link adaptation. Each scenario has been simulated with different numbers of users per site equally distributed among the sectors. The results are collected in Figure 3.15 and are expressed in terms of site throughput and percentage of users with throughput lower than 300 Kbps as functions of the number of users per site. Site capacities are found in correspondence of the percentage equal to 10% and are shown in Table 3.5 along with the capacity gains.

Scenario ID	**3-sector site capacity**	**6-sector site capacity**	**Capacity Gain**
1	44 UEs 37.56 Mbps	72 UEs 64.86 Mbps	1.64 1.73
2	20 UEs 18.22 Mbps	36 UEs 34.45 Mbps	1.80 1.89
3	24 UEs 24.80 Mbps	39 UEs 44.10 Mbps	1.63 1.78
4	39 UEs 33.19 Mbps	62 UEs 58.10 Mbps	1.59 1.75

Table 3.5: Summary of site capacities and capacity gains

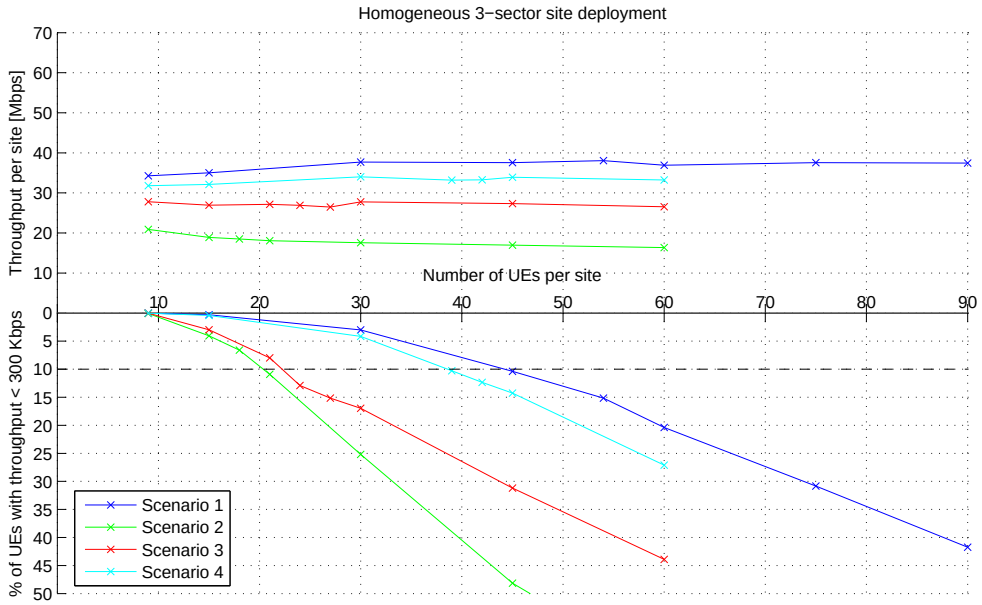

(a) Site capacity of a 3-sector site in the four scenarios

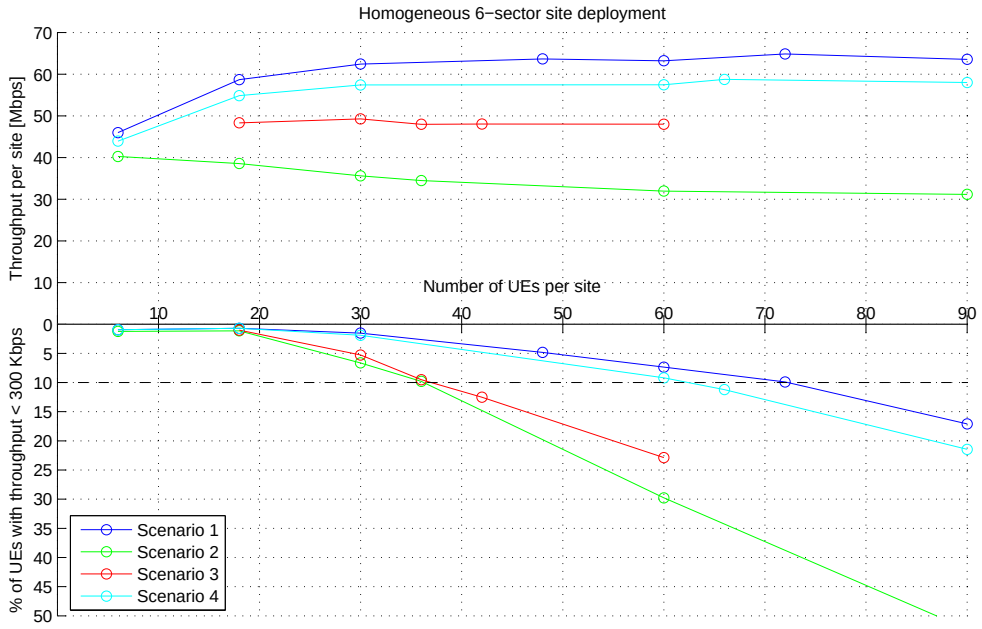

(b) Site capacity of a 3-sector site in the four scenarios

Figure 3.15: Site capacity in the four scenarios

Effect of users' speed

Downlink packet scheduling and link adaptation are based on the CQIs that are reported by the active users every sub-frame. More specifically, assuming a feedback delay of 2 ms, the scheduling decisions and the link adaptation for the current sub-frame are based on the channel conditions that were measured by the users 2 sub-frames ago. Due to user mobility and fast fading, the channel conditions may change considerably over a short period of time,

so the scheduling and link adaptation may use outdated information. The first consequence is that users may be allocated in PRBs that were favorable 2 sub-frames ago but that are not favourable now, or vice versa, resulting in lower spectral efficiency. Secondly, the modulations and coding schemes, that are chosen to provide a block error rate (BLER) below 10% with the channel conditions of 2 sub-frames ago, may result in BLER above 10% if the current channel conditions are worse. Note that, if the users' speed is low, the channel conditions change slowly over time, so the information reported at the base station are still valid and the BLER is successfully kept below 10%. However, as the users' speed increases, the channel conditions change more quickly and the link adaptation may fail to keep the BLER below 10%. This is shown in Table 3.6.

	3-sector-site	6-sector-site
3 km/h, 5 UEs/sector	2.09%	1.95%
3 km/h, 10 UEs/sector	3.88%	3.42%
30 km/h, 5 UEs/sector	49.06%	46.68%
30 km/h, 10 UEs/sector	58.94%	56.16%

Table 3.6: Values of BLER for different users' speeds and numbers of users per sector

The higher BLER for users' speed of 30 km/h is the reason of the lower site capacities achieved in scenario 2 compared to scenario 1. It clearly indicates that yet at speed of 30 km/h, the frequency domain packet scheduler and the link adaptation fail to deliver the hoped performance. In addition, Table 3.6 shows that the BLER increases when the number of users per sector increases. This is the reason for the decreasing slope of the site capacities of scenario 2 in Figure 3.15. Finally, the BLER is lower in the 6-sector-site deployment compared to the 3-sector-site deployment. Therefore, the capacity of a 6-sector site is less affected by the users' speed. In fact, as shown in Table 3.5, compared to scenario 1, the maximum number of UEs that can be allocated in a site is 55% lower for the 3-sector site and 50% lower for the 6-sector site, while the site throughput is reduced by 51% in the 3-sector site and by 47% in the 6-sector site. As a consequence, the capacity gains obtained in scenario 2 are higher. In order to give an explanations to the dependencies of the BLER to the number of users per sector and to the number of sectors, we evaluate the difference between the SINR of the TB[2] calculated two subframe ago, and the current SINR of the TB:

$$\Delta(n) = SINR_{TB}(n) - SINR_{TB}(n-2) \tag{3.8}$$

Respectively, $SINR_{TB}(n)$ is the TB's SINR in subframe n, while $SINR_{TB}(n-2)$ is the TB's SINR in subframe $n-2$ that is used to select the modulation and coding scheme of the TB in subframe n. If $\Delta(n)$ is zero, the BLER will be equal to the one expected, i.e. below 10%. If $\Delta(n)$ is positive, the BLER will be lower than expected because the channel conditions are improved. If $\Delta(n)$ is negative, the BLER will be higher than expected because the channel conditions are worse. Note that, since the MCSs are selected to keep the BLER below 10%, a high positive Δ can result in 10% lower BLER, the most, while, a high negative Δ can result in a 90% higher BLER, the most. The mean and standard deviation of Δ are reported in

[2]Transport block (TB) refers to the set of PRBs that are assigned to one user in one subframe. Even though the user indicates a different CQI for each PRB, and so in principle a different modulation can be used for each PRB to maximize the spectral efficiency, LTE specifies that the same modulation must be used for all PRBs of one TB. Therefore, the SINRs of each PRB that forms the TB are mapped to an equivalent SINR using the MIESM algorithm (see Appendix C). Finally, the SINR of the TB is used to select the modulation and coding scheme that provides a BLER lower than 10%.

Table 3.7 for different users' speeds and numbers of users per sector.

	3-sector-site	6-sector-site
3 km/h, 5 UEs/sector	(-0.024,0.162) dB	(-0.026,0.147) dB
3 km/h, 10 UEs/sector	(-0.04,0.19) dB	(-0.03,0.16) dB
30 km/h, 5 UEs/sector	(-1.34,1.42) dB	(-1.25,1.29) dB
30 km/h, 10 UEs/sector	(-1.70,1.70) dB	(-1.54,1.50) dB

Table 3.7: Values of $(\mu_\Delta, \sigma_\Delta)$ for different users' speeds and numbers of users per sector

We note that:

- When the users' speed increases, $|\mu_\Delta|$ and σ_Δ increase as well. This indicates that $SINR_{TB}$ fluctuates more over time. Hence, the BLER is higher.
- When the number of users decreases, $|\mu_\Delta|$ and σ_Δ decrease as well. Therefore, the variation of $SINR_{TB}$ over time is smaller and the BLER lower. In fact, the lower the number of users per sector, the higher the number of PRBs that are assigned to the user's transport block. Hence, the SINR variations of the single PRBs are compensated by the fact that the $SINR_{TB}$ is calculated over a wider range of PRBs.
- When the number of sectors per site is doubled from 3 to 6, $|\mu_\Delta|$ and σ_Δ slightly reduces. This indicates that in the 6-sector-site deployment, $SINR_{TB}$ fluctuates slightly less than in the 3-sector-site deployment. Consequently, the BLER is lower. Excluding all factors that do not affect the variation of $SINR_{TB}$, we found that the reason for this phenomenon is the higher number of interfering sectors. In fact, while the interfering power per PRBs in the 3-sector-site deployment is calculated as the sum of the powers that are received from 20 interfering sectors, in the 6-sector-site deployment, the interfering power is calculated as the sum of 41 interfering sectors. Intuitively, the wider sum results in a more stable interfering power, i.e. a more stable SINR per PRB, i.e. a more stable $SINR_{TB}$.
- μ_Δ is negative, so it is more likely that the current $SINR_{TB}$ is worse than the $SINR_{TB}$ of 2 subframes ago. The reason is attributable to the frequency-domain proportional fair scheduler. In fact, the PRBs that are assigned to the user's TB are the ones with higher SINR. Hence, it is more likely that the SINR worsens than improves.

In short, the 6-sector-site deployment is less affected by the users' speed than the 3-sector-site deployment. Therefore, the capacity gains obtained in scenario 2 are higher than scenario 1.

Effect of CQI compression technique

The choice of the CQI compression technique has a heavy impact on the site capacities of both deployments. With the uncompressed technique the frequency-domain proportional fair scheduler takes fully advantage of the frequency selectivity of the channel by assigning each PRB to the user that can maximize the throughput for that PRB. On the other hand, with the wideband technique, the scheduler has no information on the frequency selectivity of the channel at the user side because the CQI is the same for all the PRBs. Consequently, the uncompressed technique results in superior performance. However, there is a trade-off between performance and uplink overhead because the uncompressed technique requires 50 values of CQI per user every sub-frame, while the wideband technique requires only 1 value of CQI per user every sub-frame. The CQI compression techniques considered in this study are the two extremes of the trade-off. Several techniques that aim to achieve a compromise between

performance and uplink overhead can be found in literature.
It is worth to note that for the wideband scheme scenario, only one user is scheduled per sub-frame. In fact, since the CQI value of each user is constant for all the PRBs, if one user maximizes the scheduling metric for one PRB, it will do so for all the other PRBs, so either it gets all the PRBs or none.

Effect of feedback delay

When the feedback delay is increased, the scheduling decisions and the link adaptation are based on more outdated channel information. Therefore, the BLER is higher and the site capacity lower. Since we considered a low users' speed for scenario 4, a doubled feedback delay results in only 10-15% reduction in the site capacity of both deployments.

3.4.7 Performance in a mixed network topology

As shown in Figure 3.3, the mixed network is derived from the homogeneous 3-sector-site deployment by upgrading three sites to a six sectorized configuration. We denote the upgraded sites as *Hotspot* sites, while the other four sites as *Other* sites. In this section we evaluate the performance improvement achieved in the *Hotspot* sites, and the performance degradation, if any, achieved in the *Other* sites. The results are showen in Figure 3.17 and 3.17. The

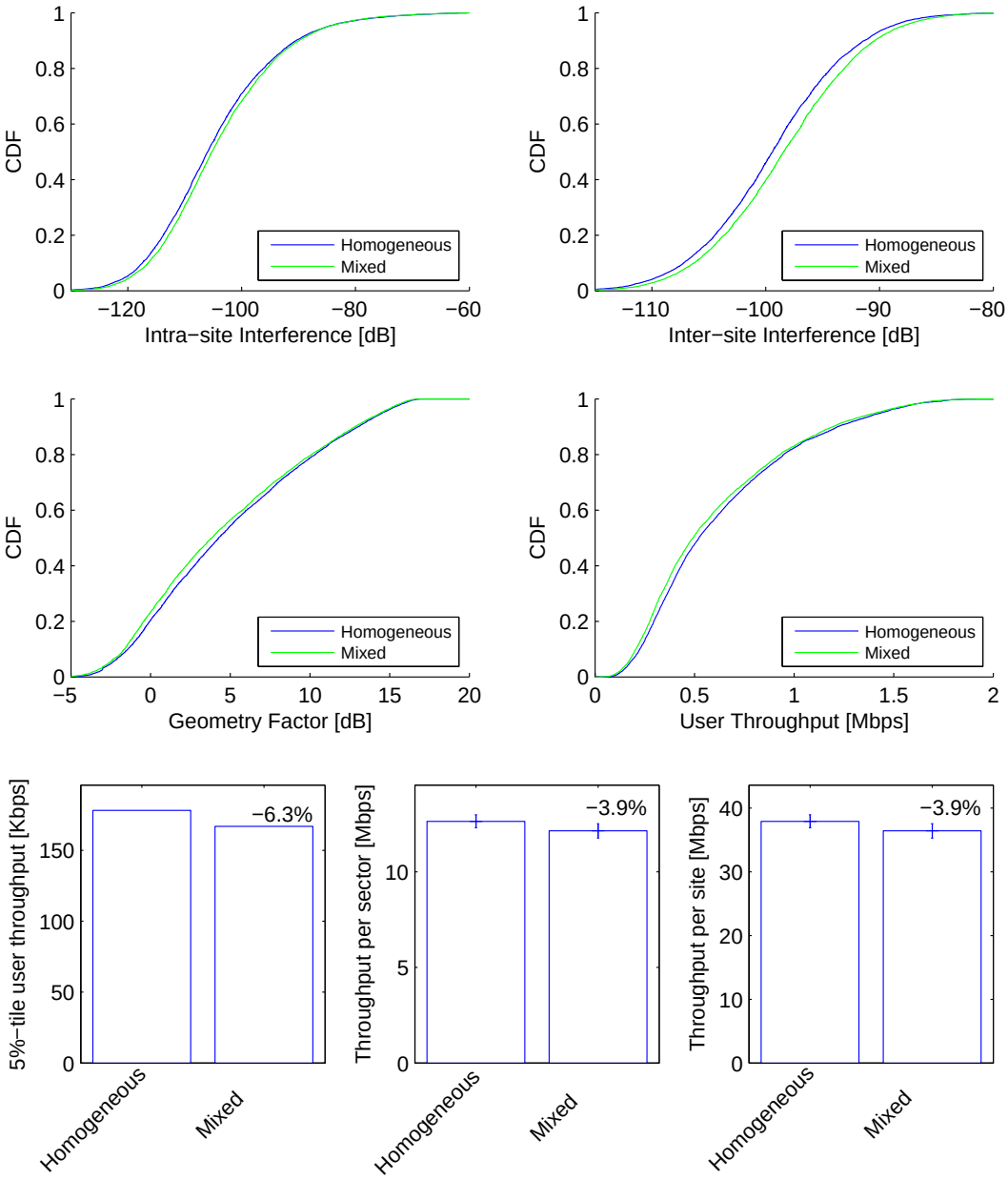

Figure 3.16: Performance of *Other* sites in the homogeneous and mixed network topologies

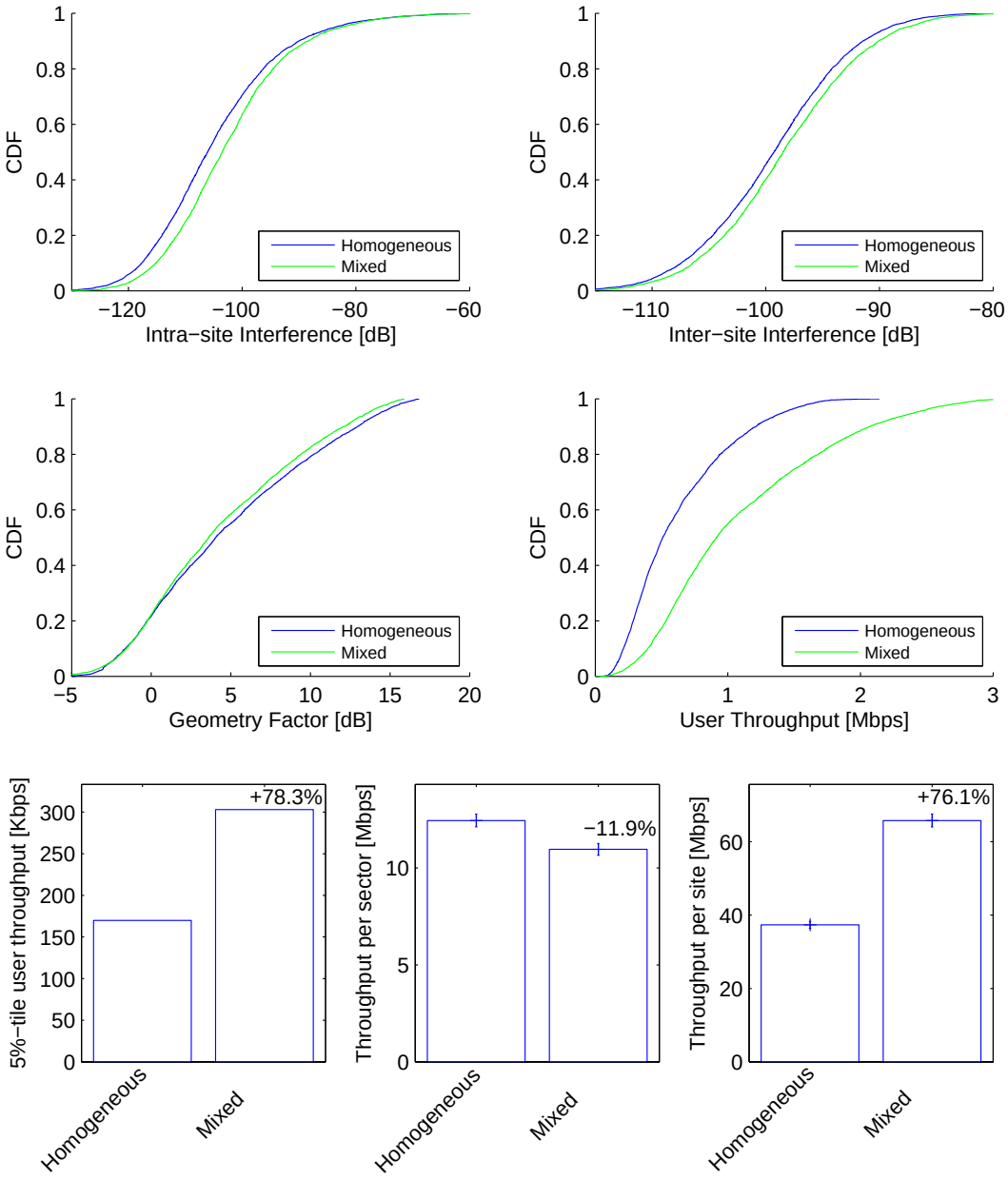

Figure 3.17: Performance of *Hotspot* sites in the homogeneous and mixed network topologies

performance of the *Other* sites are affected by the different coverage of the *Hotspot* sites that results in higher interference. However, site throughput and cell-edge coverage are only slightly reduced. On the other hand, the *Hotspot* site upgrade results in site throughput and cell-edge coverage gains of 76.1% and 78.3%, respectively. Therefore, a six sectorized configuration is able to enhance the performance of congested hotspots at the cost of a slightly performance degradation in the surrounding sites.

3.5 Summary

In this chapter we introduced the LTE System Level simulator that has been used to evaluate the performance of a 3-sector and a 6-sector site. We presented the additional capabilities that have been implemented in this project along with the simulation setup, the metrics that have been adopted, and the simulation results.
The results of paragraph 3.5.1 shown that users experience a higher intra-site and inter-site interference in a 6-sector site deployment than in a 3-sector site deployment due to wider overlapping regions, higher number of interferers, and stronger sidelobes, resulting in worse channel conditions. Therefore, the sector throughput is lower than that of a 3-sector site and the site throughput cannot be as high as twice the one of a 3-sector site. From the user side, although the resources of a sector are shared among half the number of the users, the worse channel conditions prevent to achieve a double user throughput.
In paragraphs 3.5.2, 3.5.3, and 3.5.4 we evaluated the performance of a 3-sector-site and a 6-sector-site deployment with different values of sidelobe attenuation, maximum antenna gain, and HPBW, respectively. The value of the sidelobe attenuation affects to a large extent the intra-site interference while only slightly affects the inter-site interference. A higher sidelobe attenuation results in a lower intra-site interference and consequently better performance. For the same increase in sidelobe attenuation, we observed an higher performance gain in the 6-sector-site deployment. Regarding the maximum antenna gain, the performance of both deployments are only slightly affected by a variation of this parameter. Finally, we observed that increasing the HPBW, the performance of both deployments will be worse due to the higher intra-site and the inter-site interference. For the same amount of channel dispersion we observed a stronger site throughput degradation in the 6-sector-site deployment, while the cell-edge throughput degradation is similar. In particular, for a channel dispersion of 10 degrees the site throughput is reduced by 3.9% in the 3-sector site and by 9.7% in the 6-sector site, while the cell-edge throughput is reduced by 5.2% and 5.3% respectively.
In paragraph 3.5.5 we evaluated the performance achieved with a frequency reuse factor of 1/3. The results shown that this allocation of resources among the sectors of a site consistently reduces the amount of interference. Thus, although the resources per sector are reduced by a factor of 3, the reduction of the site throughput is only 26.5% in the 3-sector-site deployment and 17.4% in the 6-sector-site deployment. Further, the cell-edge coverage is improved by 2.9% and 58.9%, respectively. Therefore, a frequency reuse factor of 1/3 can be thought as a technique to increase the cell-edge coverage in a 6-sector-site deployment at the cost of a reasonable reduction of site throughput and peak user throughput.
In paragraph 3.5.6 we determined the site capacity and the capacity gain of a 6-sector site compared to a 3-sector site. The results shown that a 6-sector site deployment is able to allocate 59% to 80% more users and offer a 73% to 89% higher site throughput, depending on the users' speed, CQI compression techniques, and uplink feedback delay.
Finally, in paragraph 3.5.7, we investigated the performance of a mixed network topology where a cluster of three sites is upgraded to a 6-sector configuration while the remaining sites are kept to a 3-sector configuration. The results shown that the 6-sector solution improves the cell-edge throughput by 78.3% and the site throughput by 76.1% while the performance of the surrounding 3-sector sites are only slightly affected.
In this simulation study we do not take into account the performance degradation due to handovers. Since the number of handovers is expected to be higher in a 6-sector-site deployment, this factor may play an important role in determining the capacity gain. Therefore, we will evaluate this effect in the measurement study. We will also measure the performance difference

between static and mobile users and between indoor and outdoor users. We will verify that in a 6-sector site the channel conditions and the sector performance are worse than in a 3-sector site. Further, the site throughput gain will be measured and compared with the ones obtained in the simulations. This allows us to determine whether the propagation models used in the simulator are correct or need to be designed again.

Chapter 4

Test Cases for the Measurements Study

4.1 Introduction

The goal of the measurements study is to determine the capacity gain, in terms of DL throughput, that can be achieved in a 6-sector site compared to a 3-sector site. Two different scenarios are investigated. The first scenario considers static users only and is denoted as *static scenario*. The second scenario considers both static and mobile users and is denoted as *mixed scenario*. The measurements will be performed in the KPN FUP network in Utrecht and are divided in four experiments. The first two experiments will determine the DL throughput of a 3-sector site in the static and mixed scenarios, while the second two experiments will determine the DL throughput of a 6-sector site in the static and mixed scenarios, respectively. The capacity gain for the static and for the mixed scenario will be calculated as the ratio of the 6-sector-site DL throughput and the 3-sector-site DL throughput.
Because of a delay in the construction of the FUP network, the measurements could not be executed. Nevertheless, this chapter includes the FUP configuration and the experiments' descriptions to allow the execution of the measurements in a follow-up project in KPN.

4.2 LTE Friendly User Pilot Network

4.2.1 Radio Access Network Configuration

The initial configuration of the FUP in Utrecht consists of four sites with three sectors each, as shown in Figure 4.1. The antenna configuration of each site and the connections to the backhauling network are summarized in Table 4.1. This configuration is used for the first two experiments that take place on site 2754.
After the completion of the first two experiments, site 2754 will be upgraded to a six sectorized configuration reported in Table 4.2. The upgrade consists of the replacement of the existing three Kathrein 80010541 antennas with six Tongyu TDJ-232720DE-33P antennas, the installation of a second FSME System Module, two additional FRHA Flexi RF Modules, a second transmission link, and the installation of the required additional power modules and connections. The upgrade of site 2754 is depicted in Figure 4.2. Sites 4618, 4619, and 8838 will remain with three sectors, as shown in Figure 4.3. This configuration is used for the last two experiments, that will take place on sector 1 and 2 of site 2754.

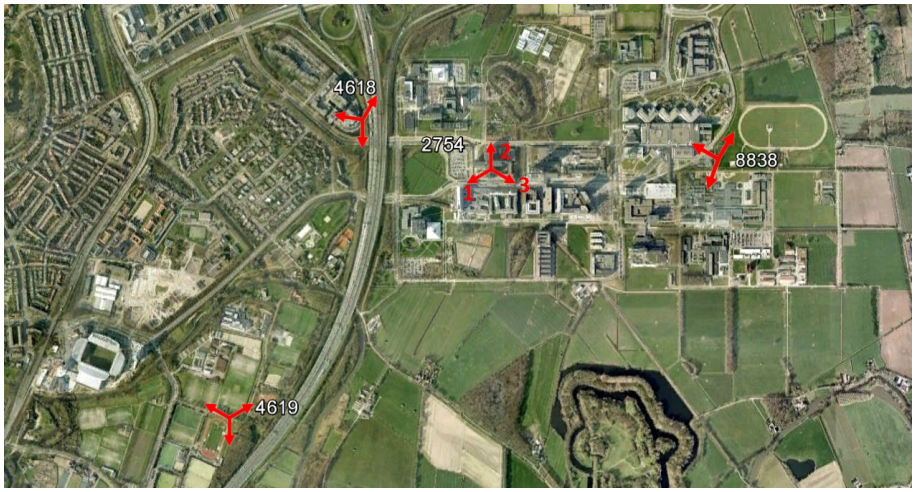

Figure 4.1: RAN layout for experiment 1 and 2

Site Number	Configuration
2754	3x Kathrein 80010541 (single-band LTE) Height 49.7 m with azimuth 0°/120°/240° 1x 50 Mbps Fixed Transmission Link
4618	3x Kathrein 80010544 (dual-band UMTS/LTE) Height 27.9 m with azimuth 30°/180°/280° 1x 50 Mbps Fixed Transmission Link
4619	3x Kathrein 80010541 (single-band LTE) Height 30 m with azimuth 60°/180°/300° 1x 50 Mbps Fixed Transmission Link
8838	3x Kathrein 80010544 (dual-band UMTS/LTE) Height 39 m with azimuth 30°/200°/300° 1x 50 Mbps Fixed Transmission Link

Table 4.1: RAN configuration for experiment 1 and 2

Site Number	Configuration
2754	6x Tongyu TDJ-232720DE-33P (single-band LTE) Height 49.7 m with azimuth 0°/60°/120°/180°/240°/300° 2x 50 Mbps Fixed Transmission Link

Table 4.2: RAN configuration update for experiment 3 and 4

Note that in the 6-sector configuration, site 2754 acts as two independent 3-sector eNodeBs located in the same site. We chose to connect sector 1 (at 180°) and sector 2 (at 240°) to two different system modules. Although the handovers between sector 1 and 2 are inter-site handovers instead of intra-site handovers, this choice was necessary because if both sectors were connected to the same system module, the transmission link capacity of 50 Mbps shared among the two sectors would be a bottleneck for the experiments. Further, we do not expect a sensible difference in performance between intra-site and inter-site handovers that would affect the results of the experiments.
The system bandwidth is 10 MHz and the transmission mode is Dynamic Open Loop MIMO,

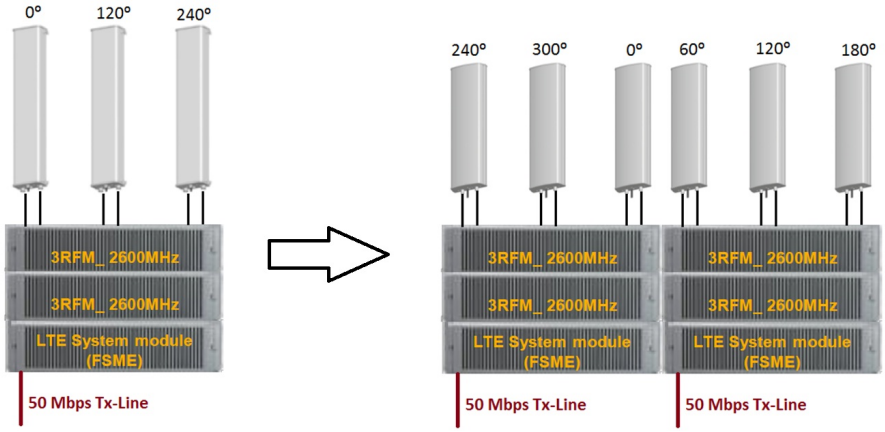

Figure 4.2: Upgrade of site 2754 for experiments 3 and 4

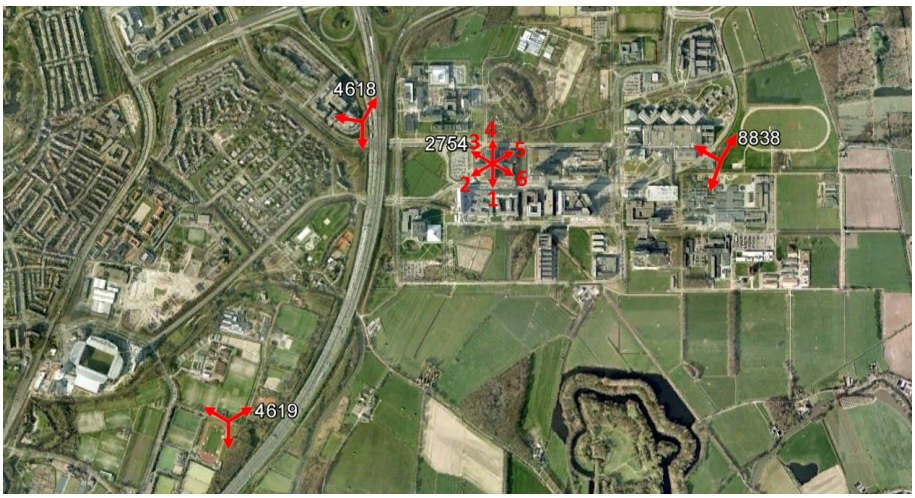

Figure 4.3: RAN layout for experiment 3 and 4

i.e. either transmit diversity or spatial multiplexing depending on the radio conditions. Site 4618 and site 8838 are equipped with dual-band UMTS/LTE antennas. They use the same antenna directions as UMTS that are optimized for the locations. Instead, site 2754 (in both 3-sector and 6-sector configurations) and site 4619 are equipped with single-band LTE antennas. They use the standard antenna directions, i.e. always the same angle between adjacent antennas. This was thought to be the best choice for the trial environment. Optimization will be performed at a later stage. All the antennas have 4 degrees electrical downtilt. Currently, RET is available in all sites except site 2754. The inter-site distances are: 560 m between site 2754 and 4618, 1480 m between site 2754 and site 4619, and 900 m between site 2754 and site 8838.

4.3 Measurements Configuration

4.3.1 Experiment 1: 3-sector, static scenario

Aim

Determine the maximum downlink throughput of a 3-sector site in a situation with static indoor and static outdoor users.

Description of the configuration

Sector 1 of site 2754 is chosen as the serving sector. The other 2 sectors of site 2754 and all sectors of sites 4618, 4619, and 8838 are configured in DL Inter-cell Interference Generation mode[1]. The number of loading terminal in the serving cell is 6:

- 2 indoor loading terminals: Commsquare DAP probes
- 4 outdoor loading terminals: laptops with LTE dongles

They are able to perform a series of FTP downloads. The file size is 800 MB. The 2 locations for the indoor users are pre-selected inside a building within the coverage area of the serving sector. For the outdoor users, 3 sets of 4 locations are randomly pre-selected within the coverage area of the serving sector.

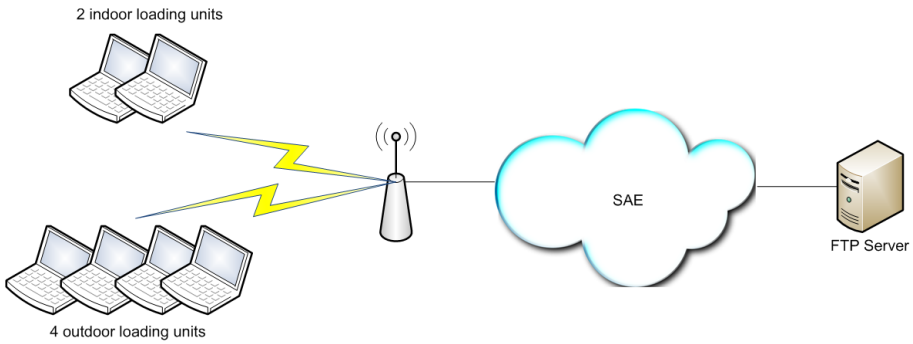

Figure 4.4: Experiment configuration

Description of the experiment

The experiment consists of 3 repetitions that differ only by the choice of the locations of the outdoor users. One set of 4 locations is used in each repetition. By contrast, the 2 locations of the indoor users are kept fixed among the repetitions. The repetitions are considered in order to take into account as much channel conditions as possible. A series of FTP downloads is performed by the loading terminals for a duration of 30 minutes. The series will start at the same time at each loading terminal.

[1] *dlInterferenceEnable* set to true, *dlInterferenceLevel* set to 70%, *dlInterferenceModulation* set to QPSK (0).

Prerequisites for the experiment

- All eNodeBs in the FUP are active and without alarms.
- The DL Inter-cell Interference Generation mode is active in sector 2 and 3 of site 2754 and in all sectors of sites 4618, 4619, and 8838.
- All 6 loading terminals are served by sector 1 of site 2754.
- All 6 loading terminals have a synchronized clock.
- The FTP server is active and connected to the Internet.
- No throughput limitations (<50 Mbps) exist on ftp-application level.
- Availability of 50 Mbps capacity on the backhauling network.
- The retransmissions of FTP packets are not counted in the calculation of the throughput.

Required time

The estimated time for the preparation of the experiment (installing the loading terminals and verifying the prerequisites) is 2 hours. The time required to perform the measurements is 1.5 hours (30 minutes for each repetition).

Required test equipment and software

- 4 x laptop (outdoor users)
- 2 x ZTE 1010 Express 100 Modem (UE Category 3)
- 1 x Samsung GT-B3740 (UE Category 3)
- 1 x LG Krypton (UE Category 3)
- 2 x Commsquare Distributed Active Probing (DAP) probes (indoor users)
- FTP server: HP Proliant DL380, 2x72 GB Hard disk, IP Address: 10.131.4.21
- 2 x TEMS license
- 2 x FTP client application (WS_FTP LE) + Throughput Log application (Net Meter)

Due to the limited availability of TEMS licenses, only one indoor laptop and one outdoor laptop are equipped with TEMS. All other terminals will be equipped with an FTP client and an application to log the throughput.

Data to be collected

- At the loading terminal side (without TEMS): downlink throughput every second.
- At the loading terminal side (with TEMS): PDCP throughput, serving cell ID + RSSI + RSRP + RSQI, neighboring cell ID + RSSI, every half second.
- At the eNodeB side: traces (including aggregate PDCP throughput every 15 minutes) and parameters settings of the network.

Procedure for processing the results and expected outcome

The downlink sector throughput of each repetition is calculated in two ways: from the PDCP throughput collected at the eNodeB side, and from the data collected at the loading terminal side. The first calculation is straightforward. The second calculation requires first the addition of all user throughputs and then the average over time. The two methods should provide the same results. Finally, the sector throughputs of all repetitions are averaged. A sector throughput of 15-25 Mbps is expected.

4.3.2 Experiment 2: 3-sector, mixed scenario

Aim

Determine the maximum downlink throughput of a 3-sector site in a situation with static indoor and mobile outdoor users.

Description of the configuration

Sector 1 of site 2754 is chosen as the serving sector. The other 2 sectors of site 2754 and all sectors of sites 4618, 4619, and 8838 are configured in DL Inter-cell Interference Generation mode. The number of loading terminal in the serving cell is 6:

- 2 indoor loading terminals: Commsquare DAP probes
- 4 outdoor loading terminals: laptops with LTE dongles

They are able to perform a series of FTP downloads. The file size is 800 MB. The locations of the static indoor terminals are pre-selected inside a building within the coverage area of the serving sector. The outdoor users are pedestrians that follow a pre-defined path carrying the laptop in their hands. Both the starting locations and the paths of the outdoor terminals are pre-selected within the coverage area of the serving sector and are different among the terminals. The choice of the paths has been driven by the goal of spanning the wider coverage area while avoiding or minimizing the intra-site and inter-site handovers. The experiment configuration is shown in Figure 4.4.

Description of the experiment

A series of FTP downloads is performed by the loading terminals for a duration of 30 minutes. The series will start at the same time at each loading terminal. At the starting time, the mobile terminals start walking along the pre-defined paths cyclically until the session of 30 minutes is terminated.

Prerequisites for the experiment

- All eNodeBs in the FUP are active and without alarms.
- The DL Inter-cell Interference Generation mode is active in sector 2 and 3 of site 2754 and in all sectors of sites 4618, 4619, and 8838.
- All indoor terminals are served by sector 1 of site 2754.
- All outdoor terminals are served by sector 1 of site 2754 at the starting locations.
- All 6 loading terminals have a synchronized clock.
- FTP server is active and connected to Internet.
- No throughput limitations (<50 Mbps) exist on ftp-application level.
- Availability of 50 Mbps capacity on the backhauling network.
- The retransmissions of FTP packets are not counted in the calculation of the throughput.

Required time

The estimated time for the preparation of the experiment (installing the loading terminals and verifying the prerequisites) is 2 hours. The time required to perform the measurements is 30 minutes.

Required test equipment and software

See 4.3.1.

Data to be collected

See 4.3.1.

Procedure for processing the results and expected outcome

Although the paths are selected to avoid or minimize the handovers, those can still occur for the mobile terminals. Since not all the mobile terminals are equipped with TEMS, it is not possible to track all the handover events and isolate the throughput from non desired sectors. Therefore, only the aggregate PDCP throughput provided by the eNodeB side is used to determine the sector throughput. The data collected by the terminals will be used only at the occurrence. A sector throughput of 15-25 Mbps is expected.

4.3.3 Experiment 3: 6-sector, static scenario

Aim

Determine the maximum downlink throughput of a 6-sector site in a situation with static indoor and static outdoor users.

Description of the configuration

Sector 1 of site 2754 is chosen as the serving sector. The other 5 sectors of site 2754 and all sectors of sites 4618, 4619, and 8838 are configured in DL Inter-cell Interference Generation mode. The number of loading terminal in the serving cell is 6:

- 2 indoor loading terminals: Commsquare DAP probes
- 4 outdoor loading terminals: laptops with LTE dongles.

They are able to perform a series of FTP downloads. The file size is 800 MB. The 2 locations for the indoor users are pre-selected inside a building within the coverage area of the serving sector. For the outdoor users, 3 sets of 4 locations are randomly pre-selected within the coverage area of the serving sector. The experiment configuration is shown in Figure 4.4.

Description of the experiment

See 4.3.1.

Prerequisites for the experiment

- All eNodeBs in the FUP are active and without alarms.
- The DL Inter-cell Interference Generation mode is active in sector 2, 3, 4, 5, and 6 of site 2754 and in all sectors of sites 4618, 4619, and 8838.
- All 6 loading terminals are served by sector 1 of site 2754.
- All 6 loading terminals have a synchronized clock.
- FTP server is active and connected to Internet.

- No throughput limitations (<50 Mbps) exist on ftp-application level.
- Availability of 50 Mbps capacity on the backhauling network connected to the serving FSME System Module.
- The retransmissions of FTP packets are not counted in the calculation of the throughput.

Required time

The estimated time for the preparation of the experiment (installing the loading terminals and verifying the prerequisites) is 2 hours. The time required to perform the measurements is 1.5 hours (30 minutes for each repetition).

Required test equipment and software

See 4.3.1.

Data to be collected

See 4.3.1.

Procedure for processing the results and expected outcome

The downlink sector throughput of each repetition is calculated in two ways: from the PDCP throughput collected at the eNodeB side, and from the data collected at the loading terminal side. The first calculation is straightforward. The second calculation requires first the addition of all user throughputs and then the average over time. The two methods should provide the same results. Finally, the sector throughputs of all repetitions are averaged. A sector throughput of 13-23Mpbs is expected.

4.3.4 Experiment 4: 6-sector, mixed scenario

Aim

Determine the maximum downlink throughput of a 6-sector site in a situation with static indoor and mobile outdoor users.

Description of the configuration

Sector 1 and sector 2 of site 2754 are chosen as the serving sectors. The other 4 sectors of site 2754 and all sectors of sites 4618, 4619, and 8838 are configured in DL Inter-cell Interference Generation mode. The number of loading terminal in the serving cell is 6:

- 2 indoor loading terminals: Commsquare DAP probes
- 4 outdoor loading terminals: laptops with LTE dongles

They are able to perform a series of FTP downloads. The file size is 800 MB. One indoor terminal is located within a building in the coverage area of sector 1, while the other indoor terminal is located in a building in the coverage area of sector 2. The outdoor users are pedestrians that follow a pre-defined path carrying the laptop in their hands. Two of the four starting locations are pre-selected within the coverage area of sector 1, while the other two locations are pre-selected within the coverage area of sector 2. The paths are pre-selected

within the coverage area of both sectors in order to force handovers between the two serving sectors. Other intra-site and inter-site handovers are avoided or minimized by the selection of the paths.

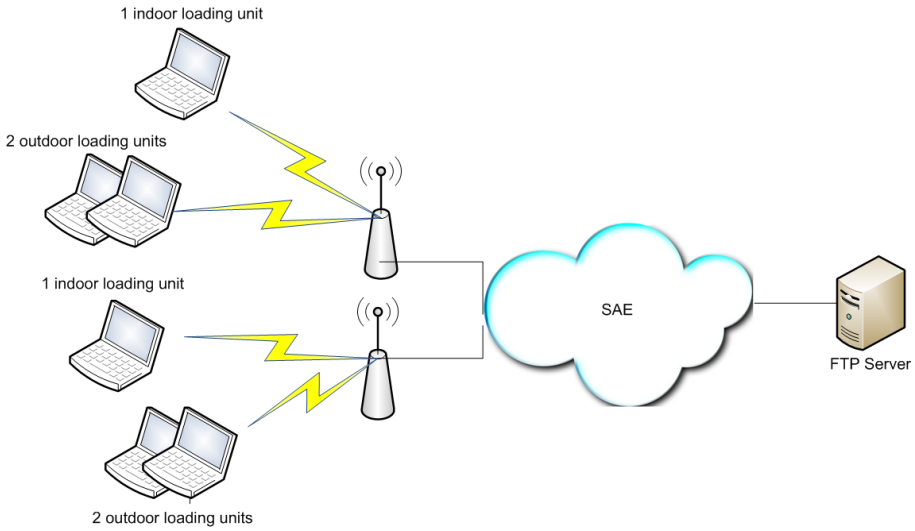

Figure 4.5: Configuration of experiment 4 at the starting time

Description of the experiment

A series of FTP downloads is performed by the loading terminals for a duration of 30 minutes. The series will start at the same time at each loading terminal. At the starting time, the mobile terminals start walking along the pre-defined paths cyclically until the session of 30 minutes is terminated.

Prerequisites for the experiment

- All eNodeBs in the FUP are active and without alarms.
- The DL Inter-cell Interference Generation mode is active in sector 3, 4, 5 and 6 of site 2754 and in all sectors of sites 4618, 4619, and 8838.
- All indoor terminals are served by the corresponding serving sector (either sector 1 or 2 of site 2754).
- All outdoor terminals are served by the corresponding serving sector (either sector 1 or 2 of site 2754) at the starting locations.
- All 6 loading terminals have a synchronized clock.
- FTP server is active and connected to Internet.
- No throughput limitations (<50 Mbps) exist on ftp-application level.
- Availability of 100 Mbps capacity on the backhauling network (50 Mbps per FSME System Module).
- The retransmissions of FTP packets are not counted in the calculation of the throughput.

Required time

The estimated time for the preparation of the experiment (installing the loading terminals and verifying the prerequisites) is 2 hours. The time required to perform the measurements is 30 minutes.

Required test equipment and software

See 4.3.1.

Data to be collected

See 4.3.1.

Procedure for processing the results and expected outcome

Since not all the mobile terminals are equipped with TEMS, it is not possible to track the handover events and the serving sector. Therefore, only the two aggregate PDCP throughputs provided by the eNodeB side are used. The data collected by the terminals will be used only at the occurrence. The sector throughput is calculated as the average of the throughputs of sector 1 and 2 of site 2754 and it is expected to be 13-23 Mbps.

Chapter 5

Conclusions and Future Work

Although potentially a 6-sector site can offer a double capacity than a 3-sector site, factors such as inter-cell interference, number of handovers, azimuth spread, spatial distribution of the users, accuracy of the site planning, and the deployment of inter-cell interference coordination techniques prevent the capacity gain to be as high as a factor of two. To quantify the impact of these factors on the capacity gain we adopted an LTE system level simulator. The simulator, that was developed by the Vienna University of Technology, has been enhanced with additional features and functionalities. We found that, for a fixed number of users per site, a homogeneous 6-sector-site deployment can offer a 73% higher site throughput and 41% higher cell-edge throughput than a homogeneous 3-sector-site deployment. Instead, when only a cluster of 3-sector sites is upgraded to a six sectorized configuration, while the surrounding sites remain with 3 sectors, for the upgraded sites this scenario results in a 76% higher site throughput and 78% higher cell-edge throughput, while for the surrounding sites this scenario results in a 4% lower site throughput and 6% lower cell-edge throughput. Therefore, a six sectorized configuration is able to enhance the performance of congested hotspots at the cost of a slightly performance degradation in the surrounding sites. Finally, when we compare the performance of the homogeneous 6-sector-site deployment and the homogeneous 3-sector-site deployment at the same cell edge user performance[1], the 6-sector-site deployment can allocate 59%-80% more users and offer a 73%-89% higher site throughput.

Besides, we performed an economic study to access the reasons for a possible deployment of 6-sector sites instead of 3-sector sites for LTE. The assessment was based on today's prices of hard/software for a 3- and a 6-sector site, today's site rents, the estimation of the capacity gain of a 6-sector site (derived from the simulation study including a safety margin), and future traffic estimation. In addition, we assumed that during the deployment of LTE a number of existing GSM/UMTS sites can be used to host a 3-sector site to reduce capital expenditures; however, only a subset of these sites can be used to host a 6-sector site, due to the extra equipment. From the analysis of the present value of the cash outflow[2], we found that it is more economically attractive to increase the capacity of the network by a combination of new 3-sector sites and upgrades of 3-sector sites to a six sectorized configuration than entirely by adding new 3-sector sites to the network. In addition, we found that the lowest present value of the cash outflow is obtained when 6-sector sites are added in all the existing locations that can host a 6-sector site, 3-sector sites are added in the remaining existing locations that cannot host a 6-sector site, and 6-sector sites are added in the new locations whenever all the existing

[1] When the percentage of active users with throughput lower than 300 Kbps is 10% (See subsection 3.4.6).

[2] The analysis is only internally available in KPN because of the presence of confidential information.

locations are used. Therefore, we can conclude that with the parameters and the assumptions that were considered in the study, the adoption of 6-sector sites along with 3-sector sites in LTE macro-cell deployments allows service operator to reduce capital expenditures compared to the only adoption of 3-sector sites.
Furthermore, in chapter 4 we defined a measurement plan for the verification of the capacity gain. As future work, the measurements will be executed to validate the results of the simulations and to refine the models used in the simulator. Further, the impact of inter-cell interference coordination techniques on the capacity gain will be investigated with simulations. Also, it would be interesting to estimate the capacity gain in uplink LTE. Regarding the economic study, an examination of the existing GSM and UMTS sites of the KPN network to determine the percentage that can host a 6-sector site, and a study to estimate the growth of the mobile traffic in The Netherlands, could be performed to refine the results.

Appendix A

LTE Standardization

A.1 Introduction

The standardization of Long term Evolution (LTE) has been carried out in the 3rd Generation Partnership Project (3GPP). 3GPP is a collaboration between telecommunication standardization bodies that is also responsible for the standardization of Wideband CDMA (WCDMA) and the later phase of GSM evolution. This chapter is organized as follows. Section 2 introduces the LTE standardization phases. Section 3 presents the LTE target requirements. Section 4 presents the 3GPP Standardization Body. Finally, section 5 introduces LTE-Advanced.

A.2 LTE Standardization Phases

The 3GPP work on LTE started with the first workshop held on November 2004 in Toronto, Canada. The workshop was open to all interested organizations, members and non members of 3GPP. Operators, manufacturers, and research institutes presented severals views and proposals on both the expected requirements for the work and the expected technologies to be adopted.
Following the workshop, the 3GPP Technical Specification Group on Radio Access Network (3GPP TSG RAN) approved the start of the study for LTE in December 2004. The goal was to develop a framework for the evolution of the 3GPP radio access technology towards a high data rate, low latency, and packet-optimized radio access technology. The first key task of the study was to define the requirements of the technology. These were mainly settled during the first half of 2005 by the 3GPP TSG RAN, with the first approved version in June 2005, as presented in section A.3. Then the work moved to the Working Groups (WGs) of 3GPP for detailed technical discussions about multiple access, protocol solutions, and architecture.
The multiple access decision was officially reached at the end of 2005. OFDMA and SC-FDMA were selected as multiple access technologies for downlink and uplink, respectively. The use of OFDMA was present in many of the presentations of the original LTE workshop in 2004, while the SC-FDMA soon emerged as the most favourable choice that was supported by many vendors and operators.
In the area of LTE architecture, it was decided to place all radio related functionalities in the base station, resulting in a single node RAN. The term for base station in 3GPP became eNodeB. In early 2007, the Packet Data Convergence Protocol (PDCP) shifted from core network side to eNodeB. The two main differences to the 3GPP Release 6 network were the lack

of the Radio Network Controller (RNC), and the net separation of the control plan and user plane in the core network functionalities.
The study item was closed formally in September 2006 and it was followed by detailed work items towards the standardization of LTE. The work on the evolution of HSPA resulted in December 2007 in the completion of the 3GPP Release 7. It introduced the HSPA+ (Evolved HSPA) standard that can be considered as the first step towards LTE; indeed, it increases the downlink/uplink data rate and reduces the latency in respect to HSDPA/HSUPA, and introduce MIMO technologies along with higher order modulation (64QAM). As further step towards LTE, it specifies an optional all IP-base architecture.
In December 2008 the first release of the LTE Standard, namely 3GPP Release 8, was completed. It includes more than 1000 specifications divided in series with numbers from 21 to 36 [25]. 3GPP Release 8 includes also HSPA+ enhancements. 3GPP Release 9 followed in 2009. It introduced enhancements to HSPA+ and LTE System Architecture Evolution (SAE). It also defined methods for interoperability between LTE and other access systems such as UMTS and WiMAX. 3GPP Release 10 was completed in 2011 and specifies LTE-Advanced. An introduction to LTE-Advanced is given in paragraph A.5. HSPA+ and Multi-RAT related enhancements are also included in this release. At the moment 3GPP is working on the 3GPP Release 11 that will specify enhancements for LTE-Advanced, HSPA+, and Multi-RAN. Table A.1 provides the 3GPP Releases[1] timeline since the first LTE workshop in 2004.

Release	**Event**	**Info**
	Workshop in Toronto Nov 2004	Start of the 3GPP work on LTE
	Study Item Dec 2004 - Sep 2006	Definition of LTE requirements and technologies
Rel-7	Stage 1 freeze Sep 2005 Stage 2 freeze Sep 2006 Stage 3 freeze Dec 2007	HSPA Evolution (HSPA+)
Rel-8	Stage 1 freeze Mar 2008 Stage 2 freeze Jun 2008 Stage 3 freeze Dec 2008	Long Term Evolution (LTE)
Rel-9	Stage 1 freeze Dec 2008 Stage 2 freeze Jun 2009 Stage 3 freeze Dec 2009	Enhancements
Rel-10	Stage 1 freeze Mar 2010 Stage 2 freeze Sep 2010 Stage 3 freeze Mar 2011	LTE-Advanced
Rel-11	Stage 1 freeze Sep 2011 Stage 2 freeze Mar 2012 ? Stage 3 freeze Sep 2012 ?	Enhancements

Table A.1: LTE standardization process

[1]3GPP standard specifications are typically released in 3 stages. Stage 1 specifications define the service requirements from the user point of view; stage 2 specifications define an architecture to support the service requirements; stage 3 specifications define an implementation of the architecture by specifying protocols in details.

A.3 LTE Target Requirements

At the start of the study item, during the first half of 2005, the 3GPP defined the requirements for LTE development. The key elements included in the target settings for the LTE feasibility study work, as defined in [26], were as follow:

- The LTE system should be packet switched domain optimized. The system is required to support IP Multimedia Sub-system (IMS) and further evolved 3GPP packet core.
- The requirement for the LTE radio round trip time is set to be below 10 ms and access delay below 300 ms.
- The requirements for data rates are defined to ensure sufficient steps in terms of data rates in contrast to HSPA. The peak rate requirements for uplink and downlink are set at 50 Mbps and 100 Mbps respectively.
- A good level of security and mobility should be sustained. This also included inter-system mobility with GSM, WCDMA, and cdma2000.
- LTE is required to improve terminal power efficiency compared to the earlier systems.
- LTE is required to facilitate frequency allocation flexibility with 1.25/2.5, 5, 10, 15, and 20 MHz allocations[1]. The possibility of using LTE in a deployment with WCDMA or GSM as the system on the adjacent band is also required.
- Depending on the case, 2- to 4-times higher capacity than provided with the Release 6 HSDPA/HSUPA reference case, is required.
- One of the drivers for the work was cost, to ensure that the new system could facilitate lower investment and operating costs compared to the earlier systems.

A.4 3GPP Standardization Body

The 3rd Generation Partnership Project (3GPP) is a collaboration agreement that was established and formalized in December 1998. The collaboration agreement brings together a number of regional and national telecommunication standardization bodies which are known as Organizational Partners. The current Organizational Partners are:

- ARIB (Japan): Association of Radio Industries and Businesses
- ATIS (USA): Alliance for Telecommunications Industry Solutions
- CCSA (China): China Communications Standards Association
- ETSI (Europe): European Telecommunications Standards Institute
- TTA (Korea): Telecommunications Technology Association
- TTC (Japan): Telecommunication Technology Committee

The 3GPP Organizational Partners determine the general policy and strategy of 3GPP and perform tasks such as approval and maintenance of the 3GPP scope and the Partnership Project Agreement; management of the Technical Specification Groups; approval of Organizational Partner funding requirements; and allocation of human and financial resources to the Project Co-ordination Group.
Along with the Organizational Partners, there are 12 Market Representation Partners (MRPs), i.e., IMS Forum, TD-SCMA Forum, GSA, GSM Association, IPv6 Forum, UMTS Forum, 3G Americans, TD-SCMA Industry Alliance, Info Communication Union, Femto Forum, CDMA

[1]Later during the course of work, the two smallest bandwidth values were slightly adjusted (to 1.4 and 3 MHz) to give a good match for both GSM and cdma2000 refarming case.

Development Group, and Cellular Operators Association of India (COAI), which provide for the maintenance of the Partnership Project Agreement and the approval of applications for 3GPP partnership.
Furthermore, 3GPP currently has three observers which are Standards Development Organizations (SDOs) who have the qualifications to become future Organizational Partners:

- TIA (USA): Telecommunications Industries Association
- ISACC (Canada): ICT Standards Advisory Council of Canada
- Communications Alliance (Australia): former Australian Communications Industry Forum (ACIF)

Along with the above partners there are more than 350 Individual Members. All entities registered as members of an Organizational Partner and eligible for participation in the technical work of that Organizational Partner can become Individual Members of 3GPP if they are committed to support 3GPP and to contribute technically or otherwise to one or more of the Technical Specification Groups (TSGs) within the 3GPP scope. An Individual Member has the right to participate in the work of 3GPP by attending meetings of the TSGs and subtending groups.

A.4.1 3GPP Scope

The original scope of 3GPP was to produce a globally applicable third-generation (3G) mobile system specifications based on evolved Global System for Mobile Communications (GSM) specifications within the scope of the International Mobile Telecommunications-2000 project of the International Telecommunication Union (ITU). The scope was later enlarged to include the deployment and maintenance of [27]: GSM including evolved radio technologies (e.g. General Packet Radio Services (GPRS) and Enhanced Data Rates for GSM Evolution (EDGE)); an evolved third generation and beyond Mobile System based on the evolved 3GPP core network, and the radio access technologies supported by the partners (i.e. UTRA both FDD and TDD modes); an evolved IP Multimedia Subsystem (IMS) developed in an access independent manner.

A.4.2 Structure of 3GPP

As shown in Figure A.1, 3GPP is organized in one Project Co-ordination Group (PCG) and four Technical Specification Groups (TSGs). The PCG is responsible for overall time-frame and management of technical work to ensure that the 3GPP specifications are produced in a timely manner as required by the market place according to the principles and rules contained in the Project reference documentation. The technical specification development work within 3GPP is accomplished by TSGs that report to the PCG. Each TSG has the responsibility to prepare, approve and maintain the specifications within its terms of reference, and it organizes its work in Working Groups (WGs).
The 3GPP TSG RAN is responsible for LTE specification deployment. TSG RAN has a total of five WGs. The physical layer specifications are in the 36.2 series and are developed by WG1. Respectively, the Layer 2 (L2) and Layer 3 (L3) specifications are in the 36.3 series from WG2, internal interfaces in the 36.4 series from WG3, and radio performance requirements in the 36.1 series from WG4. The LTE terminal test specifications are developed by WG5.
The specifications for the Evolved Packet Core (EPC) are covered in TSG SA and TSG CT, while the TSG GERAN is responsible for the necessary Release 8 changes in GSM/EDGE specifications to facilitate the LTE-GERAN inter-working from GERAN perspective.

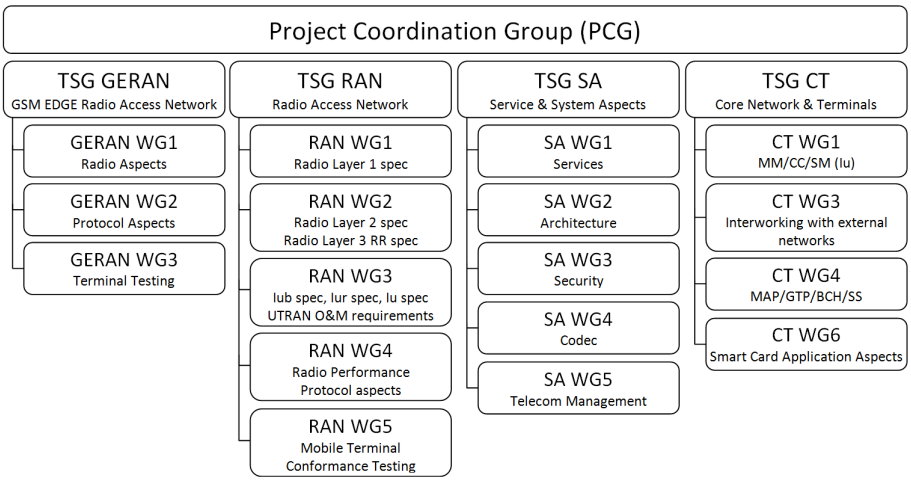

Figure A.1: 3GPP structure

A.4.3 3GPP Support Organizations

Next generation mobile networks (NGMN) and LTE/SAE Trial Initiative (LSTI) are supporting organizations that help 3GPP in defining the standards. Various vendors and operators have come together to facilitate the LTE standard setting by providing recommendations and providing feedback by knowledge gathered during trials.

Next Generation Mobile Network (NGMN) alliance

NGMN is an alliance of major service providers who are also early adopters of mobile communication technology. Several operators (Sprint Nextel, China Mobile, Vodafone, Orange, T-Mobile International, KPN Mobile, and NTT DoCoMo) formed the alliance in September 2006. Subsequently, NGMN defined the high-level requirements for all next generation broadband wireless networks, not just LTE. This type of initiative is one of the key differences between LTE and its predecessors, which were primarily vendor driven technologies. The NGMN alliance's mandate is to complement and support the work within standardization bodies by providing a coherent view of what the operator community is going to require in the decade beyond 2010. NGMN has provided 3GPP with recommendations on optimized networks, self organized networks and higher performance networks. These recommendations, which LTE has been developed around, are incorporated into the standards. One of the benefits of NGMN is that service providers have buy-in throughout the standardization process. As a result, they will be more comfortable with the standards when they are completed and LTE will be optimized for operators.
In addition to a service providers' role as NGMN members, various types of vendors play the role of sponsors of NGMN alliance's activities. Universities and non-industrial research institutes are also contributing to NGMN's activities in their role of advisors to the alliance.

LTE/SAE Trial Initiative (LSTI)

LSTI is a global, collaborative technology trial initiative focused on accelerating the availability of commercial and interoperable LTE mobile broadband systems. Major vendors (Nortel, Alcatel-Lucent, Ericsson, Nokia and Nokia Siemens Networks) and operators (Orange,

T-Mobile and Vodafone) founded the initiative and have added more stakeholders (chipset vendors, operators and equipment vendors) since its inception. Vendors and operators began testing LTE early in the development process. The test results are shared with operators and 3GPP in an effort to improve the standards as the technology is being defined. Moreover, LSTI collaboration ensures that operators can rely on published results since they participate in the process. LSTI testing helps remove the hype from LTE and make the results more realistic. The efforts of NGMN and LSTI in conjunction with 3GPP are driving LTE to be a comprehensive technology with early interoperability testing and operator confidence. Objectives of LSTI include:

- Driving the industrialization of 3GPP LTE and SAE.
- Demonstrating the 3GPP LTE capabilities.
- Promoting 3GPP LTE to operators, vendors, analysts and regulators.
- Simplifying the technology with a full packet-based network and developing newer business models for service providers, vendors and operators.
- Evolving the 3GPP LTE standard with findings from the proof-of-concept and interoperability trials.

A.4.4 Roles of NGMN, LSTI, and service providers in LTE standardization

This paragraph focuses on the roles that NGMN and LSTI alliances, and service providers have played in the overall developments towards LTE standardization. Three phases can be identified.
Phase 1 started in September 2006 with the NGMN alliance formation among major service providers to formulate their requirements for a 4G wireless communication system and set the stage for various vendors to standardize the same in LTE specification. The formation of the LSTI alliance and LTE Proof-of-Concept (PoC) trials occurred in this phase as well. Phase 1 ended with the stage 2 freeze of the LTE standard.
Phase 2 has seen LTE gaining more emphasis and importance between vendors at the expense of other competing technologies, and also it has seen major development in LTE technology. This phase started in July 2008 when NGMN approved LTE as it first compliant technology. That triggered Sprint, which was one of the founders of the alliance, to leave NGMN. This is partly due to Sprint's decision to adopt WiMAX as choice of technology for their next generation network. In November 2008, Qualcomm halted the UMB project and shifted focus fully on to LTE technology. In January 2009, Nokia ended the production of its only WiMAX device. In October 2008, Bell and Telus declared a joint plan to move from CDMA to HSPA in 2010 and then to LTE in 2012. Regarding the alliances, LSTI members continued their focus on performing the technology trials and interoperability trials to refine the technology, while NGMN released its final requirements. Stage 3 freeze of the LTE standard was achieved in this phase.
Phase 3 (1Q 2009) started with commitments to adopt LTE by the biggest service providers which started to award the commercial contracts to deploy LTE to the vendors. In February 2009, Verizon announced their LTE deployment plans and selected various vendors for the network. The global mobile suppliers association announced that 26 major service providers have committed to deploy LTE systems.

A.5 Introduction to LTE-Advanced

In March 2008, the ITU-R[1] called for the submission of proposals for candidate radio interface technologies for IMT-Advanced[2]. Proposals must fulfil the ITU-R's requirements for IMT-Advanced [30]. The new capabilities of these IMT-Advanced systems are envisaged to handle a wide range of supported data rates according to economic and service demands in multi-user environment with target peak data rates of up to 100 Mbps for high mobility and 1 Gbps for low mobility such as nomadic/local wireless access.
In response to the call for proposals from ITU-R, a workshop of 3GPP TSG RAN took place in April 2008 to identify targets and potential techniques for further advancements of LTE. These targeted advancements became LTE-Advanced, specified as LTE Release 10 and beyond. LTE-Advanced was the 3GPP candidate radio interface technology for IMT-Advanced. It was designed to meet the requirements of mobile network operators for the evolution of LTE, and to exceed the IMT-Advanced requirements. An evaluation of LTE-Advanced was carried out by 18 companies in 3GPP, showing that LTE-Advanced completely satisfies the criteria set by the ITU-R for IMT-Advanced. As a result, LTE-Advanced was accepted by the ITU as an IMT-Advanced technology in October 2010.
The main components of LTE-Advanced that are added to LTE in Release 10 are [28]:

- Carrier aggregation
- Enhanced downlink multiple antenna transmission
- Uplink multiple antenna transmission
- Relaying
- Support for heterogeneous network deployments

Up to five component carriers with a bandwidth of up to 20 MHz each can be aggregated in LTE-Advanced to make efficient use of the available spectrum and achieve the desired total bandwidth and peak data rate. Each component carrier within a carrier aggregation is designed to be fundamentally similar to an LTE Release 8 carrier so that it can be configured in a backward-compatible way and used by legacy UEs if desired. This allows network operators to continue serving existing LTE customers while their network equipment is progressively upgraded.
Although the use of larger bandwidths by means of carrier aggregation allows higher peak data rates to be achieved, it does not increase the spectral efficiency. LTE-Advanced therefore supports enhanced downlink MIMO transmission by increasing the number of antennas at the eNodeB and UE. The maximum number of spatial transmission layers for Single-User MIMO (SU-MIMO) is increased from four in LTE Release 8 to eight. Similarly to the downlink, the number of spatial layers supported in the uplink for SU-MIMO is increased from one in LTE Release 8 to two. In addition, transmit diversity is introduced for the uplink control signaling.
In order to further improve the spectral efficiency, especially at the cell edge, a later release of LTE-Advanced may incorporate an enhanced support for Coordinated Multi-Point (CoMP) scheme, which in downlink entails the coordination of transmission from multiple cells.
Relay nodes enable the deployment of small cells at locations where conventional fixed line or microwave backhaul is not possible or commercially viable. Relay nodes use the LTE-Advanced air-interface for self-backhaul to a so-called donor eNB. For the user equipment, the relay node is just a cell of the donor eNB.

[1] International Telecommunication Union Radiocommunication Bureau
[2] International Mobile Telecommunications-Advanced

LTE-Advanced supports deployments of heterogeneous networks to improve the spectral efficiency per unit area. An heterogeneous network consists of a regular placement of macrosites that typically transmit at high power level, overlaid with several picosites and femtosites which transmit at substantially lower power. The low-power base stations can be deployed to eliminate coverage holes in the macro system and improve the capacity in hot-spots. Since interference among macrosites and pico/femtosites can lead to significantly sub-optimal performance, advanced techniques for efficient interference management need to be considered in LTE-Advanced. More information on LTE-Advanced can be found in [28], [32].

Appendix B

LTE System Description

B.1 Introduction

This chapter reviews the 3GPP System Architecture Evolution (SAE), the physical layer of LTE, and the Radio Resource Management (RRM), with particular focus on the downlink. Providing a detailed description of these aspects is far from the goal of this chapter. Instead, we would like to provide the reader with an insight to the most important concepts that are needed to have a better understanding of the report. The review presented in this chapter is based on [1], and [28]. For an extensive description please refer to these references.

B.2 System Architecture

Figure B.1 describes the basic system architecture configuration where only E-UTRAN access network is involved. The architecture is divided in four main high level domains: User Equipment (UE), Evolved UTRAN (E-UTRAN), Evolved Packet Core Network (EPC), and the Services domain. The new architectural development is limited to the Radio Access Network and the Core Network, i.e. the E-UTRAN and the EPC, respectively. UE and Services domains remain architecturally intact, but functionally evolution has also continued in those areas.
UE, E-UTRAN, and EPC together represent the Internet Protocol (IP) Connectivity Layer. This part of the system is also called the Evolved Packet System (EPS). The main function of this layer is to provide IP based connectivity, and it is highly optimized for that purpose only. All services will be offered on top of IP, and circuit switched nodes and interfaces seen in earlier 3GPP architectures are not present in E-UTRAN and EPC at all.

B.2.1 Logical Elements

This section introduces the logical network elements for the basic architecture configuration.

User Equipment (UE)

UE is the device that the end user uses for communication. UE also contains the Universal Subscriber Identity Module (USIM) that is a separate module from the rest of the UE. USIM is used to identify and authenticate the user and to derive security keys for protecting the radio interface transmission. Functionally, the UE is a platform for communication applications, which signals with the network for setting up, maintaining and removing the communication

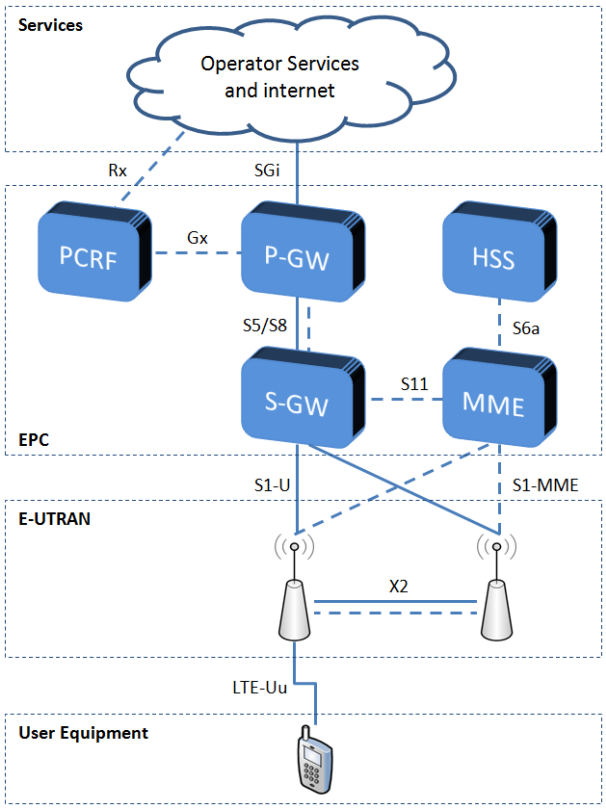

Figure B.1: EPS network architecture

links the end users needs.
In LTE, there are five UE capability classes, as shown in Table B.1. The supported data ranges from 10 to 300 Mbps in downlink and from 5 to 75 in uplink. All devices support the 20 MHz bandwidth, QPSK/16QAM/64QAM modulation in downlink, QPSK/16QAM modulation in uplink. Only a category 5 device support 64QAM in uplink. Further, receiver diversity and MIMO is supported in all categories, except in category 1.

	Peak rate	Max supported modulation in DL/UL	Max number of supported layers for DL MIMO
Category 1	DL: 10 Mbps UL: 5 Mbps	DL: 64QAM UL: 16QAM	1
Category 2	DL: 50 Mbps UL: 25 Mbps	DL: 64QAM UL: 16QAM	2
Category 3	DL: 100 Mbps UL: 50 Mbps	DL: 64QAM UL: 16QAM	2
Category 4	DL: 150 Mbps UL: 50 Mbps	DL: 64QAM UL: 16QAM	2
Category 5	DL: 300 Mbps UL: 75 Mbps	DL: 64QAM UL: 64QAM	4

Table B.1: LTE UE capability categories [29]

E-UTRAN NodeB (eNodeB)

E-UTRAN is simply a mesh of eNodeBs connected to neighbouring eNodeBs with the X2 interface. All radio functionalities of the fixed part of the network are concentrated in the eNodeB. Being the termination point of all the radio protocols, the eNodeB acts as a layer 2 bridge between UE and the EPC, i.e. it relays data between the radio connection and the corresponding IP based connectivity towards the EPC. In this role, it performs ciphering/deciphering of the User Plane (UP) data, and also IP header compression/decompression.
The eNodeB is also responsible for many Control Plane (CP) functions such as Radio Resource Management (RRM). In addition, it has an important role in Mobility Management (MM). Based on signal level measurements carried out by the UE, it makes decisions to handover UEs between cells. This includes exchanging handover signaling between other eNodeBs and the MME. The eNodeB is also responsible for routing the UE's request of network connection to the MME that previously served that UE, or selecting a new MME if a route to the previous MME is not available or routing information is absent. Thus, the eNodeB may need to connect to many eNodeBs, MMEs and S-GWs. However, each UE will be served by only one eNodeB, MME and S-GW at a time, and the serving eNodeB has to keep track of the association with the serving MME and S-GW.

Mobility Management Entity (MME)

The MME is the main control element in the EPC. It operates only in the CP, and it is not involved in the path of the UP data. The main MME functions are: Authentication and Security, Mobility Management, and Managing Subscription Profile and Service Connectivity. The inter-MME connection with neighbouring MMEs is used in handovers. In principle the MME may be connected to any other MME in the system, but typically the connectivity is limited to one operator network only. The remote connectivity between MMEs may be used when a UE that has traveled far away while powered down registers to a new MME, which then retrieves the UE's permanent identity, the International Mobile Subscriber Identity (IMSI), from the previously visited MME.
Connectivity to a number of HHSs will also need to be supported. The HHS is located in each UE's home network and a route to that can be found based on the IMSI. The HSS provides the MME with the authentication vectors needed in the authentication mechanism, and the subscription profile that determines what Packet Data Network (PDN) connections should be allocated to the UE at network attachment.

Serving Gateway (S-GW)

The high level function of the S-GW is UP tunnel management and switching. It relays the data between eNodeB and P-GW in form of GTP tunnel. When a UE is in idle mode, the resources in eNodeB are released, and the data path terminates in the S-GW. If the S-GW receives data packets from the P-GW on any such tunnel, it will buffer the packets, and request the MME to initiate paging of the UE. Paging will cause the UE to re-connect, and when the tunnels are re-connected, the buffered packets will be sent on. In addition, the S-GW monitors the tunnels and may collect data for user charging and legal interception.
The S-GW has minor role in control functions of its own resources. It allocates them only based on requests from MME or P-GW, which in turn are acting on the need to set up, modify or clear bearers for the UE. If the request was received from the P-GW, the S-GW will also rely the command to the MME so that it can control the tunnel to the eNodeB. Similarly,

when the MME initiated the request, the S-GW will signal to the P-GW.
During mobility between eNodeBs, the S-GW acts as the local mobility anchor. The MME commands the S-GW to switch the tunnel from one eNodeB to another. The MME may also request the S-GW to provide tunneling resources for data forwarding, when there is a need to forward data from source eNodeB to target eNodeB during the time UE makes the radio handover. The mobility scenarios also include changing from one S-GW to another, and the MME controls this change accordingly, by removing tunnels in the old S-GW and setting them up in the new S-GW. The S-GW should be able to connect to any P-GW in the whole network, because P-GW will not change during mobility, while S-GW may be relocated when the UE moves.

Packet Data Network Gateway (P-GW)

The P-GW is the edge router between the EPS and external packet data networks. The UP traffic between P-GW and external networks is in the form of IP packets that belongs to various IP services flows, while the UP traffic between P-GW and S-GW is in form of GTP tunnels, which represent the bearer. Thus, the P-GW is responsible for the mapping of the IP data flows to GTP tunnels. The mapping is performed according to the policies set defined by the Policy and Charging Enforcement Function (PCEF) for every UE and the service in question. The PCEF that resides in the P-GW is also responsible for collecting and reporting the related charging information for every bearer.
The P-GW is the highest level mobility anchor in the system. When a UE moves from one S-GW to another, the bearers have to be switched in the P-GW. The P-GW is also responsible for the IP address allocation for the UE.

Policy and Charging Resource Function (PCRF)

The PCRF is responsible for policy control decision-making, as well as for controlling the flow-based charging functionalities in the PCEF which resides in the P-GW. The PCRF provides the QoS authorization (QoS class identifier and bit rates) that decides how a certain data flow will be treated in the PCEF and ensures that this is in accordance with the user's subscription.

Home Subscription Server (HSS)

The HSS is the subscription data repository for all permanent user data. It also records the location of the user in the level of visited network control node, such as MME. The HSS stores the master copy of the subscriber profile, which contains information about the services that are applicable to the user, including information about the PDN connections, and whether roaming to a particular visited network is allowed or not. The permanent key, which is used to calculate the authentication vectors that are sent to a visited network for user authentication and deriving subsequent keys for encryption and integrity protection, is stored in the Authentication Center (AuC) which is typically part of the HSS. In all signaling related to these functions, the HSS interacts with the MME. Therefore, the HSS needs to be able to connect with every MME in the whole network, where its UEs are allowed to move.

Services Domain

Three categories of services will be made available: IMS based operator services, non-IMS based operator services, and other services not provided by the mobile network operator (e.g.

services provided through the internet).

B.2.2 Interfaces and Protocols

Figure B.2 shows the CP protocols related to a UE's connection to a PDN. The topmost layer in the CP is the Non-Access Stratum (NAS), which consists of two separate protocols that are carried on direct signaling transport between UE and MME. The eNodeB is not involved in these transactions by any other means besides transporting the messages, and providing some additional transport layer indication along with the messages in some case. The NAS layer protocols are EPS Mobility Management (EMM) and the EPS Session Management (ESM). The EMM protocol is responsible for handling the UE mobility within the system. Authentication and protection of the UE identity, NAS layer security functions, encryption and integrity protection are parts of the EMM protocol as well. The EPS protocol may be used to handle the bearer management between the UE and the MME, and for E-UTRAN bearer management procedures.
The radio interface protocols are:

- Radio Resource Control (RRC): the RRC protocol controls the radio resource usage. It manages UE's signaling and data connections, and includes functions for handover.
- Packet Data Convergence Protocol (PDCP): the main functions of the PDCP protocol are IP header compression (UP), encryption and integrity protection (CP only).
- Radio Link Control (RLC): the RLC protocol is responsible for segmentation/concatenation of the PDCP-PDUs for radio interface transmission. It also performs error correction with the Automatic Repeat Request (ARQ) method.
- Medium Access Control (MAC): the MAC layer is responsible for scheduling the data according to priorities, and multiplexing data to Layer 1 transport blocks. It also provides error correction with Hybrid ARQ.
- Physical Layer (PHY): it is the Layer 1 of the LTE-u radio interface.

The S1 interface connects the E-UTRAN to the EPC, and involves the following protocols:

- S1 Application Protocol (S1AP): the S1AP protocol handles the UE's CP and UP connections between E-UTRAN and EPC, including participating in handover when EPC is involved.
- Stream Control Transmission Protocol IP (STCP/IP): the STCP protocols provides the reliable transport and sequenced delivery functions suitable for signaling messages.

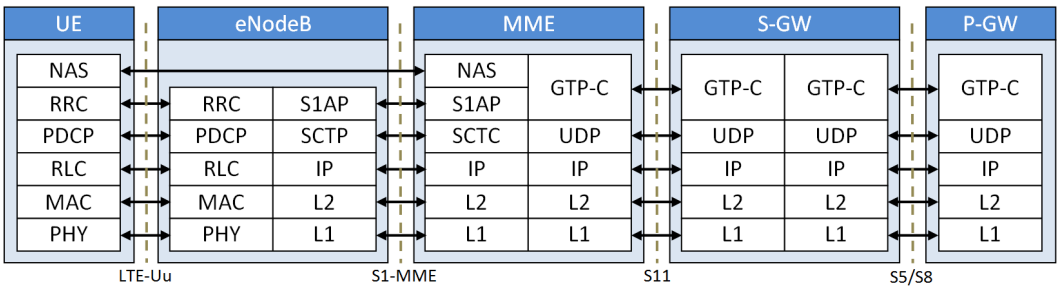

Figure B.2: Control plane protocol stack in EPS

The following additional protocols are involved in the EPC:

- GPRS Tunneling Protocol Control Plane (GTP-C): it manages the UP connections in the EPC. This role includes signaling the QoS and other parameters, and performing mobility management functions within the EPC, e.g. when the GTP-U tunnels of a UE need to be switched from one node to another.
- UDP/IP: UDP and IP are used as the standard and basic IP transport on top of a variety of L2 and L1 technologies. UDP is used instead of TCP because the higher layers already provide reliable transport with error recovery and re-transmission.

Figure B.3 illustrates the UP protocol structure for UE connecting to P-GW. The protocol structure is very similar to the CP. this highlights the fact that the whole system is designed for generic packet data transport, and both CP signaling and UP data are ultimately packet data. Only the volumes are different. Most of the protocols have been introduced above, with the exception of the following one:

- GPRS Tunneling Protocol User Plane (GTP-U): it forms the GTP-U tunnel that is used to send end-user IP packets belonging to one EPS bearer.

Figure B.4 illustrates the X2 interface protocol structure, which resembles that of the S1 interface. Only the CP application protocol is different. X2 interface is used in mobility between the eNodeBs, and the X2AP includes functions for handover preparation, and overall maintenance of the relations between neighbouring eNodeBs. The UP in the X2 interface is used for forwarding data in a transient state during handover, when the radio interface is already disconnected on the source side, and has not yet resumed on the target side. Data forwarding is done for the DL data, since the UL data can be throttled effectively by the UE.

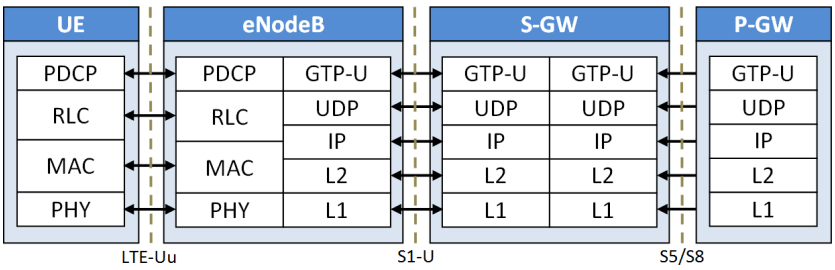

Figure B.3: User plane protocol stack in EPS

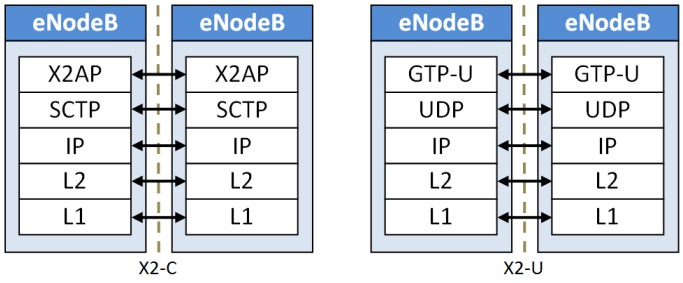

Figure B.4: Control and user plane protocol stacks for X2 interface

B.3 Physical Layer

B.3.1 System Bandwidth and Frame Structure

LTE is defined to operate in a wide range of frequency bands. Table B.2 gives details of the frequency bands for FDD and TDD operations. The system bandwidth of LTE can be chosen among 6 values: 1.4, 3, 5, 10, 15, and 20 MHz. In all cases, the bandwidth is divided in 15 KHz sub-carriers.

Band Number	Uplink Band (MHz)	Downlink Band (MHz)	Duplex Mode
1	1920 - 1980	2110 - 2170	FDD
2	1850 - 1910	1930 - 1990	FDD
3	1710 - 1785	1805 - 1880	FDD
4	1710 - 1755	2110 - 2155	FDD
5	824 - 849	869 - 894	FDD
(6)	Not applicable	Not applicable	FDD
7	2500 - 2570	2620 - 2690	FDD
8	880 - 915	925 - 960	FDD
9	1749.9 - 1784.9	1844.9 - 1879.9	FDD
10	1710 - 1770	2110 - 2170	FDD
11	1427.9 - 1447.9	1475.9 - 1495.9	FDD
12	699 - 716	729 - 746	FDD
13	777 - 787	746 - 756	FDD
14	788 - 798	758 - 768	FDD
(15)	Reserved	Reserved	FDD
(16)	Reserved	Reserved	FDD
17	704 - 716	734 - 746	FDD
18	815 - 830	860 - 875	FDD
19	830 - 845	875 - 890	FDD
20	832 - 862	791 - 821	FDD
21	1447.9 - 1462.9	1495.9 - 1510.9	FDD
22	3410 - 3490	3510 - 3590	FDD
23	2000 - 2020	2180 - 2200	FDD
24	1626.5 - 1660.5	1525 - 1559	FDD
25	1850 - 1915	1930 - 1995	FDD
...			
33	1900 - 1920	1900 - 1920	TDD
34	2010 - 2025	2010 - 2025	TDD
35	1850 - 1910	1850 - 1910	TDD
36	1930 - 1990	1930 - 1990	TDD
37	1910 - 1930	1910 - 1930	TDD
38	2570 - 2620	2570 - 2620	TDD
39	1880 - 1920	1880 - 1920	TDD
40	2300 - 2400	2300 - 2400	TDD
41	2496 - 2696	2496 - 2696	TDD
42	3400 - 3600	3400 - 3600	TDD
43	3600 - 3800	3600 - 3800	TDD

Table B.2: LTE frequency bands [33]

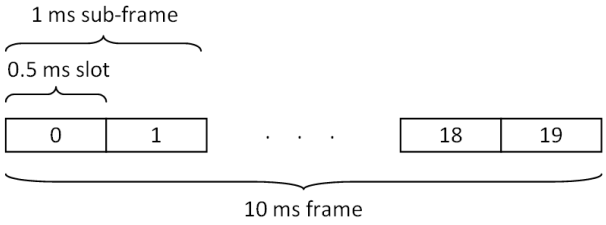

Figure B.5: LTE FDD frame structure

Regarding the time division, LTE FDD adopts a 10 ms frame structure as illustrated in Figure B.5 for both downlink and uplink transmissions. Each frame is divided in 0.5 ms slots and the shortest allocation period is 1 ms (1 subframe). The resources consisting of 12 contiguous sub-carriers (180 KHz) and a duration of 1 ms subframe are known as Physical Resource Block (PRB). One PRB is the smallest amount of resources that can be allocated to one UE. Table B.3 summarizes the number of available PRBs as a function of the system bandwidth.

System Bandwidth (MHz)	1.4	3	5	10	15	20
Number of PRBs	6	15	25	50	75	100

Table B.3: Number of PRBs for different LTE system bandwidths

B.3.2 Downlink Physical Layer

The multiple access scheme chosen for downlink LTE was OFDMA. Therefore each sub-carrier is transmitted as a parallel 15 KHz sub-carrier. One 0.5 ms slot can accommodate 6 or 7 OFDM symbols per sub-carrier, depending on whether an extended or short cyclic prefix is used.
The user data in the downlink direction is carried out on the Physical Downlink Shared Channel (PDSCH). Based on the Channel Quality Information (CQI) received from the terminals, the scheduler in every eNodeB's sector performs the resource allocation for the active users in its serving area every subframe. The resources are allocated in both time and frequency domain. The PRBs are not necessary having continuous allocation in the frequency domain. The Physical Downlink Control Channel (PDCCH) informs the device about the PRBs that are allocated to it, dynamically with 1 ms granularity. PDSCH data occupy between 9 and 13 symbols per 1 ms subframe depending on the allocation for PDCCH and depending whether a short or extended cyclic prefix is used. Within the 1 ms subframe, only the first 0.5 ms slot contains PDCCH while the second 0.5 ms slot is purely for PDSCH data. The number of symbols for PDCCH within a subframe can vary between 1 and 3. With the smallest bandwidth of 1.4 MHZ, the number of symbols varies between 2 and 4 to enable sufficient signal capacity and enough bits to allow for good enough channel coding in range critical cases. Figure B.6 illustrates the downlink slot structure assuming short cyclic prefix, bandwidth above 1.4 MHz, and 3 symbols for PDCCH.
In addition to the control symbols for PDCCH, space from the user data is reduced due to the reference signals (RS), synchronization signals, and broadcast data. Figure B.7 shows an example of resource allocation for PDSCH and PDCCH along with the RS pattern that is defined when 2 antennas are used for downlink transmissions. The figure on the left refers to the antenna port 1, while the figure on the right refers to the antenna port 2. Note that when a resource element is used to transmit an RS on one antenna port, the corresponding OFDM

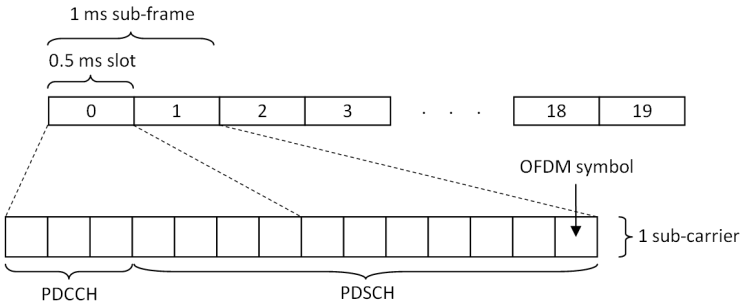

Figure B.6: Downlink slot structure for bandwidths above 1.4 MHz

symbol on the other antenna port is not used.
The modulation methods available in PDSCH are QPSK, 16QAM and 64QAM. In theory, an OFDM system could use different modulations for each sub-carrier. However, to have CQI and signaling with such granularity would not be feasible due to the resulting excessive overhead. Indeed, if modulation was sub-carrier specific, there would be too many bits in the downlink for informing the receiver of parameters for each sub-carrier and in the uplink the CQI feedback would need to be too detailed to achieve sub-carrier level granularity in the adaption. Therefore, it was chosen to adapt the modulation on a per user and subframe basis. Meaning that PRBs that are intended for one user will have the same modulation. The PDCCH uses either Binary Phase Shift Keying (BPSK) or QPSK.
The channel coding chosen for LTE user data in the downlink direction was 1/3-rate turbo coding. The encoder is Parallel Concatenated Convolution Coding (PCCC), the same as in WCDMA/HSPA. The turbo interleaver of WCDMA was modified to better fit LTE properties and slot structures and also to allow more flexibility for implementation of parallel signal processing with increased data rates. The maximum block size for turbo encoding is limited to 6144 bits to reduce the processing burden, higher allocations are then segmented to multiple encoding blocks.
LTE also uses physical layer retransmission combining, often referred to as Hybrid Adaptive

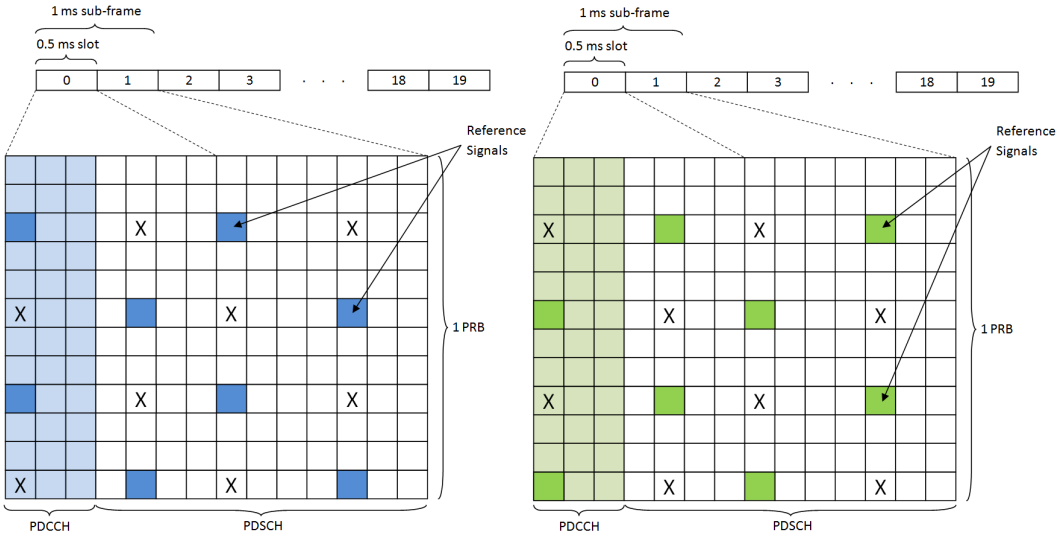

Figure B.7: Example of downlink resource sharing between PDSCH and PDCCH

Repeat and Request (HARQ). In a physical layer HARQ operation, the receiver also stores the packets with failed CRC checks and combines the received packets when a retransmission is received. Both soft combining with identical retransmissions and combining with incremental redundancy are facilitated.
The instantaneous data rate for downlink depends on the modulation, the allocated amount of PRBs, the channel encoding rate, and the transmission mode (MIMO operation). Assuming all resources to a single user and counting only the physical available resources available, an instantaneous peak data rate for downlink of 300 Mbps can be expected if using 4x4 MIMO operation [25].

B.3.3 Uplink Physical Layer

The multiple access scheme chosen for uplink LTE was SC-FDMA. The user data in the uplink direction is carried on the Physical Uplink Shared Channel (PUSCH). The same 1 ms resource allocation is also valid in the uplink direction. The resource allocation comes from a scheduler located at the eNodeB. Based on the buffer status received from the active users, the uplink scheduler allocates the resources and communicates the allocation to the active users. Without prior signaling from the eNodeB, only random access resources may be used.
The allocated bandwidth to a user in a sub-frame may be between 0 and 20 MHz, in steps of 180 KHz. In uplink, the allocation of PRBs to the active users must be contiguous. In fact only one SC-FDMA symbol can be transmitted at a time using the entire allocated bandwidth. Conversely, we have seen that in downlink, one OFDMA symbol per sub-carrier is transmitted at a time, thus an active users may be assigned with not contiguous PRBs.
The channel coding for user data in the uplink direction is also turbo coding, as in the downlink direction. Besides the turbo coding, uplink also has the physical layer HARQ with the same combining methods as in the downlink direction.
The instantaneous uplink user data rate depends on the modulation, the number of PRBs allocated, the amount of control information overhead, and the rate of channel coding applied. When calculated from the physical layer resources, an uplink peak data rate of 75 Mbps can be expected [25].

B.3.4 LTE MIMO

In the basic configuration, only one transmitter and one receiver antenna is used at the eNodeB and UE side. This is known as Single Input Single Output (SISO) transmission mode. However, in order to improve the cell coverage, as well as the average cell throughput and the spectral efficiency, LTE adopted various MIMO technologies in downlink and uplink. A brief overview of these technologies is presented in the following sections. More information can be found in [31],[28].

MIMO in Downlink

LTE supports up to four transmit antennas at the eNodeB and up to four receive antennas at the UE. The MIMO technologies adopted in downlink LTE are:

- *Single-User MIMO (SU-MIMO).* In SU-MIMO, the transmissions of multiple streams of data to a given user are overlapped in the same time-frequency resources by exploiting the spatial diversity of the propagation channel. The maximum number of supported spatial

layers is two, when the transmit and receive antennas are two, and four, when the transmit and receive antennas are four. There are two operation modes in SU-MIMO spatial multiplexing: open-loop spatial multiplexing and closed-loop spatial multiplexing. In the *closed-loop spatial multiplexing mode*, the eNodeB applies the spatial domain precoding on the transmitted signal taking into account the precoding matrix indicator (PMI) reported by the UE so that the transmitted signal matches with the spatial channel experienced by the UE. In the *open-loop spatial multiplexing mode*, the PMI feedback is not available at the eNodeB, thus a fixed set of precoding matrices are applied cyclically across all the scheduled subcarriers in the frequency domain.
To support both operation modes, the UE needs to feedback the rank indicator (RI) in addition to the PMI. The RI indicates the number of spatial layers (rank) that can be supported by the current channel experienced at the UE. The eNodeB may decide the transmission rank based on the RI reported by the UE as well as other factors such as traffic pattern, available transmission power, etc.

- *Transmit Diversity.* Transmit diversity is used when the selected transmission rank is one. Thus, switching between SU-MIMO modes is possible depending on channel conditions. In transmit diversity only one stream of data is transmitted to a given UE. Multiple transmit antennas are used to reduce the fading experienced at the UE rather than simultaneously transmit different streams of data. The fading reduction is obtained by transmitting each sub-carrier symbol in two different sub-carriers (one sub-carrier per antenna). Transmit diversity is specified for two and four transmit antennas.
- *Multi-User MIMO (MU-MIMO).* As in SU-MIMO, multiple antennas are used to transmit different streams of data in the same time-frequency resources. However, while in SU-MIMO different streams are transmitted to a given user, in MU-MIMO different streams are transmitted to different users. Since transmissions to several terminals are overlapped in the same time-frequency resources, MU-MIMO aims to enhance the capacity of a cell, rather than increasing the user peak rate. In order to fully exploit MU-MIMO transmission modes, the spatial streams intended to the targeted terminals need to be well separated, ideally orthogonal at both transmit and receive sides.
- *Closed-loop rank-1 precoding.* In the closed-loop rank-1 precoding mode, the eNodeB operates the closed-loop SU-MIMO scheme based on the cell-specific common reference signal with the limitation of selecting a rank-1 precoding matrix for transmission to a UE among the ones defined for two and four transmit antennas. The aim is to improve data coverage without relying on the UE-specific reference signal. Further, since the transmission rank is fixed, the related control signaling overhead is smaller than the case of operating the closed-loop SU-MIMO scheme.
- *Dedicated beamforming.* Dedicated beamforming is used to improve data coverage when the UE supports data demodulation using the UE-specific reference signal. The eNodeB generates a beam using the array of antenna elements, and then applies the same precoding to both the data payload and the UE-specific reference signal with this beam.

MIMO in Uplink

In order to avoid additional cost required to implement two or more power amplifiers at the UE, only one transmit antenna can be used at a time. The eNodeB can use up to four receive antennas, therefore receive diversity is supported. The MIMO technologies adopted in uplink LTE are:

- *Transmit antenna selection diversity.* In case of the closed-loop transmit antenna selection, the eNodeB selects the antenna to be used for uplink transmission and communicate this selection to the UE using the downlink control message. For the open-loop transmit antenna selection, the UE autonomously selects the transmit antenna to be used for transmission without eNodeB's intervention.
- *MU-MIMO.* In uplink MU-MIMO, the eNodeB schedules more than one UEs to transmit in the same time-frequency resources. In order for the eNodeB to be able to correctly differentiate and demodulate these UEs' signals, eNodeB needs to assign orthogonal reference signals for these UEs scheduled for the MU-MIMO transmission.

B.4 Radio Resource Management

B.4.1 Introduction

The role of Radio Resource Management (RRM) is to ensure that the radio resources are efficiently used, taking advantage of the available adaptation techniques, and to serve the users according to their configured Quality of Service (QoS) parameters [1]. The family of RRM algorithms at the eNodeB exploits various functionalities from Layer 1 to Layer 3 as listed below:

- *Layer-3 (PDCP/RRC)*: QoS management, Admission control, Persistent scheduling;
- *Layer-2 (RLC/MAC)*: HARQ, Dynamic scheduling, Link adaptation;
- *Layer-1 (PHY)*: PDCCH adaptation, CQI manager, Power control.

The RRM functions at Layer 3 are characterized as semi-dynamic mechanisms, since they are mainly executed during setup of new data flows. Instead, the RRM algorithms of Layer 1 and Layer 2 are highly dynamic functions with new actions conducted every TTI.
The CQI manager processes the received CQI reports and Sounding Reference Signals (SRSs) from active users in the cell. The CQI report is related to the channel conditions experienced at the UE in downlink and indicate a combination of modulation scheme and channel coding rate that the eNodeB should use to ensure that the block error rate probability at the UE will not exceed 10%. The SRSs are used in uplink in order for the eNodeB to be able to estimate the channel condition in uplink. Each received CQI report and SRS is used by the eNodeB for scheduling decision and link adaptation in downlink and uplink, respectively.
A complete description of the RRM functions is out of the goals of this report. In the next section, we will focus on the Layer 2 downlink dynamic scheduling and link adaptation, which are more relevant in relation of our work.

B.4.2 Downlink Dynamic Scheduling and Link Adaptation

The dynamic packet scheduler (PS) and the link adaptation entity are Layer 2 RRM entities, as illustrated in Figure B.8. The former performs scheduling decisions every TTI by allocating PRBs to the users, while the latter selects the modulation and coding scheme based on

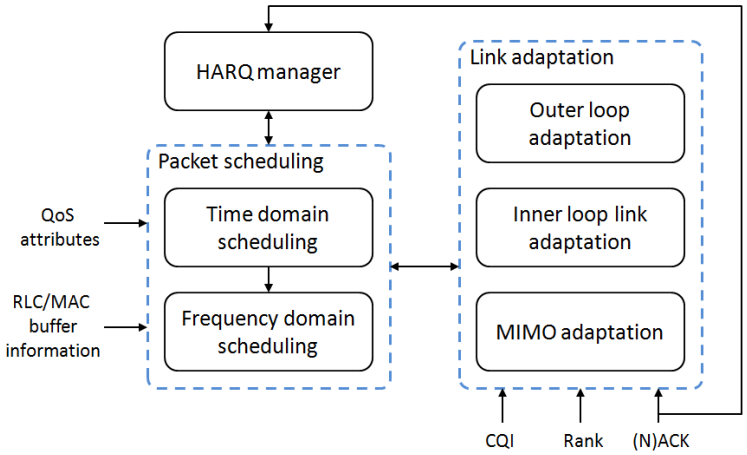

Figure B.8: Layer 2 RRM functionalities

the CQI reported by the UEs. The allocated PRBs and the selected modulation and coding scheme are signaled to the scheduled users on the PDCCH. The overall packet scheduling goal is to maximize the cell capacity, while making sure that the minimum QoS requirements for the EPS bearers are fulfilled and there are adequate resources also for best-effort bearers with no strict QoS requirements.

Figure B.8 illustrates a two-step packet scheduling implementation. The first step consists of the time-domain packet scheduler (TDPS). From the set of active users for which data is available for transmission, the TDPS selects a subset of M users for which resources have to be allocated in the TTI being scheduled. This subset forms the candidate set of users for the frequency-domain packet scheduler (FDPS). For each UE, the TDPS calculates a scheduling criterion that may depends on the QoS requirements, the presence of HARQ retransmissions, the past throughput, etc. All UEs are then listed in decreasing order in respect of the scheduling criterion, and the first M entries in the list are selected as candidate for the frequency domain scheduling.

The FDPS allocates the available PRBs to the users selected by the TDPS. The FDPS principle exploits the frequency selective power variations of the received signal by only scheduling users on the PRBs with high channel quality, while avoiding the PRBs where a user experiences deep fades. The overall objective of FDPS is to maximize the benefit from the frequency selectivity, while still guaranteeing a certain fairness. The FDPS is responsible for allocating the PRBs to users with new transmissions and also to users with pending HARQ retransmissions. Note, however, that it is not possible to simultaneously schedule new data and pending HARQ retransmissions to the same user in the same TTI.

Appendix C

Overview of the LTE System-Level Simulator

The LTE system-level simulator v1.3r427 [15], developed by the Vienna University of Technology, is capable of evaluating the performance of the PDSCH of LTE networks using SISO and MIMO transmit modes including Transmit Diversity, Open Loop Spatial Multiplexing, and Closed Loop Spatial Multiplexing. In addition it offers the possibility to adjust the number of TX and RX antennas, uplink delay, network layout, channel model, and scheduling algorithm. The LTE system-level simulator supplements an already freely available LTE link-level simulator [16]. This combination allows fast network performance investigations because the physical layer in the system-level simulator is abstracted by a simplified model that is based on results of the link-level simulator.
Figure C.1 shows a schematic block diagram of the LTE system level simulator and its relation with the LTE link-level simulator. The core part of the system-level simulator consists of a Link Measurement Model and a Link Performance Model. The Link Measurement Model is responsible for the calculation of the SINR of each UE. The SINR calculation is done per-layer and per sub-carrier and it is based on a simple Zero Forcing (ZF) receiver that includes three categories of losses: macroscopic pathloss, shadow fading, and fast fading. The macroscopic pathloss is implemented as an array of pathloss maps, where each map is associated to a different transmitter as shown in Figure C.2. Each map specifies the macroscopic pathloss

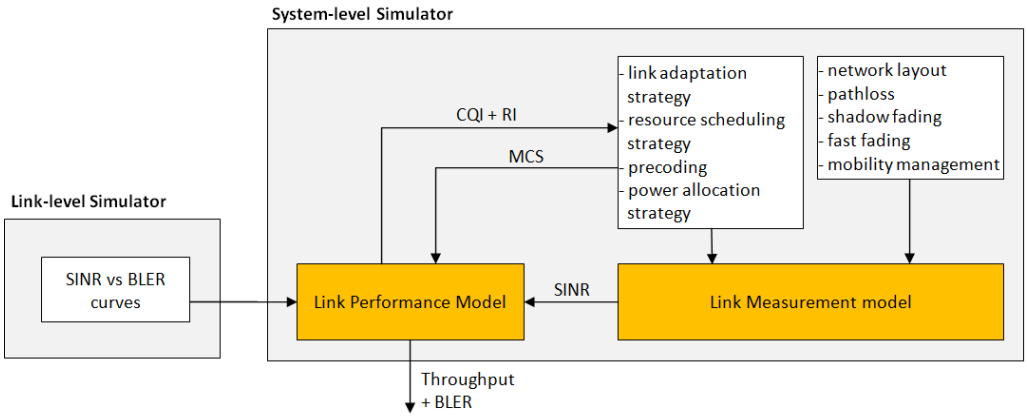

Figure C.1: Schematic block diagram of the LTE system level simulator

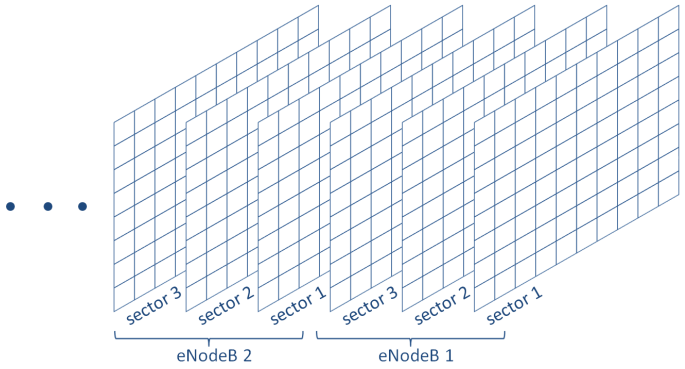

Figure C.2: Macroscopic pathloss implementation

between any point (x,y) in the region and the transmitter associated to the map. The same implementation has been selected for the shadow fading. This choice allows the simulator to calculate all the maps once, and as long as the network layout is kept the same, reuse the same maps. While the losses caused by the macroscopic pathloss and the shadow fading are position-dependent and time-invariant, fast fading is modeled as a time-dependent process. In this case, a trace of fading parameters modeling the time-and-frequency variant behaviour is generated at the beginning of the simulation and then accessed at the corresponding TTI.
The Link Performance Model is responsible for the calculation of the BLER of the received Transport Blocks (TBs) in order to determine whether the TB has been received correctly or not. The calculation is based on the SINRs calculated in the Link Measurement Model, the resource allocation, the TB's modulation and coding scheme (MCS), and a set of Additive White Gaussian Noise (AWGN) BLER curves, obtained from the link-level simulator. First, the set of SINRs of the PRBs assigned to the UE's TB are mapped to an equivalent-SINR using the Mutual Information Effective SINR ratio Mapping (MIESM). Then, the BLER of the received TB is found from the BLER curve of the TB's MCS in correspondence of the equivalent-SINR value. It is then decided via a coin toss, with probability of success equals to (1-BLER), whether the given received TB was received correctly. ACK reporting is subsequently generated.
Related to the Link Performance Model, the CQI feedback reporting provides the eNodeB with information of the channel condition at the UE. This information is used by the eNodeB in the link adaptation, in order to select the most appropriate MCS, and in the scheduling, in order to exploit the frequency selectivity. For the CQI feedback strategy, the SINR-to-CQI mapping is realized by selecting the MCS that offers a BLER lower than 10% in correspondence of the equivalent-SINR. If the SISO transmission scheme is selected, the UE feedback consists only of the CQI per PRB. Instead, if the OLSM transmission mode is selected, the Rank Indicator (RI) is also included in the feedback. In addition, the CQI is reported for both layers. The RI indicates the transmission rank that conveys more information in the current channel condition. Therefore, it provides the eNodeB with information on whether to transmit over one or two layers. Finally, if the CLSM transmission mode is selected, the Precoding Matrix Indicator (PMI) is also included in the feedback. It indicated to the eNodeB which precoding matrix to use for the spatial precoding of the transmitted signal.
The simulation is performed by defining a Region Of Interest (ROI) in which the eNodeBs and UEs are positioned, and a simulation length in Transmission Time Intervals (TTIs). It is only in this area where the UE movements and downlink transmissions are simulated. Each

simulated TTI, the simulator performs the following actions:

- The UEs' positions are updated according to their directions and speeds. If a position does not belong to the ROI, the UE is placed randomly within the ROI.
- Each sector receives the feedbacks from the attached UEs. Based on the received feedbacks, it determines the MCS and the transmission layers, and schedules the UEs.
- Each UE calculates the SINR for each PRB as defined by the link measurement model. It also calculates the CQI, RI, PMI, BLER, and throughput as defined by the link performance model. Finally it sends the CQI, RI, and PMI feedback, or a subset of those depending on the transmission mode, to the serving sector.

Appendix D

Feasibility study of an antenna array for a 6-sector site

D.1 Introduction

This section presents a radiation pattern study of an antenna array that is obtained combining the left side and right side of a Kathrein 80010622. The goal of the study is to determine whether this antenna array can be used as a sector antenna in 6-sector-site deployments. The investigation was driven by the poor availability of sector antennas intended for 6-sector-site deployments at the frequency range of 2.49-2.69 GHz. Indeed, directional antennas with 33° Half Power Beamwidth (HPBW) and dual-beam antennas with aggregate HPBW of 65° were widely available only for the frequency range of 1.71-2.2 GHz.
The strategy of the feasibility study can be summarized as follow. A mathematical model for the radiation pattern of the antenna array is derived from the antenna array theory. The radiation pattern of the antenna array is measured in order to verified the model. Finally, the performance of a 6-sector-site deployment are evaluated with the LTE System Level simulator presented in chapter 3 using the antenna array as sector antenna. This will give an insight on whether the antenna array can be used as a sector antenna in a 6-sector-site deployment.
This chapter is organized as follows. Section C.2 introduces the main characteristics of the Kathrein 80010622 along with the configuration of the antenna array. Section C.3 presents the mathematical model for the radiation pattern of the antenna array. Section C.4 presents the measurements of the radiation pattern. Section C.5 shows the simulation results obtained with the LTE System Level simulator using the radiation pattern of the antenna arrays. Finally, section C.6 provides the conclusion of the feasibility study.

D.2 Antenna Configuration

The Kathrein 80010622 is a panel antenna that consists of two identical antennas placed side by side in the same radome. Each of the two antennas is a slanted dual polarization (Xpol) multi-band antenna that operates in the frequency range of 1.71-2.69 GHz. Each Xpol antenna consists of two independently working slanted dipole systems, one for $+45°$ polarization and the other for $-45°$ polarization. The HPBW of each Xpol antenna is 65°, making the Kathrein 80010622 a suitable sector antenna for 3-sector-site deployments. For the antenna specifications please refer to [23].
In a standard configuration, the Kathrein 80010622 allows two service providers (SPs) to

use the same panel antenna for MIMO transmissions. Each service provider has access to both polarizations of one side of the panel antenna as shown in Figure D.1(a). This study proposes a new configuration. The $+45°$ polarization of the left side is connected with the $+45°$ polarization of the right side using a power splitter/combiner. The same is done for the $-45°$ polarization, as shown in Figure D.1(b). The result is the establishment of two independently working antenna arrays of two elements each, one for $+45°$ polarization and the other for $-45°$ polarization. In this configuration, the Kathrein 80010622 can be used by only one service provider for MIMO transmissions. Because of the array configuration, we expect a narrower HPBW compared to the standard configuration.

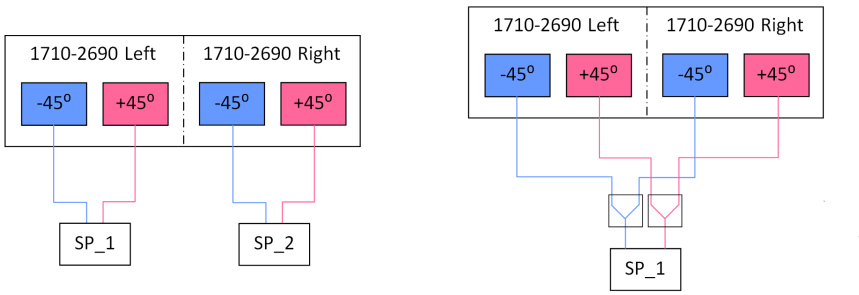

(a) Standard configuration (b) Array configuration

Figure D.1: Layout of interface (bottom view)

D.3 Theoretical Study

The voltage radiation pattern of a linear antenna array of K elements is calculated as the multiplication of two factors [24]:

$$S(\theta) = S_e(\theta)S_a(\theta), \tag{D.1}$$

where $S_e(\theta)$ is the element factor and $S_a(\theta)$ is the array factor. The element factor is the voltage radiation pattern of a single element, while the array factor is the voltage radiation pattern of an array of K isotropic radiators. The array factor is expressed as:

$$S_a(\theta) = \sum_{i=1}^{K} e^{jk_0(K-i)d\sin(\theta)} \tag{D.2}$$

The absolute value of the array factor can be simplified to:

$$|S_a(\theta)| = \left| \frac{\sin\left(\pi \frac{Kd}{\lambda_0}\sin(\theta)\right)}{\sin\left(\pi \frac{d}{\lambda_0}\sin(\theta)\right)} \right|. \tag{D.3}$$

Instead of the voltage radiation pattern, antenna manufacturers usually provide the power radiation pattern. Therefore, (C.1) can be written in the following form:

$$S_{dB}(\theta) = S_{e,dB}(\theta) + 20\log\left(\frac{|S_a(\theta)|}{K}\right), \tag{D.4}$$

where $S_{dB}(\theta)$ is the power radiation pattern of the antenna array, $S_{e,dB}(\theta)$ is the power radiation pattern of the single element, and $20\log\left(|S_a(\theta)|/K\right)$ is the normalized power radiation pattern of an array of K isotropic radiators.
The antenna array considered in this study is a 2 elements antenna array, where each element is a column of dipoles with $-45°$ polarization. The target frequency is 2600 MHz. From (C.3) and (C.4) with K = 2, the power radiation pattern of the antenna array can be calculated as:

$$S_{dB}(\theta) = S_{e,dB}(\theta) + 20\log\left(\frac{1}{2}\left|\frac{\sin\left(\pi\frac{2d}{\lambda_0}\sin(\theta)\right)}{\sin\left(\pi\frac{d}{\lambda_0}\sin(\theta)\right)}\right|\right), \tag{D.5}$$

where $S_{e,dB}$ is the power radiation pattern of the left element of the Kathrein 80010622 with $-45°$ polarization, measured at a frequency of 2620 MHz and a $0°$ of downtilt angle.
Figure D.2 shows the power radiation pattern of the element, the power radiation pattern of the array factor, and the power radiation pattern of the antenna array calculated with (C.5). The HPBW of the antenna array is $21°$ and the sidelobe attenuation is 5.5 dB.

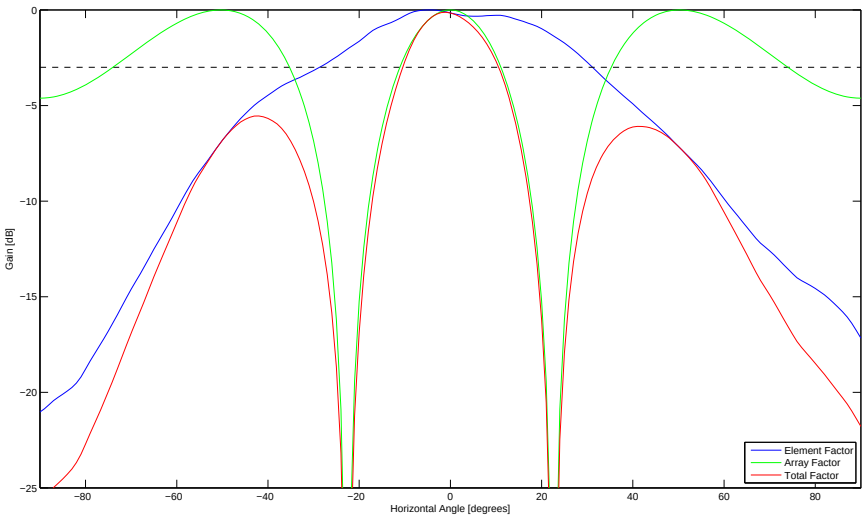

Figure D.2: Element, Array, and Total factor power radiation patterns

In the calculations above, we have implicitly assumed that the radiation pattern of an individual radiator remains the same upon placing it in an array environment. Apart from the interaction introduced by the inter-element distance and the phase difference this distance causes, no further interations between the radiators is assumed. In other words the mutual coupling between the radiators has been neglected. Since this assumption is a possible error source, we planned to measure the radiation pattern in order to verify the simulation results. The results of the measurements are presented in the next section.

D.4 Measurement Results

This section presents the results of two measurements. The first measurement aims to measure the radiation pattern of the left element of the Kathrein 80010622 with $-45°$ polarization and $0°$ tilt. The second measurement aims to measure the radiation pattern of the two elements array obtained combining the received power of the left and right element of the Kathrein 80010622 with $-45°$ polarization and $0°$ tilt.
The instruments that have been used in the measurements are:

- 1x Aaronia Hyperlog 7060 (Tx antenna)
- 1x Kathrein 80010622 (Rx antenna)
- 1x SiteMaster S251B
- 1x Power splitter/combiner
- Tripods, coaxial-cables, connectors, adapters

The parameters and settings of the measurements are summarized below:

- Frequency of the transmitted signal: 2500 MHz (maximum allowed by the signal generator in the SiteMaster S251B)
- Distance Tx-Rx: 30 meters (far-field region). It has been chosen as $2D^2/\lambda$ with D being the largest dimension of the antenna aperture.
- Angular rotation of the Rx antenna: steps of 3 degrees between -90 and +90 degrees
- Location: TU/e campus

Both measurements follow the same methodology, i.e. the received power is registered for every 3 degrees rotation of the Rx antenna while the Tx antenna is kept fixed. Figure D.3 depicts the configuration layouts of the two measurements, while Figure D.4 shows the actual configuration for measurement 2 at the TU/e campus.

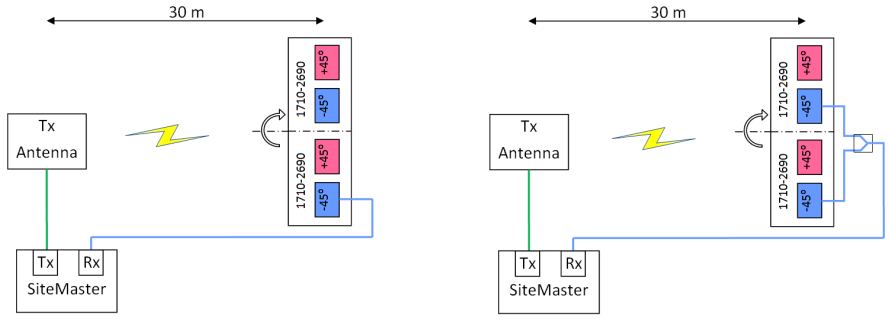

Figure D.3: Configuration layout of measurement 1 (left) and measurement 2 (right)

D.4.1 Results

Figure D.5 shows the measured radiation pattern of the left element of the antenna along with the radiation pattern provided by Kathrein for a frequency of 2490 MHz. The measured radiation pattern is quite closed to the one provided by Kathrein, therefore, the choice of the settings and the location of the measurements were appropriate.
Figure D.6 shows the measured radiation pattern of the array antenna along with the simulated radiation pattern of (C.5) with $d = 15$ cm and $f = 2500$ MHz. In this case, $S_{e,dB}(\theta)$ in (C.5) is the power radiation pattern of the left element of the Kathrein 80010622 at 2490 MHz with

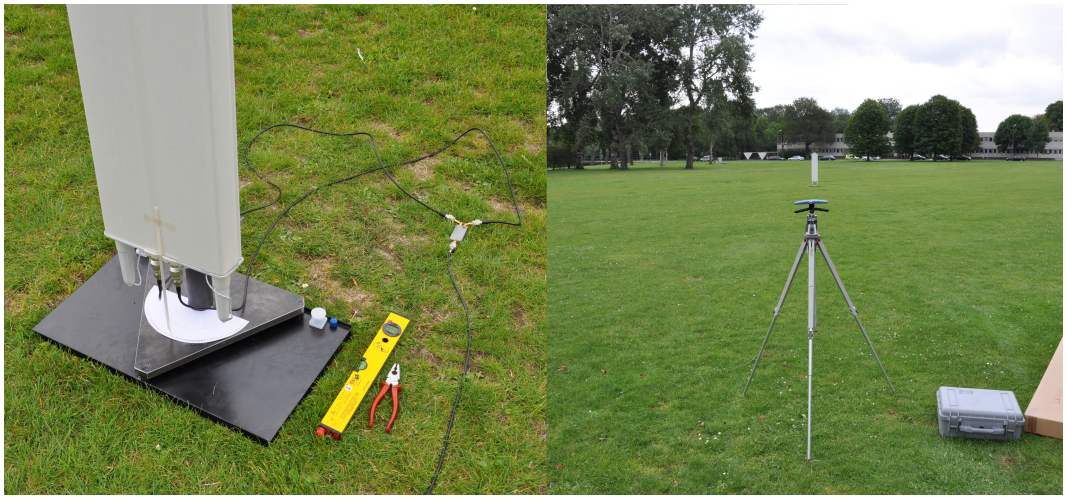

Figure D.4: Configuration of measurement 2 at the TU/e campus

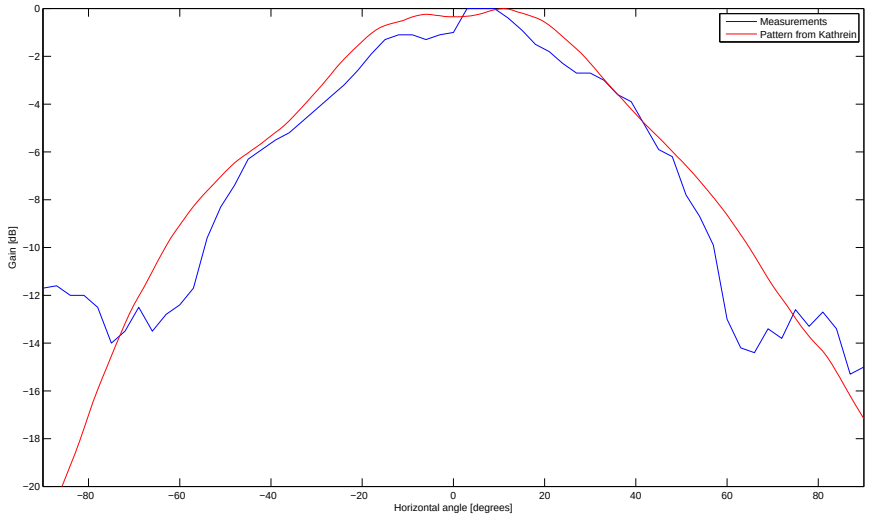

Figure D.5: Radiation pattern of the left element (−45° pol, 0° tilt)

−45° polarization and 0° of downtilt angle. The measured radiation pattern shown in Figure D.6 matches the simulated radiation pattern obtained with equation (C.5). Therefore, we can conclude that at 2500 MHz the mutual coupling between the elements has minor effects, if any, on the radiation pattern, and that equation (C.5) is a good model for the calculation of the radiation pattern of the antenna array. Furthermore, the assumption of a distance of 15 cm between the elements is realistic.

Because of the frequency limitation of the signal generator of the SiteMaster, it was not possible to perform the measurements at 2600 MHz and directly verify the equation (C.5) for this frequency. However, since the equation is verified at a frequency of only 100 MHz lower, we can extend the same conclusion to 2600 MHz.

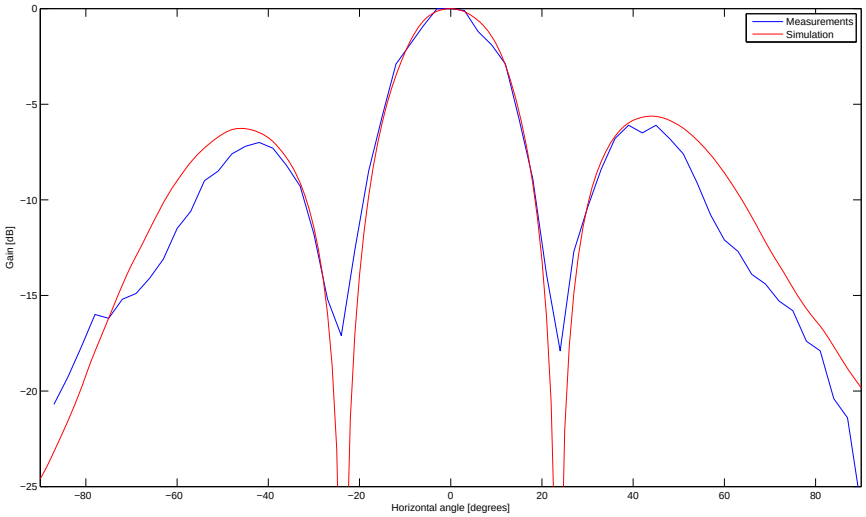

Figure D.6: Radiation pattern of the array configuration (−45° pol, 0° tilt)

D.5 Simulation Results

In order to determine whether this antenna array is suitable to be used as 6-sector antenna, we evaluated the performance of a 6-sector-site deployment with the LTE System Level simulator presented in Chapter 3 where the radiation pattern of the antenna array, as depicted in Figure D.2 (red line), is used as the radiation pattern of each sector antenna. A users' speed of 3 Km/h, 10 users per sector, Open Loop Spatial Multiplexing, and a frequency domain Proportional Fair packet scheduler have been considered in the simulations. To facilitate the performance evaluation, we compared the results achieved with the antenna array with the results achieved with two other antennas. The first antenna is a 6-sector antenna with 33° HPBW and radiation pattern defined by (3.3). The second antenna is the Kathrein 80010622 used in standard configuration. This antenna is normally deployed as a 3-sector antenna and its radiation pattern is depicted in Figure D.2 (blu line). For each antenna, the same radiation pattern has been used for both polarizations. The results comparison is shown in Figure D.7, where 'Model' stands for the 6-sector antenna, 'Std config' stands for the Kathrein 80010622 in standard configuration, and 'Array config' stands for the Kathrein 80010622 in array configuration.
Compared to Kathrein 80010622 in standard configuration, the antenna array results in lower intra-site and inter-site interference. The reason is quite straightforward if we observe Figure D.2. Since for every horizontal angles the gain of the antenna array is not greater then the gain of the single element, the level of interference that is generated in the adjacent sectors or in the surrounding sites is lower. The radiation nulls between the main lobe and the sidelobes affect the received power in the serving sector. However, as the geometry factor is higher, this effect is compensated by the reduction of the interference.
Compared to the 6-sector antenna, due to the poor sidelobe attenuation, the antenna array results in a much higher intra-site interference. In contrast, the inter-site interference is slightly lower. This is due to the narrower HPBW and the lower maximum gain. As result, the geometry factor and consequently the user throughput are lower.

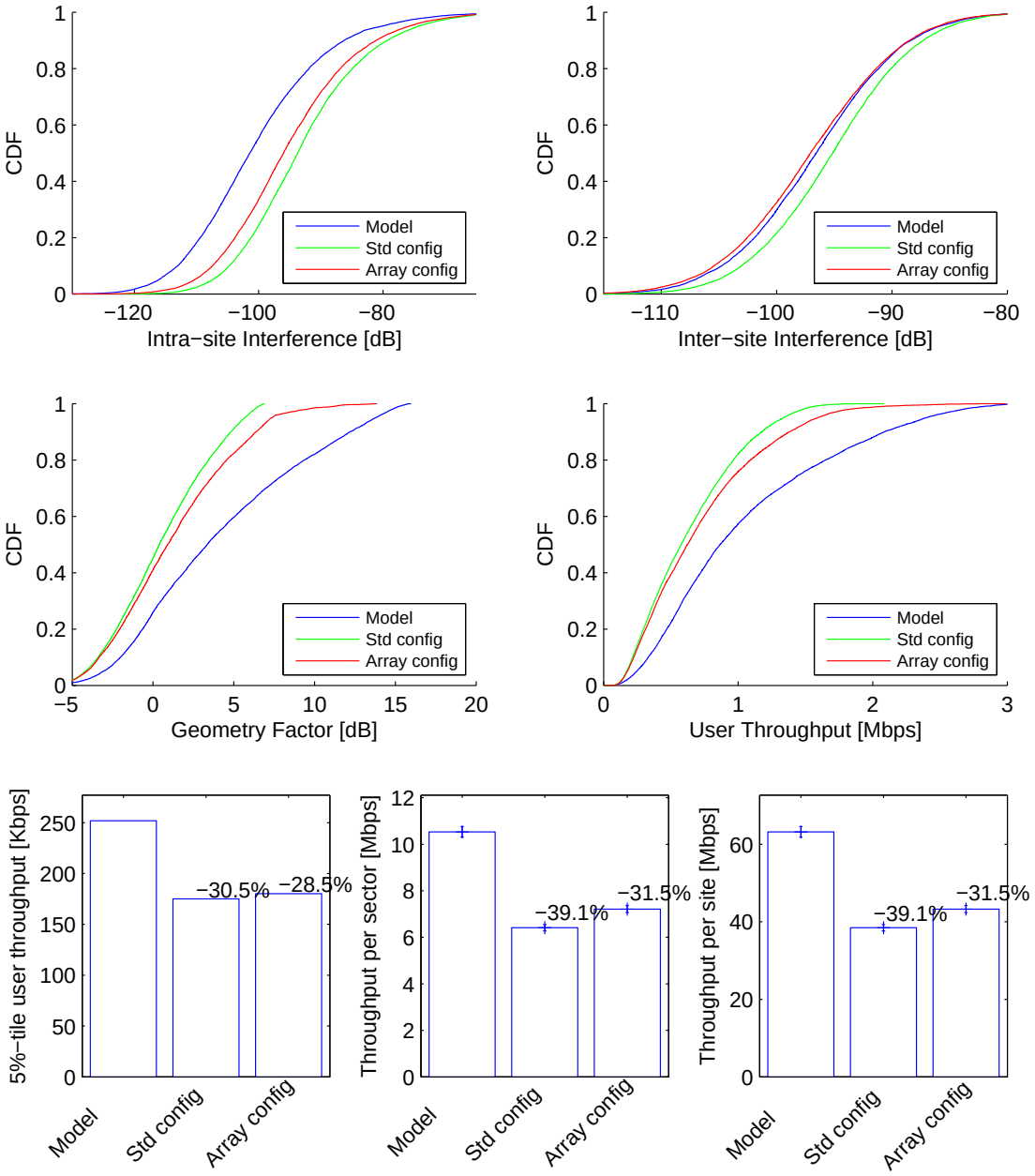

Figure D.7: Performance of 6-sector site with different antenna radiation patterns

Compared to the 6-sector antenna, the Kathrein 80010622 in the standard configuration provides a 30.5% lower cell-edge coverage and a 39.1% lower site throughput, while the Kathrein 80010622 in the array configuration provides a 28.5% lower cell-edge coverage and a 31.5% lower site throughput.

D.6 Conclusions

In this chapter we investigated the radiation pattern of the antenna array obtained combining the received power from the left and right element of a Kathrein 80010622. A mathematical model of the radiation pattern has been derived from antenna array theory. The radiation pattern has also been measured for a frequency of 2500 MHz. The measurements results confirmed the mathematical model. Although it was not possible to perform the measurements at 2600 MHz, we stated that the model can be considered valid also at 2600 MHz because of the small frequency difference. The simulations results of a 6-sector-site deployment shown that the Kathrein 80010622 in array configuration provides only slightly better performance than the Kathrein 80010622 in standard configuration and around 30% lower performance than a 6-sector antenna. Therefore, we conclude that it is not profitable in terms of performance to employ the antenna array presented in this study as sector antenna in a 6-sector-site deployment at 2600 MHz.
The main limitation of the considered antenna array is that the distance between the elements cannot be changed. If we were able to place the two sides of the antenna at a distance of 0.75λ (i.e. 8.65 cm), the radiation pattern of the antenna array would have been suitable for a 6-sector antenna as it would have an HPBW of 33° and a sidelobe attenuation of 17 dB. In this context, we took into consideration an antenna array consisting of two Kathrein 84010077 placed side by side. The configuration is similar to the one considered in this study with the difference that the two antennas are not kept together by the same radome but instead their distance can be adjusted. However, it cannot be lower than 155 mm, therefore also this solution is not feasible for a 6-sector site.

Appendix E

Baseline Document

The last version of the baseline document that has been written for the course Project Based Management is presented in this appendix. It refers to the finalization of the project.

E.1 Introduction

3GPP Long Term Evolution (LTE) is one of the latest standards for mobile communications and it represents the evolution of the widely deployed UMTS/3G cellular communication system. Among all performances, LTE can offer reduced delays, in terms of both connection establishment and transmission latency, increased user data rates, reduced cost per bit, and simplified network architecture. Currently, publicly available LTE services can be found in Stockholm, Oslo, and Denmark. However, many service providers in Europe have built their own LTE network to perform performance measurements and research activities.
KPN is a Dutch landline and mobile telecommunication company based in The Hague. In February 2011, KPN started with a series of tests and measurements on its LTE trial network in The Hague. Among its goals, KPN is interested in accessing the capacity gain of a 6-sector-site deployment compared to a 3-sector-site deployment. Currently, each base station of the LTE network is provided with 3 directional antennas (3-sector site). Increasing the number of antennas to 6 is expected to increase the site capacity and the user rates. However, due to the lack of studies on this topic, the capacity gain cannot be estimated and the most profitable solution cannot be determined. The aim of this project is to access the capacity gain through a simulation study and a measurement study.
This project is executed as the final project of the Professional Doctorate in Engineering (PDEng) in Information and Communication Technology, a two years program that is offered by the Stan Ackermans Institute (SAI) at the Eindhoven University of Technology (TU/e). The mentor of the project is Mr. Matthijs Klepper from the Radio Access Innovation department of KPN. The supervisors of the project are Mr. Arie Verschoor, from the Radio Access Innovation department of KPN, and Mr. Erik Fledderus, from TU/e.

E.2 The project result

E.2.1 Problem definition

Global mobile data traffic is expected to grow at a CAGR (Compound Annual Growth Rate) of 78% from 2011 to 2016. One reason of the strong growth is the accelerated adoption of

smartphones and mobile-connected tablets, laptops, and netbooks. The other reason is the rapid increase of the traffic per device due to a higher usage of VoIP applications, mobile gaming, mobile P2P, and mobile M2M, along with an increasing request of high-definition video and TV services.
In order to support the rapid growth in mobile subscribers and bandwidth demand per subscriber, service operators must increase the capacity of their network. One technique to achieve this goal consists in upgrading the existing site from a 3-sector configuration to a 6-sector configuration. Although several simulation studies have been conducted to investigate the performances of a six sectorized site compared to those of a three sector site in GSM and WCDMA systems, no extensive simulation studies nor measurement studies are available in literature for LTE systems. This leads to an uncertainty on the magnitude of the capacity gain that can be achieved in the downlink channel of LTE when upgrading the existing sites from three to six sectors.

E.2.2 Project goal

The goals of this project are:

A) Determine the capacity gain of a 6-sector-site deployment compared to a 3-sector-site deployment through a simulation study and a measurement study.

B) Determine whether the 6-sector-site deployment is economically more attractive than a 3-sector-site deployment through an economic study.

C) Determine whether an antenna array derived from two 3-sector-site antennas can be used as 6-sector-site antenna or a specific 6-sector antenna needs to be used.

E.2.3 Deliverables

At the end of the project the deliverables will be the following. Next to each deliverable we reported the corresponding goal.

1) Report that includes: the results of the simulation study, the results of measurements study, the comparison of the results of the two studies, and the answer to the problem [A]. In addition, the feasibility study of the antenna array is also included in the report [C].

2) Report on the economic study [B].

3) LTE system level simulator [A]: MATLAB code, and documentations.

4) Antenna support [C] designed for sector antennas that allows rotation over the vertical axes.

E.2.4 Delimiters

The project does not include capacity gain investigation in uplink UTRAN LTE and higher order sectorization than 6.

E.2.5 Progress of the project

This baseline document refers to the finalization of the project. At the final stage, the measurement study is not completed. The test cases for the measurements have been designed

but the measurements could not be performed because of a delay in the construction of the KPN network. Therefore, the measurements results are not part of the report. Every other activities and the corresponding deliverables are accomplished.

E.3 Phasing Plan

E.3.1 Strategy

The project consists of four subprojects. The first subproject involves the design and realization of an antenna support and the execution of measurements with the antenna array. The second subproject consists in the simulation study. It involves the choice of the simulator, the development of additional capabilities, and the execution of an extensive set of simulations. The third subproject consists in the measurement study. It involves the design and execution of a set of measurements in a LTE network. The results of the second and third subprojects will be analyzed and compared in order to solve the uncertainty on the capacity gain of a 6-sector-site deployment over a 3-sector-site deployment. Finally, the fourth subproject consists in the economic study. The activities and the outcome of each phase of each subproject are described below.

E.3.2 Init phase

- Investigate overall- and sub-goals and problems.
- Define desired results and deliverables.

The outcome of this phase it the first version of the baseline document.

E.3.3 Definition phase

Common activity:

- Acquiring knowledge on LTE physical layer and on 6-sector-site deployment.

Subproject 1 - Antenna array investigation:

- Collecting antenna specifications
- Defining requirements for the support
- Reviewing existing tripods/supports

Subproject 2 - Simulation study:

- Defining requirements for the simulator
- Reviewing existing simulators

Subproject 3 - Measurement study:

- Acquiring knowledge on the LTE trial network: structure and elements
- Acquiring knowledge on what is possible to measure from the network
- Defining the requirements of the measurements and what I am going to measure

The outcome of this phase are the list of requirements and the project plan.

E.3.4 Design phase

Subproject 1 - Antenna array investigation:

- Developing a general design
- Testing against requirements
- Developing a detailed design with a 3D graphic toll in cooperation with GTD-TNO
- Testing against requirements

Subproject 2 - Simulation Study:

- Choice of the simulator out of the reviewed ones
- Study of the simulator
- Developing of additional capabilities to the simulator
- Testing against requirements
- Developing a set of scenarios to simulate

Subproject 3 - Measurement study:

- Choice of the 6-sector antenna
- Developing a test case for the measurements

The outcome of this phase are the design of the antenna support, the extended version of the LTE system level simulator with the additional capabilities, and a set of test cases for the measurements.

E.3.5 Preparation phase

Subproject 1 - Antenna array investigation:

- Obtaining funds approval for the antenna support
- Contracting and instructing realizers of the antenna support (GTD-TNO)

Subproject 2 - Simulation Study:

- Obtaining rights of using an adequate PC for the simulations
- Setting parameters for the simulations
- Planning simulations

Subproject 3 - Measurement study:

- Ordering 6 items of 6-sector antennas
- Construction of the LTE Friendly User Pilot (FUP)[1]
- Obtaining equipment for the measurements

The outcome of this phase are the realization scripts for each subproject.

[1] Activity done by KPN

E.3.6 Realisation phase

Subproject 1 - Antenna array investigation:

- Production of the antenna support[2]
- Execution of the radiation pattern measurements with the antenna array mounted on the support
- Writing the report section related to the antenna array investigation

Subproject 2 - Simulation Study:

- Execution of the planned simulations
- Results analysis
- Writing the report section related to the simulation study

Subproject 3 - Measurement study:

- Execution of the planned measurements
- Results analysis
- Writing the report section related to the measurements study
- Finalizing the report

Subproject 4 - Economic study:

- Writing the economic study report

The outcome of this phase are the project report, the economic study report, and the antenna support.

E.4 Control plan

E.4.1 Time

	Date
Starting date of the project	07-02-2011
Completing date of the project	30-03-2012
Delivery date for the results	25-03-2012
Final Presentation	28-03-2012
	Man hours
Capacity - Damiano	40 hours/week
Capacity - TU/e supervisor	1-5 hours/month
Capacity - KPN supervisor	5-10 hours/month

Table E.1: Overview of time/capacity

For the duration of phases, see Figure E.1.

[2]Activity done by GTD-TNO

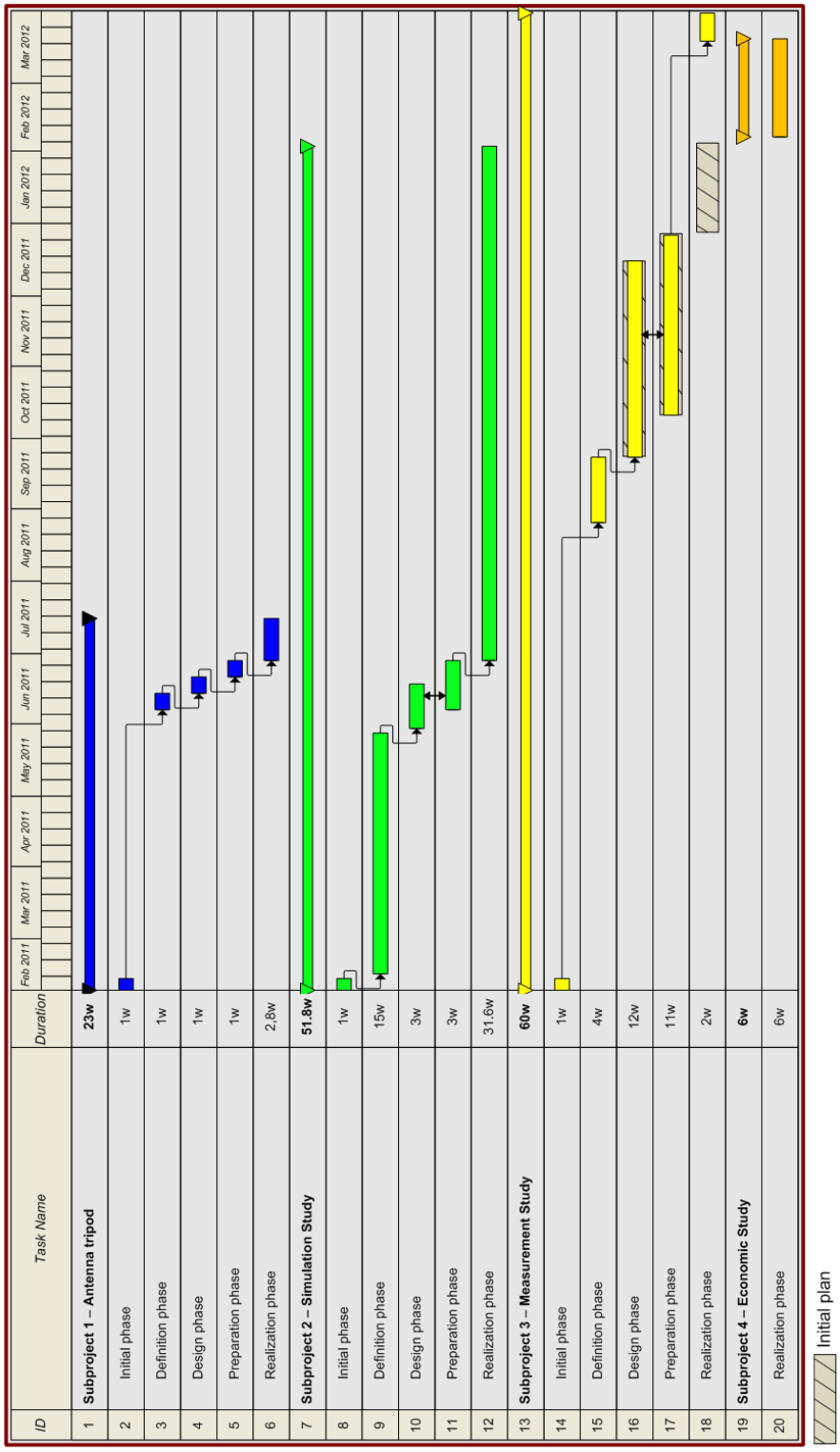

Figure E.1: Gantt chart of the project. The definition phase of the subproject 1 is delayed because of capacity reason. The definition phase of subproject 3 is delayed because it cannot start before the main settings of the trial network are defined. This has to be done by KPN, the project leader cannot influence it.

E.4.2 Progress control

- Weekly meetings with KPN supervisor in The Hague.
- Monthly meetings with both KPN and TU/e supervisors in The Hague.

E.4.3 Costs

The costs involved in the project include:

- My salary
- My travel expenses
- The salary of the people involved in the project as supervisors or consultants
- The office room and equipment costs
- Production cost of the antenna support

All costs have been covered by TU/e with funds provided by KPN. The TU/e Financial Department has estimated the integral costs for a PDEng Traineeship to be around 210,000 €.

E.4.4 Quality

Demands for the Antenna support:

- It has to allow the antenna to rotate among its vertical axis
- It has to include an angular plot with 3 degrees precision
- Height adjustments of the support base of +/- 3 cm should be possible
- Vertical axes movements should be kept lower than 3 degrees

Demands for the Simulation Study:

- Possibility to adjust the number of sectors, the number of users per sector, users' speed, CQI reporting delay, and CQI compression technique
- Possibility to use any antenna pattern defined by the user, and different propagation models
- Assess the capacity gain in an extensive set of scenarios
- Reliability of the results

Demands for the Measurement study:

- Assess the capacity gain in an extensive set of scenarios
- Reliability of the results

The activities performed to guarantee the quality of the results in this project are summarized in Table E.2.

Phase	What (by who)
Definition phase	Check if the set of reviewed simulators is extensive (D) Discuss about measurement requirements (D+S)
Design phase	Design validation/verification tests (D) Validation of the antenna support design (D) Verification of added capabilities in the simulator (D)
Preparation phase	Verification of the whole simulator (D) Check if simulator parameters are set according to 3GPP standards (D) Check sector antenna specifications before ordering (D)
Realization phase	Monitor production of antenna support (D) Monitor the construction of the FUP (D+S) Define reliability of simulation results and measurements (D+S) Check reliability of simulation results (D) Check the reliability of the measurements (D+S)

Table E.2: Activities to guarantee quality of results. Notation: (D) indicated an activity performed by Damiano, while (D+S) indicates an activity performed by Damiano and the supervisors.

Phase	**Documents, etc.**	**Recipients**
Init phase	Project assignment	Supervisors
Definition phase	Project plan	Supervisors
Design phase	Design of the antenna support	GTD-TNO
	Extended version of the LTE system level simulator	Supervisors
	Test cases for the measurements	Supervisors
Preparation phase	Realization script for the antenna support	GTD-TNO
	Realization script for simulations	Supervisors
	Realization script for the measurements	Supervisors
Realization phase	Report	Supervisors
	Economic report	Supervisors
Along all project	Monthly presentation to illustrate the progress	Supervisors

Table E.3: Information delivery plan

E.4.5 Information

The plan for output distribution is summarized in Table E.3.

E.4.6 Organization

The people who are involved in this project are:

- Project owner: dr. ir. Matthijs Klepper (Radio Access Innovation department at KPN)
- Contractor: ir. Arie Verschoor (Radio Access Innovation department at KPN)
- Project leader: Dipl. Eng. Damiano Scanferla
- TU/e Supervisor: prof. dr. ir. Erik Fledderus
- Director of SAI-ICT program: prof. Dr.-Ing. Leon Kaufmann

- Project manager of the LTE FUP: dr. ir. Redert Steens (KPN)

Third parties:

- GTD-TNO. Contact person: A.R. van Dommele.
- Argus Antenna. Contact person: Jonathan Hicks.
- Tongyu Communication Inc. Contact person: Kevin Wang.

E.5 Risk Analysis

E.5.1 Risk list

The risks that can occur in the project are identified and evaluated in Table E.4. Equation E.1 provides a formula to prioritize the risks according to their severity[3] and frequency of occurrence[4],

$$Priority = Effect * Chance \tag{E.1}$$

Possible risks identified	**Effect**	**Chance**	**Priority**
Delay on delivery of antennas	2	2	4
Delay on the construction of the FUP	3	2	6

Table E.4: List of possible risks

E.5.2 Risk management

The risk of a delay in the construction of the LTE FUP eventually occurred. In version 1.0 of this document, a set of actions were identified to handle this risk:

1. Extension of the project duration according to the delay of the construction.
2. Plan a follow project for the execution of the measurements.

The management plan number 1 has been selected. The project duration and the contract of the project leader have been extended from the 31st of January 2012 to the 30th of March 2012.

[3]Effect (severity): 1 = small, 2 = medium, 3 = big.
[4]Chance (occurrence): 1 = rare, 2 = sometimes occur, 3 = frequently.

Bibliography

[1] H.Holma and A.Toskala, "LTE for UMTS: OFDMA and SC-FDMA based radio access", John Wiley & Sons, 2009.

[2] 3GPP Technical Specifications TS 36.213 v10.2.0, Physical layer procedures, June, 2011.

[3] Cisco Visual Networking Index: Global Mobile Data Traffic Forecast Update, 2011-2016; February 14, 2012.

[4] M. Schacht, A. Dekorsy, P. Jung, "System capacity from UMTS Smart Antenna Concepts", *In Proc. of the 58th IEEE Veh. Tech. Conf.*, October 2003.

[5] J. Laiho, A. Wacker, T. Novosad, "Radio Network Planning and Optimization for UMTS", John Wiley & Sons, 2006.

[6] A. Wacker, J. Laiho, K. Sipila, K. Heiska, "The impact of the base station sectorization on WCDMA radio network performance", *In Proc. of VTC*, 1999.

[7] B. Hagermann, D. Imbeni, J. Barta, A. Pollard, R. Wohlmuth, P. Cosimini, "WCDMA 6-sector Deployment - Case Study of a Real Installed UMTS-FDD Network", *Vehicular Technology Conference*, Vol. 2, pp. 703-707, Spring 2006.

[8] Press Release: Espoo, Finland - November 4, 2009, "All-in-one mobile site solution boosts 2G, 3G and LTE network coverage and capacity", http://www.nokiasiemensnetworks.com/news-events/press/press-releases.

[9] Press Release: London, UK - June 9, 2010, "Upgrade for O2 delivers superior smartphone experience in London", http://www.nokiasiemensnetworks.com/news-events/press/press-releases.

[10] News: SK Telecom - January 1, 2011, "SK Telecom Plans LTE Launch in 2011", http://www.sk.com/happychannel/news/news_list.asp.

[11] S. Kumar, I.Z. Kovács, G. Monghal, K.I. Pedersen, P.E. Mogensen, "Performance Evaluation of a 6-Sector-Site Deployment for Downlink UTRAN Long Term Evolution", *IEEE Proc. Vehicular Technology Conference*, September 2008.

[12] K.I. Pedersen, P.E. Mogensen, B.H. Fleury, "Spatial channel characteristics in outdoor environments and their impact on BS antenna system performance", *Proc. IEEE Vehicular Technology Conf. 1998*, pp/719-724, 1998.

[13] http://www.tenxc.com.

[14] http://www.nokiasiemensnetworks.com.

[15] J.C. Ikuno, M. Wrulich, M. Rupp, "System level simulation of LTE networks", *IEEE Vehicular Technology Conference VTC2010 spring*, Taipi, Taiwan, May 2010.

[16] C. Mehlführer, M. Wrulich, J.C. Ikuno, D. Bosanska, M. Rupp, "Simulating The Long Term Evolution Physical Layer", *in Proc. of the 17th European Signal Processing Conference (EUSIPCO 2009)*, Glasgow, Scotland, August 2009.

[17] A. Pokhariyal, T. E. Kolding, P. E. Mogensen, "Performance of Downlink Frequency Domain Packet Scheduling for the UTRAN Long Term Evolution", *The 17th Annual IEEE International Symposium on Personal, indoor and Mobile Radio Communications*, Helsinki, September 2006.

[18] 3GPP Technical Report TR 36.942 v10.2.0, Radio Frequency (RF) system scenarios, December 2010.

[19] H. Claussen, "Efficient modeling of channel maps with correlated shadow fading in mobile radio systems", September 2005.

[20] Y. R. Zheng, C. Xiao, "Simulation models with correct statistical properties for rayleigh fading channels", *Communications, IEEE Transactions on*, June 2003.

[21] T.B. Sorensen, P.E. Mogensen, F. Frederiksen, "Extension of the ITU Channel Models for Wideband (OFDM) Systems", *in Proc. IEEE Vehicular Technology Conf.*, Dallas, USA, September 2005.

[22] http://www.kathrein.de.

[23] https://www.kathrein.de/de/mcs/produkte/download/9363621b.pdf.

[24] H.J. Visser, "Array and Phased Array Antenna Basics", John Wiley & Sons, 2005.

[25] www.3gpp.org.

[26] 3GPP Technical Report TR 25.913 v7.0.0, Requirements for Evolved UTRA (E-UTRA) and Evolved UTRAN (E-UTRAN), June 2005.

[27] 3GPP Scope and Objectives, 31 August 2007.

[28] S. Sesia, I. Toufik, M. Baker, "LTE - The UMTS Long Term Evolution: From Theory to Practice", John Wiley & Sons Ltd., 2011.

[29] 3GPP Technical Specifications TS 36.306 v8.8.0, User Equipment (UE) radio access capabilities, June 2011.

[30] ITU-R Report M.2134, 'Requirements related to technical performance for IMD-Advanced radio interace(s)', www.itu.int/itu-r, 2008.

[31] J. Lee, J.-K. Han, J. Zhang, "MIMO Technologies in 3GPP LTE and LTE-Advances", *EURASIP Journal on Wireless Communications and Networking*, vol. 2009, Article ID 302092, doi:10.1155/2009/302092.

[32] "4G Mobile Broadband Evolution: 3GPP Release 10 and Beyond - HSPA+, SAE/LTE and LTE-Advanced", 4G Americas, February 2011.

[33] 3GPP Technical Specifications TS 36.104 v10.5.0, Base Station (BS) radio transmission and reception, December, 2011.